Onshore to offshore trends in carbonate sequence development, diagenesis and reservoir quality across a land-attached shelf in SE Asia

Moyra E.J. Wilson[1*], Eva Chang Ee Wah[2], Steven Dorobek[3] and Peter Lunt[4]

[1]Department of Applied Geology, Curtin University, GPO Box U1987, Perth, Western Australia 6845, Australia.

[2]BHP Billiton, Perth, Western Australia.

[3]BHP Billiton Petroleum, 1360 Post Oak Boulevard, Houston TX 77056.

[4]Mitra Energy Limited, Level 24, Menara IMC, Jalan Sultan Ismail, 50250 Kuala Lumpur, Malaysia.

Corresponding author e-mail: m.wilson@curtin.edu.au

Keywords: Neogene, mixed carbonate-siliciclastic shelf, reefs, diagenesis, SE Asia, reservoir quality

Abstract

Although isolated Miocene buildups in SE Asia commonly form prolific hydrocarbon reservoirs, their equivalents on clastic-dominated land-attached shelves remain poorly known and underexplored. Here, onshore to offshore trends in carbonate development and reservoir quality are assessed across the NW Borneo shelf through study of surface outcrops and subsurface wells. A multidisciplinary programme of fieldwork, petrography and geochemical analyses allowed evaluation of spatio-temporal variations in deposition, diagenesis and pore system development, together with an assessment of controlling

influences. In addition to field logging and sample collection >200 samples were studied via transmitted light, cathodoluminescent and scanning electron microscopy together with stable isotopic characterisation (O, C and Sr).

Carbonates developed as localised low-, and higher-relief buildups, as well as more continuous sheet-like deposits in near-coast to shelf margin positions. Molluscs, corals, larger benthic foraminifera and coralline algae are common constituents. Most samples show evidence for marine micritisation, and just in shelf margin positions isopachous cements. However, burial diagenesis predominates in the form of compaction, neomorphism, fracturing, late leaching and dolomitisation. Near-coastal carbonates commonly contain siliciclastics, as do some shelf margin deposits that interdigitate with, or are covered in siliciclastics. Some early, probable meteoric leaching affected inner shelf deposits prior to pervasive neomorphic to blocky/poikilotopic calcite cement formation. On the basis of δ^{18}O V-PDB values of –4.5 to –7.9‰ equivalent to δ^{18}O V-SMOW values of 0 to –4‰ at 25–40°C and δ^{13}C V-PDB values of –0.6 to +1.6‰ cementation probably reflects alteration from terrestrial groundwaters in meteoric aquifers derived from the humid landmass of Borneo. Despite this cementation, moderate energy inner- to mid-shelf grainstones from the core of mounded carbonates still retain, or have enhanced porosity (<8%) over their lower energy counterparts (<4% porosity). Retention of primary porosity and/or late burial dissolution (often associated with saddle dolomite formation) enhancing predominantly primary and minor secondary porosity is key to reservoir quality development in outer-shelf deposits. Best porosity (<20–35%) is in high energy grainstones and rudstones from outer-shelf to shelf-margin positions that experienced minimal clastic influx, most commonly from backstepping to aggradational carbonate sequences. Although

stable isotopes for shelf margin calcite cements are consistent with precipitation from marine derived fluids ($\delta^{18}O$ V-PDB values of –3.6 to –5.4‰), those for the late dolomites are suggestive of fluids of meteoric origin ($\delta^{18}O$ V-PDB values of –5.2 to –7.4‰ equivalent to values of –0.3 to –6.3‰ V-SMOW at 40 to 60 °C). Critical factors for reservoir quality development in carbonates from siliciclastic dominated shelves in the equatorial tropics are: (1) development and preservation of primary porosity, (2) cementation associated with meteoric aquifers draining large humid equatorial landmasses, and (3) burial leaching and fluid pathways.

Introduction

Isolated Miocene buildups in SE Asia commonly form prolific hydrocarbon reservoirs (Epting, 1980; Fulthorpe and Schlanger, 1989; Vahrenkamp et al., 2004; Bachtel at al., 2004), however, their equivalents on clastic-dominated land-attached shelves remain poorly known and underexplored (Wilson, 2002; Wilson and Lokier, 2002; Wilson, 2012). Although 69% of the 250 shallow-water or shelfal/neritic carbonate formations of Tertiary age in SE Asia developed as attached systems, 83% of economic hydrocarbon discoveries by formation to date, and >96% of reserves are in isolated carbonates (Wilson and Hall, 2010). Does this apparent mismatch in SE Asian carbonate systems development versus their reservoir development reflect: (1) underevaluation, (2) paucity of reservoir development, (3) lack of trap formation, or (4) 'failure' of other aspects of petroleum system development all within attached carbonate systems? The hypothesis here is that potential reservoir development in attached carbonate systems from predominantly clastic shelves in SE Asia will be strongly influenced by local environmental conditions associated with their development in the equatorial tropics adjacent to large landmasses. Additionally, there may

be significant variations in carbonate and potential reservoir development across broad land-attached shelves. Local environmental conditions that may all influence depositional and post-depositional basin margin carbonate development in the equatorial tropics include significant and near-continuous influx of siliciclastics and/or nutrients together with sustained large-scale palaeoaquifer flow (Hendry et al., 1999; Wilson and Lokier, 2002; Wilson, 2002; 2005; 2008; 2011; 2012; Madden and Wilson, 2012).

Herein, the deposition, diagenesis and reservoir quality of Miocene carbonates from across the broad (>100 km wide) siliciclastic-dominated shelf of NW Borneo, offshore Sarawak, is assessed (Figure 1). As the world's third largest island, with significant Neogene uplift and a humid equatorial climate, the terrestrial runoff from Borneo results in some of the most globally significant annual discharges of freshwater, clastics and nutrients to the surrounding seas (Hall and Nichols, 2002). Basins around Borneo conservatively contain up to 9 km of sediment derived from the island (Hamilton, 1979), and the sediment supplied during the Neogene is similar to that per unit area of the Himalayas (Hall and Nichols, 2002). Although excessive clastic influx can be detrimental to carbonate production, recent studies have shown that many carbonate producers can adapt to a significant influx (Wilson and Lokier, 2002; Sanders and Baron–Szabo, 2005; Hallock, 2005; Wilson, 2005; Lokier et al., 2009). A range of modern and Tertiary carbonate systems have been documented from the predominantly clastic shelves of Borneo, including delta-front patch reefs, coastal fringing reefs, admixed carbonate-siliciclastic biostromes, intra-shelf reefs or buildups, and shelf margin buildups or barrier systems (Agostinelli et al., 1990; Netherwood and Wight, 1992; Ali, 1995; Roberts and Sydow, 1996; Noad, 2001; Tomascik et al., 1997; Wilson et al., 1999; Wilson and Lokier, 2002; Hook and Wilson, 2003; Wilson, 2005; Saller et al., 2010). Recent

studies have shown that large-scale sustained palaeoaquifer flow has significantly impacted the diagenesis of carbonate systems from around Borneo (Warrlich et al., 2010; Madden and Wilson, 2012) as well as other shelfal carbonates that developed in the humid tropics (Hendry et al., 1999). This is the first study aiming to: (1) assess trends in deposition, diagenesis and reservoir quality of carbonates developed across a broad >100 km wide equatorial siliciclastic-dominated shelf and (2) evaluate controlling influences on carbonate system development, including the impacts of climatic setting and basin margin history.

Geological Setting

The marine shelf offshore Northwest Borneo borders the S. China Sea: a basin formed by oceanic spreading during the middle Oligocene to the Early Miocene (Figure 2; Taylor and Hayes, 1983; Briais et al., 1993; Barckhausen and Roeser, 2004). The NW Borneo margin has a complex Cenozoic tectonic history (Hall, 2002a; Hutchison, 2005). The area includes thinned continental crust and/or microcontinental blocks originating from Indochina and South China that during the Paleogene were situated on the north side of oceanic crust of the proto-South China Sea (Hall, 1996; Hall and Nichols, 2002). Sea floor spreading in the S China Sea resulted in a number of these microcontinental blocks, including the Dangerous Grounds and Reed Bank, drifting south during the Oligocene and colliding with the NW Borneo margin (Holloway, 1982). Concurrent with the southward drift of microcontinental blocks the proto S China Sea was being consumed by subduction beneath Borneo (Figure 2; Hall, 1996). Subduction ceased during the Early Miocene due to jamming by the Dangerous Grounds attenuated crust (Hall, 1996; Hutchison et al., 2000; Morley et al., 2003). Formation of the Rajang accretionary complex associated with subduction together with earlier uplift and deformation and weathering under the humid tropical climate resulted in

significant supply of clastics to the NW Borneo Shelf (Figure 2; Hinz and Schlüter, 1985; Hall and Nichols, 2002; Hutchison, 2005). Uplift and deformation of Borneo continued until at least the latest Tertiary and there is still significant shedding of terrestrial derived material into the seas off NW Borneo (Morley et al., 2003; Hall and Nichols, 2002). This study focuses on Neogene carbonates within the Sarawak Basin that is located inboard of the Luconia Block and adjacent to the coast of Borneo (Figure 2). The Sarawak Basin may include thicknesses up to, or in excess of 8–12 km of Tertiary sedimentary fill, most of which is siliciclastics (Hamilton, 1974; 1979; Madon, 1999b; Hall and Nichols, 2002).

The area of this study is on the continental shelf of Sarawak between the present day Baram and Balingian Delta in the northeastern part of the Balingian Province (Figures 1, 2 and 3; or the East Balingian Subprovince: Madon, 1999a; Madon and Abolins, 1999). The East Balingian Subprovince consists of a series of NE-SW trending horst blocks and grabens that underlie the Neogene shelf deposits and were affected by transpression in the late Neogene (Figure 3; Hazebroek et al., 1994; Madon, 1999b; Hutchison, 2005). Some early Tertiary carbonate development is inferred to have taken place in wedge-top basinal settings (Figure 4; e.g. Melinau and Batu Gading Limestones, Wannier, 2009). This study focuses on subsequent Miocene shelfal carbonates that developed over the deeper NW-SE trending structural Serunai High (Figure 3; Agostinelli et al., 1990). The Serunai High lies directly to the NW of the younger Anau Nyalau Thrust Fault that borders the present day coast (Figure 3; Madon, 1999a). The area of study is bounded to the NW by the Cochrane Graben and extends as far NE as the West Baram Line: a major fault zone that may mark a change in the nature of the underlying crust and across which there are significant changes in geothermal gradients and patterns of Tertiary sedimentation (Hutchison, 2005). The area of palaeoshelf studied extends 80 km in a NW direction perpendicular to the modern coast

across the shelf, 20 km in a south-easterly direction onshore and ~100 km in a SW-NE direction (Figures 1 and 4). The position of the shelf margin may have varied during the Cenozoic (Agostinelli et al., 1990; Madon, 1999a), and the schematic shelf-margin location illustrated on figure 4 best reflects that for Miocene deposits.

Methods

Study of part of a ~12,000 km^2 2-D seismic survey together with subsurface well reports, wireline data and cuttings from 10 wells penetrating carbonates allowed evaluation of sequence development, platform geometries and age dating from a range of inner shelf to shelf margin carbonate systems across the Sarawak Shelf (Figures 4 and 5). One hundred thin sections of Miocene carbonates from six of these wells and/or outcrops from the North Borneo Shelf and onshore Sarawak together with 30 of the corresponding subsurface limestone samples were available for petrographic and further geochemical analyses. This manuscript focuses just on the offshore subsurface carbonates with further research being undertaken on the carbonates that crop out onshore Sarawak (Figure 4). Lithological, diagenetic and pore system evaluation of samples was undertaken via transmitted light microscopy, cathodoluminescent study of polished thin sections (CL: 14 samples), scanning electron microscopy (SEM: 10 samples), and stable isotope analyses ($\delta^{18}O$ and $\delta^{13}C$: 50 samples). Age dating of samples was via foraminiferal biostratigraphy and strontium isotope analysis (41 samples), with the results of the dating briefly summarised here (Figures 4 and 5; Lunt, pers. obs., 2007; Allan, pers. comm., 2007; following van der Vlerk and Umbgrove, 1927; Blow, 1969; 1979; Adams, 1970; McArthur et al., 2001; Lunt and Allan, 2004; McArthur and Howarth, 2004).

Lithological components, microfacies, diagenetic phases, the relative timing of diagenetic events and pore systems were evaluated through thin-section petrography. All samples were impregnated with blue epoxy resin to aid pore system characterisation. Half of each thin section was stained with Alizarin Red S and potassium ferricyanide to allow identification of dolomite, ferroan and non-ferroan calcite (Dickson, 1965). The relative abundance of components and diagenetic phases were recorded semi-quantitatively (visual estimates; after Mazzullo and Graham, 1988). Facies nomenclature follows the textural classification scheme of Dunham (1962), modified by Embry and Klovan (1971), with components given in lithology names where they exceed 10–15%. Nomenclature on carbonate cement geometries follows Flügel (2004). Cold cathodoluminescent (CL) microscopy study of polished sections was via an ELM-3R luminoscope (after Witkowski et al., 2000). Samples for CL analysis were selected to investigate the range of coarse (>250 μm) cement phases present.

Stable-isotope analysis ($\delta^{18}O$ and $\delta^{13}C$) was undertaken on 50 samples micro-drilled from the rock off-cut counterpart of the thin sections. Drilling sites matched directly to the off-cuts, correspond to a range of depositional and diagenetic features identified in thin section. Drilled samples include bioclasts, matrix and cements with varied morphologies including those filling fractures. Oxygen and carbon isotope analyses were run on a GasBench II system coupled online to a stable-isotope-ratio mass spectrometer in continuous flow (Skrzypek and Paul, 2006), with all data normalised to NBS-19 (standard) and reported relative to V-PDB. External errors for $\delta^{18}O$ and $\delta^{13}C$ were ±0.1‰.

Carbonate development across the North Borneo Shelf: distribution and age dating

Early Miocene (Aquitanian) carbonate development was extensive across the Serunai Horst Block to the southwest of the West Baram Line. Thin sections of fullbore core and/or rotary sidewall cores of these Lower Miocene carbonates were available from 3 offshore wells (Wells C, D and W; Figure 4). Cuttings and core were available from a further three wells for which thin sections were not available. The presence of *Miogypsina* and *Eulepidina* in carbonates from wells D and W are indicative of an Aquitanian age (Te5; East Indian larger benthic foraminifera Letter Classification; Figure 4). Strontium isotopic dating was carried out within well W to confirm the upper age limit of the carbonate (between 20 and 20.5 Ma; Figures 4 and 5) since the environmentally sensitive marker *Eulepidina* was so rare. Carbonate systems from the three wells studied in detail are all examples of inner- to mid-shelf carbonates located >30, and >15 km from the shelf margin, respectively, as inferred from seismic (Figures 4 and 5). Thicknesses of the inner shelf carbonates vary but are typically ~100 m in the wells.

Carbonate deposits of Early and Middle Miocene age younger than 20 Ma (Burdigalian and younger) are much more areally restricted than the Aquitanian carbonate succession (Figures 4, 5 and 6) and are localised to shelf margin areas bordering the West Baram Line and the SW part of the Serunai High. Thin carbonate stringers developed within the clastic shelf succession in an outer shelf location to the SW of the Serunai High were studied in detail in one well and have been dated at 12–13 Ma (Well A; Figure 4). In well A the side wall core samples below the main limestone unit contain common *Miogypsina* indicative of Lower Tf (Figure 4). However, cuttings from the overlying limestone include much less diverse foraminifera faunas and lack *Miogypsina*, so the Sr dating of 12.6 and 13.4 Ma (i.e.

within the Serravallian) at this transition is important data to fix the Lower to Upper Tf Letter Stage boundary to other time scales.

A thicker stacked carbonate succession over 1400 m developed at the NE margin of the Serunai High adjacent to the West Baram Line. These shelf margin carbonates in the West Baram Hinge area have backstepped from the more areally extensive Aquitanian carbonate succession and during their development successively reduce, then increase and reduce again in areal extent (Figures 4, 5 and 6). The upper part of these shelf margin carbonates were studied in two well in the West Baram Line area with the ages of studied samples ranging from 13 to 7 Ma (Wells G and Z; Figures 4 and 5). In the lower cores from well G the diverse foraminifera faunas lack *Eulepidina* and are post-Te in age (agreeing with Sr dating). The *Miogypsina* species based on grade of evolution (Lunt and Allan, 2004) are *M. tani-globulina,* consistent with an age in basal Tf (i.e. Burdigalian). The highest core (3836–3845 m) however contains *Lepidosemicyclina*, which evolved from the *Miogypsina* lineage in later Early Miocene times (with Sr dates of 15.3 to 15.7 Ma in the same core also indicating late Burdigalian to Langhian ages). The distinct species *Nephrolepidina ferreroi* is also frequent and restricted to this highest core, and is a later Lower Tf index fossil. The samples in well Z have a fauna similar to the cuttings in well A, devoid of the diverse Tf foraminifera, and strontium isotopes suggest an age slightly younger than well A that is right on the Lower to Upper Tf boundary (i.e. Tortonian).

The characteristic of the Aquitanian inner shelf carbonates versus the Burdigalian and younger outer shelf to shelf margin carbonates are described below under the headings of: (a) inner shelf and (b) outer shelf and shelf margin carbonate systems. However, it is

recognised that some of the variation within the carbonate systems may relate to different ages of the deposits and their sequence development in addition to their broad depositional setting. Wells within 5–10 km of the margin are considered to be in outer shelf or shelf margin locations.

Inner-shelf carbonate systems

Regional distribution and carbonate platform development – Inner-shelf carbonate systems of earliest Miocene (Aquitanian) age consist of an extensive sheet-like carbonate package interstratified with siliciclastics up a few tens of metres thick over much of the Serunai Horst block with localised mounded carbonate development (Wells C, D, E, F and W; Figures 4 and 5). Well penetrations and carbonate samples are from the mounded carbonate features that are typically up to ~100 m thick, but may be as much as ~200 m thick. Mounded features with low relief (perhaps up to a few tens of metres) are present as both more extensive ramp-type carbonate development and localised platforms around 2–10 km across. Gamma-rays logs and samples indicate both some interstratification and admixing of siliciclastics within the mounded predominantly carbonate features. The top of the sheet-like carbonate package and its associated mounded features are characterised by high to moderate amplitude, laterally continuous seismic reflectors (Figure 7). Internally the sheet-like to mounded carbonates commonly have good lateral continuity of moderate amplitude reflectors (Figure 7). However, more chaotic reflectors are also seen in the mounded features, most commonly in southerly deposits (Figures 7 and 8). Particularly towards the SW on the Serunai High, seismic facies within, or towards the margins of, the carbonate package consist of several shingled wedges with very low-angle progradational reflectors and overlapping lenses.

Depositional features of the inner-shelf mounded carbonates – Samples from inner-shelf carbonate mounds consist of mollusc and coral or larger benthic foraminifera packstones (Well D; Figures 4 and 9a–g). Molluscs comprise between 10 and 30% of each sample together with corals (up to 20%), and larger benthic foraminifera (up to 20% including *Miogypsina* and Lepidocyclinids; Figure 9d–f). Admixed siliciclastic content of silt to medium sand-size may be up to 15% of each sample and commonly includes angular quartz grains (Figure 9a, c and e). Up to 3% disseminated carbon or other organics are present in individual samples. Micritic matrix content with some admixed clays and other fine siliciclastics is generally up to 40–50% (Figure 9g). Other components, present mainly in amounts of <5%, include *Halimeda,* coralline algae, echinoderm debris and imperforate foraminifera with the later including miliolids and *Austrotrillina* (Figure 9b–f). Most bioclasts show little evidence for abrasion, but may be fragmented, and are commonly recrystallised (Figure 9a–g; see diagenesis section).

Inner- to mid-shelf mounds tend to be less mollusc-rich (<5% of each sample) than those sited inboard (Well W: Figure 4). Corals (up to 15%) and larger benthic foraminifera (up to 20% including *Miogypsina* and Lepidocyclinids) are common in many samples (Figure 9a and g). Packstone, wackestone and floatstone textures predominate (more than 80% of samples) and micritic matrix, commonly with an admixed clayey and/or silty siliciclastic fraction may be up to 65% of each sample (Figure 9g). Other subsidiary components are similar to the inboard mounds, with the addition of up to 1–2% planktonic foraminifera. Less than 20% of inner to mid-shelf mound samples are grainstones and grain/packstones, and these are mostly located towards the centre of the mounded carbonate systems (Well W; Figure 9h and i). Coralline algae together with larger benthic foraminifera are the most

common components in the grainstones and pack/grainstones, with each comprising up to 20–30% of individual sample. Other components in the grain/packstones are comparable with those in samples having mainly matrix-supported textures. Abrasion and fragmentation of bioclasts is generally low in the packstones, wackestones and floatstones, but more significant in the grainstones.

Diagenesis and pore systems of the inner-shelf mounded carbonates – Initial diagenetic features from inner- to mid-shelf carbonate mounds are micritisation of bioclasts with micritic rims up to 50 µm, followed by minor mechanical compaction (Figure 9a–f). These two initial features may be followed by dissolution of aragonitic bioclasts (~40% of samples), further mechanical compaction and some limited bladed to blocky cement development in secondary biomolds (~20% of samples and crystal sizes between 200 and 400 µm; Well D: Figure 9d–f). Subsequent neomorphic granular mosaic cement replacement of matrix is pervasive with cements retaining micritic inclusions of the original matrix (Figure 9a, c and e–g). The granular mosaic cements all show uniform dull- to slightly bright-luminescence in CL, whereas bioclasts and matrix show either brighter or duller luminescence (Figure 10). Dissolution and cement precipitation is most common in inner- as opposed to mid-shelf deposits (Figure 11). Early isopachous cements forming <100 µm fringes around bioclasts are only present as a very minor feature in grainstones from inner- to mid-shelf carbonates (<5% of samples). Syntaxial overgrowth cements around echinoderm debris are most common in the grainstone units, and present to a lesser extent in packstones. If earlier dissolution of aragonitic bioclasts has not occurred, further pervasive neomorphism near contemporaneous with that of the matrix results in originally aragonitic bioclasts replaced by granular mosaic cements including ‘ghost fabrics’ of the original allochem (Figure 9a, c, f

and g). Additional granular to equant or poikilotopic cement infill is seen in 70% of samples, most commonly in those affected by earlier dissolution of bioclasts (Figure 9e and f). Crystal sizes of these later cements range mostly from 200 to 600 µm with the larger poikilotopic cements of up to 4 mm just present in the inner-shelf carbonates. The late equant cements infilling fractures are brightly luminescent under CL (Figure 10). Stable isotopic values for marine bioclasts, matrix (commonly neomorphosed), neomorphic granular mosaic to equant cements are almost all within the range –4.5 to –7.9‰ δ^{18}O V-PDB and –0.6 to +1.6‰ δ^{13}C V-PDB (Figure 12). Exceptions are two equant fracture filling cements with values of –9.6 and –10.1‰ δ^{18}O V-PDB and –1.8 and –7.4‰ δ^{13}C V-PDB, respectively (Figure 12). Chemical compaction features post-date cementation with anastomosing dissolution seams and 'jagged' stylolites developed in more siliciclastic-rich, and less siliciclastic-rich samples, respectively (Figure 9h). Just in inner- to mid-shelf carbonates chemical compaction is followed by microdolomite rhomb formation in 25% of samples (<50 µm), minor leaching and precipitation of saddle dolomite in <10% of samples (200–600 µm; Well W; Figure 9a, g, h and i). Dolomite is non-luminescent under CL (Figure 10).

Porosity in inner-shelf samples and 85% of inner- to mid-shelf samples with matrix-supported depositional textures is generally <4% and commonly <1–2%. Pores types include intercrystalline (including within cement-lined biomolds), intragranular and vuggy, some associated with secondary dissolution (Figure 9d, h and i). Most pores are <400 µm across. Permeability appears low with few interconnecting pores. Biomoldic porosity is also present in <10% of inner to mid-shelf samples associated with leaching near saddle dolomites (Figure 9i). Coarse-grained grainstones from the cores of the inner to mid-shelf mounds may have porosity up to 5–8% with pores sizes up to a few mm, although not all pores appear interlinked (Well W; Figure 9h and i).

Outer-shelf and shelf-margin carbonate systems

Regional distribution and carbonate platform development – Outer-shelf to shelf-margin carbonates developed best on the NE part of the Serunai High in the region of the West Baram Line hinge zone where they form a stacked carbonate succession over 1400 m thick (Wells G and Z; Figures 4, 5 and 6). Low relief carbonate stringers are also locally present within the predominantly clastic post-Lower Miocene succession at the NW margin of the Serunai High where it borders the Cochrane Graben (Well A; Figure 4). Both the stacked shelf margin carbonates and the localised stringers along the NW and NE margins of the Serunai High have well penetrations with carbonates <20 Ma available for study (i.e. Burdigalian and younger). Earlier shelf margin carbonates were imaged on seismic in the West Baram Line hinge zone vicinity, but were not penetrated by wells. Through correlation of reflectors across the seismic lines the early shelf margin carbonates are linked to the Aquitanian inner shelf carbonate successions described above (Figures 4 and 5). Locally the upper part of the Aquitanian extensive carbonate succession has chaotic seismic character and potential 'sinkhole' features (Figure 8). From the seismic data there is also the possibility of some Aquitanian, or perhaps Oligocene, shelf margin carbonate development pre-dating the laterally extensive carbonates packages that includes the inner shelf carbonate systems.

The stacked carbonates in the area of the West Baram Line Hinge Zone comprise a predominantly aggradational to backstepping or locally 'out-building' succession on seismic (Figures 4, 5 and 6). Early carbonate development thickens considerably from the apparently age equivalent Aquitanian inner shelf deposits to over ~300 m in the Hinge Zone area. Where the carbonates thicken, internal lateral reflector continuity decreases and the

seismic facies appear more massive. Poorly-imaged, shingled, wedge-like carbonate platforms extend north of the West Baram Line Fault. After inner-shelf carbonate development the system backsteps to the region of Hinge Zone with continued further aggradation, some localised 'buildout' and backstepping of a further 5 to 6 carbonate sequences during much of the Miocene (Figures 4, 5, 6 and 13). In general the shelf margin carbonates have steeper, seismically better-defined margins than the inner shelf systems, and commonly show 'shingled' development (as described directly above). In a number of sequences the SW carbonate margin is very steep, appears reef-rimmed with evidence for margin collapse, whereas clinoforms are better developed along the eastern margin (Figure 13). On the Hinge Zone high the carbonates commonly appear massive or have weak to chaotic internal reflectors, with rare complex coalescence of platforms. Within individual sequences that have seismically imaged features of inferred karstic origin on platform tops there is some downstepping of carbonates into the bathymetric low of the West Baram depocentre. Some sequences appear highly faulted and have thickness and seismic facies changes across faults (Figure 14), as well as 'intrastratal slides with thrust-like geometries'. A package of siliciclastic strata downlaps the carbonate system post 19 Ma, before the resumption of shelf margin carbonates (Figures 4, 5 and 6). Subsequent shelf margin carbonate systems 'build-out' over, and interdigitate with, adjacent siliciclastics until ~12.5 Ma (Figures 6 and 15). After ~12.5 Ma there is renewed carbonate backstepping (Figures 5, 6 and 14). Associated with the phase of 'build-out', and during the transition to backstepping geometries, carbonate platforms are areally extensive with low relief and include additional platforms or 'stringers' within the predominantly clastic shelf succession in both shelf margin positions and inboard from the margin (Figures 4, 5, 6 and 15). The last

phases of carbonate development are areally restricted isolated platforms with mounded profiles (Figures 5, 6 and 14).

Depositional features of the outer-shelf and shelf-margin carbonates – The oldest deposits penetrated by wells in the stacked shelf margin carbonate succession at depths of >4460 to 4570 m date to around 19.0 Ma (from Sr isotopic dating; Well G; Figure 4; i.e. Burdigalian). These deep shelf margin well penetrations are from the backstepping sequence that immediately post-dates the shelf-wide Aquitanian carbonate sequence. These deepest shelf margin samples consist mainly of larger benthic foraminifera bioclastic packstones and pack/grainstones containing up to 25% miogypsinids and lepidocyclinids (Figure 16a–b). Coralline algae fragments and echinoderm material are other common components at up to 15% and 5%, respectively. Above 4567 m grainstone textures become more common (Figure 16b), as do imperforate foraminifera (up to 15%), including miliolids, with molluscs locally forming up to 12% of individual samples. Allochems are commonly fragmented and abraded. Micritic matrix is commonly partially recrystallised and comprises up to 40% in the packstones and <15–20% in the grainstones. The uppermost samples from 4460 to 4463 m sampled individual massive corals with fine grained matrix in chambers and borings (Figure 16c).

Between 4414 and 4460 m just below the intra-carbonate siliciclastic succession that progrades out over the shelf margin, the carbonates are both texturally and compositional varied and date to around 18.7 Ma from Sr isotopes (i.e. Burdigalian; Well G; Figure 4). Lithologies between 4414 and 4460 m include siliciclastic bioclastic packstones, larger benthic foraminifera and coralline algal or coral bioclastic pack/grainstones as well as coral bioclastic wacke/packstones (Figure 16d–i). Siliciclastics including angular to sub-rounded

silt to fine sand-grade quartz and undifferentiated clays are present in all samples between 4414 and 4460 m comprising 3–40%. In individual samples siliciclastics may be disseminated throughout the lithology, or concentrated within burrows or along dissolution seams (Figure 16d and h). Types of carbonate allochems and their abundance vary between samples, but are generally similar to those from the underlying interval (4460–4570 m). An exception is that imperforate foraminifera, predominantly in the form of miliolids and alveolinids, are only locally seen and never in abundances of > 5% (Figure 16e, g and i). Larger perforate foraminifera and coralline algae are locally abundant, collectively up to 70% in coarse grainstones (Figure 16e and f). Planktonic foraminifera make up 1–3% of some individual samples from 4423 to 4414 m (Figure 16i).

The first of the 'build-out' carbonate sequences directly proceeding the phase of siliciclastic progradation over the shelf margin was sampled between 3837 and 3847 m and dates from between 15.7 and 15.3 Ma on the basis of Sr isotopic analysis (Well G; Figure 4). The sampled interval consists predominantly of larger benthic foraminifera bioclastic pack/grainstones and grainstones, some containing corals (Figure 17a–d). Siliciclastics, as clays, comprise <2–3% of individual samples. Perforate larger benthic foraminifera including miogypsinids, lepidocyclinids, heterostegids and amphisteginids are abundant comprising up to 40% of samples (Figure 17a–d). Coralline algae and corals are locally abundant at up to 20% and 30% of individual samples, respectively. Planktonic foraminifera, echinoderm debris and calcareous sponge spicules may all comprise up to 1–3% of individual samples. Partially recrystallised micritic matrix forms up to 20–30% of pack/grainstone samples. Many of the shallow water bioclasts from this interval are fragmented and/or abraded.

Outer shelf deposits sampled from the transition of the 'build-out' to final backstepping and aggradational phases are from a broad carbonate package within the

clastic succession at the SW margin of the Serunai Block adjacent to the Cochrane Graben (Well A; Figures 3 and 4). These southwesterly deposits are dated as 12.6 perhaps up to 15.2 Ma, and from depths of 620–883 m are significantly shallower than all other shelf margin deposits sampled from the West Baram Hinge Zone. Southwesterly carbonate samples consist of silty dolomitised bioclastic or foraminifera packstones, wacke/packstones and packstones between 620–730 m (Figure 18a, c and f). Larger benthic foraminifera (dolomitised) bioclastic packstones and grainstones predominate from 864–883 m (Figure 18b, d and e). Bioclasts within the wacke/packstone include *Amphistigina* (up to 15%), coralline algae (up to 15%) and *Halimeda* (up to 5%), sometimes together with comminuted bioclastic debris in a pervasively dolomitised fine groundmass (Figure 18a and f). Siliciclastics may comprise up to 15% of individual samples and include angular to sub-rounded quartz grains (Figure 18c). Robust, commonly fragmented or abraded amphisteginid and heterosteginid foraminifera (up to 50%) dominate in the grain/packstones together with coralline algae (up to 20%) and echinoderm material (up to 8%).

The youngest aggradational to backstepping terminal shelf margin carbonate sequences in the Baram Hinge Zone were sampled from depths of 3400–3440 m and have been dated as 7.0–11.4 Ma from Sr isotopic analysis (Well Z; Figure 4). All samples from the terminal shelf margin carbonates are coral bioclastic pack/grainstones or grain/rudstones (Figure 17e–i). Branching corals, commonly encrusted by coralline algae and/or foraminifera, and highly fragmented material comprise up to 50% of individual samples (Figure 17e–i). Molluscs and larger benthic foraminifera (including heterosteginids, miogypsinids, lepidocyclinids and amphisteginids) locally may each make up to 30% of individual samples. Other common components are coralline algae (up to 20%) and

echinoderm fragments (up to 8%). Imperforate foraminifera, including alveolinids and miliolids, comprise up to 3% of some samples. Most bioclasts are highly fragmented and commonly abraded. Up to 40% micritic matrix is present between, and within chambers of, bioclasts and is most common in the packstone lithologies (Figure 17f–g).

Diagenesis and pore systems of the outer-shelf and shelf-margin carbonates – Outer-shelf-margin deposits from the West Baram Hinge Zone area have porosity between 2–20% (Wells G and Z at depths of 4570–3837 m and 3400–3440 m, respectively). Pore types include cement-lined intergranular, intragranular, vuggy, biomoldic, fracture and along seams or stylolites (Figures 17, 19 and 20). Pores are on a micron- to millimetre-scale and many appear connected. Best porosity preservation is in grainstone and/or pack/grainstone samples from the upper shelf-margin sequences above 4000 m (Figure 17). Samples from below 4000 m show similarities in biota, lithologies, clastic content and diagenesis to the inner-shelf carbonates, and also in having low (up to 2–4%) porosity development (Figures 9 and 16). Cathodoluminescent characteristics of just the shelf-margin sequences from above 4000 m are illustrated (Figure 21), since those from samples deeper than 4000 m are comparable with the inner-shelf carbonates (Figure 10).

Initial minor to moderate micritisation of bioclasts with micritic rims mostly <40 µm, is followed by syntaxial cements on echinoderm debris and minor isopachous fringing cements (<100 µm; Figures 16c, 17a–c and 22). Syntaxial overgrowth cements are non-luminescent sometimes with a thin (<100 µm) brightly-luminescent rim, whereas bioclasts and matrix generally show dull- to bright-luminescence (Figure 21). Early cements commonly partially infill pore space in samples with grain-supported textures (i.e. ~30% of samples; Figure 17b–c). Dissolution of aragonitic bioclasts is common from samples of the

upper terminal aggradational buildups and the lower backstepping to aggradational buildup (Figures 16, 17, 22 and 23). Leaching is followed by localised mechanical fracturing. Blocky to equant cement precipitation with crystals sizes of 100–500 µm is common in most samples (Figures 16 and 17). Up to 30% neomorphic granular mosaic cements together with blocky and equant cements are also present in the samples with admixed siliciclastic content between 4423 and 4414 m and those from the 'build-out' carbonate sequence sampled between 3837 and 3847 m (Figure 16). These blocky to equant and mosaic cements all show relatively uniform dull- to non-luminescence, with non-luminescence character dominating in equant cement fracture fills (Figure 21). Stable isotopic values for marine bioclasts, matrix and blocky to equant cements are all within the range –2.4 to –5.4‰ δ^{18}O V-PDB and –1.1 to +0.6‰ δ^{13}C V-PDB (Figure 10). Poikilotopic cements are a minor cement phase (<5% of individual samples), from just the lower siliciclastic admixed samples (Figures 16 and 20). Chemical compaction features post-date cementation with anastomosing dissolution seams and 'jagged' stylolites developed in more siliciclastic-rich, and less siliciclastic-rich samples, respectively (Figures 16a, 16h and 21). Fracturing both pre- and post-dates equant cement precipitation. Minor microdolomite (<50 µm) precipitation is mostly along dissolution seams. Microdolomites developed along seams or stylolites may show zoned bright- and non-luminescence (Figure 21). Some dissolution enhancement of pore spaces by late leaching, precipitation of clear dolomite and equant calcite cements are the final diagenetic phases affecting ~70% of shelf margin samples (Figures 16, 17, 20 and 21). Clear dolomite crystals are up to 200 µm have rhombic shapes, or partially curved 'saddle dolomite' geometries and comprise up to 5% of individual samples partially infilling pore space. Dolomite cements are mostly brightly luminescent

under CL. Stable isotopic values for clear dolomite cements all range from –5.2 to –7.4‰ δ^{18}O V-PDB and +0.5 to +1.5‰ δ^{13}C V-PDB (Figure 12).

The outer shelf deposits from the SW margin of the Serunai High have significant porosity (5–35%) present as intergranular, intragranular and biomoldic pores, as well as microporosity between crystals in dolomitised units (Well A; Figure 18). Many pores appear well-connected and highest porosity (10–35%) is present in grainstone lithologies. Minor micritisation of bioclasts affects some samples. Dissolution of aragonitic bioclasts and precipitation of granular mosaic cement with a meniscate habit is present in 20% of samples (Figures 18e and 24). Isopachous fringing cements up to 200 µm, post-date meniscate cements and are most common in grainstones, or within areas of shelter porosity in finer-grained units (Figure 18d). Syntaxial overgrowth cements are locally present on echinoderm debris. Mechanical compaction and grain suturing, post date cementation but are minor feature with the later mainly seen in deeper subsurface samples (to depths of 883 m; Figure 24). The matrix of wacke/packstone samples is pervasively replaced by microdolomite rhombs (<50 µm) with a dusty appearance (Figure 18a, c and f). Some further bioclast leaching followed by minor precipitation of clear dolomite rhombs (<100 µm) are the final diagenetic processes affecting samples with microdolomite (Figures 18c, 13d, 13e and 19).

Interpretation and discussion

Onshore to offshore trends in carbonate development and controlling influences

The abundance of light-dependent, stenohaline biota such as corals and larger benthic foraminifera in all the shelf carbonate deposits studied is indicative of their formation under normal marine conditions within the photic zone. The common occurrence of siliciclastics in the inner shelf carbonates reflects carbonate accumulation and *in situ*

admixing with siliciclastics derived from the nearby landmass and/or reworked on the predominantly siliciclastic shelf (Figure 25). The presence of disseminated carbon and other organic matter is also likely to relate to terrestrial runoff. The mounded carbonate development seen on seismic together with well-preserved abundant coral, mollusc and larger benthic foraminifera likely reflect localised shallow water patch reef development (2–10 km across). In inner- to mid-shelf areas these patch reefs had low relief, on the order of metres to perhaps a few tens of metres, sloping gently down into the more extensive shelf deposits. Although corals are common, reefal framework deposits are not present in the samples. Fine siliciclastic input, resulting in turbid inner shelf conditions in which the photic zone is condensed into the upper few metres to tens of metres of the water column are factors that may contribute to a paucity of framework reefal development and promote low relief, gently sloping carbonate systems (Tomascik et al., 1997; Wilson and Lokier, 2002; Wilson, 2005; 2012). The predominance of wacke-, pack- and floatstone textures in the inner- to mid-shelf carbonates is indicative of low energy conditions. Low energies are consistent with the dissipation of wave and current energy across the broad NW Borneo Shelf, that lies outside the typhoon belt (as is the case at the present day: Wang and Li, 2009). The addition of some pack/grainstone textures together with fragmentation and abrasion of components in the core of some inner- to mid-shelf mounded carbonates indicates that on moving seawards more moderate energy conditions developed locally. Low abundances of planktonic foraminifera in the shallow water inner- to mid-shelf mounds indicate open circulation of marine waters. The good lateral continuity of internal seismic reflectors and their moderate to high amplitudes throughout much of the Aquitanian broad inner shelf carbonate package are interpreted to reflect: (1) interbedding of carbonates and siliciclastics and/or admixed silty content (also inferred from wireline gamma response), (2)

paucity of faulting, and (3) 'less intense diagenesis' and/or less secondary porosity development in comparison with the contemporaneous shelf-margin deposits. Some general decrease in lateral seismic reflector continuity associated with thickening of the Aquitanian carbonates is consistent with the higher carbonate content and higher porosity seen samples from the core of the inner- to mid-shelf mounded carbonates.

The extensive carbonate development over much of the Serunai Horst Block during the Aquitanian is probably in part a response to transgressive to perhaps highstand carbonate expansion during the 'equable' greenhouse conditions of the Early Miocene (Zachos et al., 2001) and relative shoreward movement of siliciclastic systems (cf. Wilson, 2005). However, enhanced aragonite saturation state of marine waters for the region, linked to regional relative low climatic seasonality and low atmospheric CO_2 levels during the Aquitanian may have also been influential (Wilson, 2008; 2012). The mounded carbonate development, some with flat tops, during the Aquitanian with thicknesses of up to 200 m (and locally significantly more in shelf margin areas) indicates carbonates locally building to sea level but not filling the shelfal accommodation space, and the additional role of differential tectonic subsidence across the region. The Baram depocentre remained underfilled during the Early Miocene as indicated by shelf margin carbonates that developed on the West Baram Hinge prograding and downstepping into this depocentre. The margins of the outer-shelf carbonates are generally seismically better defined and steeper than the inner and mid shelf mounds. The occurrence of thicker carbonates with more massive appearance on seismic and steeper platform margins on the West Baram High than compared with inner-shelf areas is interpreted to reflect cleaner carbonate development with probable reefal development in shelf-margin positions. The presence of potential 'sinkhole' features and chaotic seismic appearance of the top of the pre-20 Ma extensive

carbonate package is suggestive of exposure prior to carbonate systems backstepping to shelf-margin areas (Figures 7 and 8).

Backstepping of the carbonate sequence to the shelf margin area within the Early Miocene may reflect eustatic sea level rise and/or outbuilding of clastic systems across the North Borneo Shelf. Notwithstanding this, the aggradational development of >1400 m of Miocene carbonates in the shelf margin area indicate significant local tectonic subsidence. At times active faulting affected carbonate facies variability and potentially margin collapse (Figure 14). The steepness of some of the SW facing margins in shelf margin areas suggests these may have been windward margins of rimmed carbonate platforms; an interpretation supported by more extensive clinoform development on eastern sides (Figure 13). This windward to leeward orientation is similar to that inferred for the Luconia Platforms during the Miocene and to inferences of monsoonal development from global climate models (Vahrenkamp *et al*., 2004). The coralline algal and larger benthic foraminifera pack/grainstone that are the deepest subsurface shelf margin deposits sampled indicate moderate to higher energy deposits for the middle of the backstepping to aggradational sequence. Moderately robust foraminifera together with the faunal assemblage are suggestive of moderate photic depth deposits and consistent with a transgressive carbonate sequence (cf. Vahrenkamp et al., 2004). The appearance of imperforate foraminifera and increasing abundance of molluscs passing upwards through the aggradational carbonate succession is indicative of shallowing conditions, with some coral development around 4460 m. The increase in grainstone textures together with fragmentation and abrasion of allochems reveal that depositional energies increased concomitant with the upward shallowing. The appearance of between 3–40% siliciclastic content in samples between 4414 and 4460 m records the encroachment and admixing of siliciclastics before they

prograde over the shelf margin carbonate succession. Depositional energies varied prior to siliciclastic covering of the carbonates as inferred from wacke/packstones and grainstone textures. Planktonic foraminifera in the uppermost samples from the sequence indicate open oceanic conditions. Also, most of the deposits just prior to siliciclastic covering are moderate to shallow photic depth, but probably not very shallow (<~5 m), deposits as inferred from the biotic assemblage and the moderately robust forms of larger benthic foraminifera (diameter to thickness ratio of 2–3). An abundance of coralline algae in grainstones is consistent with moderate to high energy shelf margin conditions, perhaps with some upwelling along the margins, or with some nutrient influx associated with the encroaching siliciclastics (cf. Erlich et al., 1990; 1993). The shallowing trend in the upper part of the aggradational carbonate succession and the progradation of siliciclastics occur at a time of eustatic sea level fall towards the end of the Early Miocene and probably at least partially reflect sea level lowering (Figure 4). However, the end of the Early Miocene was a time of tectonic uplift, unroofing and increased siliciclastic derivation from Borneo with considerable deltaic progradation and siliciclastic infill of adjacent marine basins (Hall and Nichols, 2002). The encroachment of clastics to the shelf margin may have resulted in environmental deterioration for carbonate development, perhaps in the form of nutrient loading and/or increased turbidity and there is no evidence for exposure just prior to covering by the siliciclastics.

The ‘build-out’ carbonate sequences that overlies and interdigitates with siliciclastics mostly correspond to periods of eustatic sea level highs (Figure 4). Conversely, phases of renewed siliciclastic progradation over the margin roughly, although not precisely, correspond to three periods of eustatic lows during the Middle Miocene (Figure 4). Mat–Zin and Tucker (1999) noted that on a larger-scale than covered in this work the pre-Pliocene

Sarawak Shelf sequences do not correspond to eustatic sea-level variations, and suggested that tectonisn was important in generating sequence boundaries. Fine siliciclastic content within the build-out carbonates attest to admixing of siliciclastics within the shelf margin deposits. The presence of planktonic foraminifera, local abundance of corals, coralline algae as well as sponge spicules indicate open oceanic circulation in shallow to moderate photic depths perhaps with some nutrient influence. The morphologies and types of foraminifera are consistent with shallow to moderate photic depth conditions. Pack/grainstone to grainstone textures are indicative of moderate to higher energies. Some of the youngest carbonate platforms within the clastic succession do not stack directly on top of underlying ones. Locally, siliciclastic strata or flanking deposits from neighbouring platforms filled accommodation space between neighbouring platforms, smoothed subtle bathymetric variability and collectively acted as antecedent topography for the development of younger platforms. The flat topped development of carbonates platforms, their complex stacking patterns and interrelationship with clastics within this interval are all consistent with carbonates building to sealevel, building-out and vying with siliciclastics during a phase of limited accommodation space compared with sediment generation and/or infilling.

Outer shelf deposits sampled from the SW margin of the Serunai Block that date from 12.6 to 15.2 Ma lack coral material and on the basis of seismic geometries have sheet-like geometries. Deposition within the photic zone from a range of energies is inferred on the basis of common well preserved larger benthic foraminifera and varied wacke/pack and grainstone textures. Siliciclastic content indicates admixing and the carbonate package interdigitates with shelfal clastics along its borders. These sheet-like carbonates correlate on seismic to the transition of the ‘build-out’ to final backstepping and aggradational phase of carbonate sequence development on the West Baram High. The lack of evidence for

framework builders, sheet-like geometries and range of energies inferred for the SW Serunai carbonate package and their correlation to a package that transitions from 'build-out' to backstepping carbonates are all consistent with a transgressive sequence and this unit did form at a time of eustatic sea level rise (Figure 4; Haq *et al*., 1987). The high energy grainstones deepest in the SW Serunai package may reflect initial transgressive scouring and the wacke/packstone that precede them are moderate to deeper photic depth deposits that formed under lower energy.

Coral-rich bioclastic pack/grainstone and grain/rudstones from the youngest backstepping to aggradational terminal shelf margin carbonate sequences are interpreted as reefal or near-reefal shelf margin deposits. The high degree of bioclast fragmentation, together with pack/grainstone and grain/rudstone textures indicates high energy depositional conditions. The abundance of molluscs together with corals and the presence of imperforate foraminifera are indicative of shallow water depositional conditions. The terminal phase of backstepping to aggradational shelf margin carbonate formed initially during a period of eustatic sea level rise (as documented directly above for the SW Serunai carbonate package), followed by a highstand, then a lowstand and then a further eustatic sea level rise (Figure 4; Haq et al., 1987). The shallow photic deposits sampled date back to 11.4 Ma: the time of the 3rd order eustatic lowstand and the subsequent rise in sea level. Apparent terminations of seismic reflectors at the outer margins of the mounded terminal carbonate buildups are suggestive of gradual drowning. For this sequence, as with the underlying ones, there is some, but not precise, concordance with eustatic sea level change (Figure 4). Carbonate sequence development was also influenced by clastic progradation and tectonics; the later linked to differential subsidence and/or tectonic tilting, strike-slip

deformation and formation of flower structures in the West Baram Hinge Zone area (Figure 14).

Onshore to offshore trends in carbonate diagenesis and controlling influences

Grain micritisation is the first diagenetic process affecting most samples and is linked to boring and alteration of allochem surfaces by microbes during marine diagenesis (Bathurst, 1966; Gunther, 1990). The more common occurrence of micritisation and thicker micrite rims to bioclasts in inner-shelf carbonates and/or those with admixed siliciclastic content is consistent with increased microbial activity in low energy warm waters and/or local environments with some nutrient influx (Gunther 1990; Perry 1999). The development of isopachous fringing cements predominantly in outer shelf deposits, and to a lesser extent in mid-shelf grainstones, reflects early cement precipitation in moderate to higher energy settings in which marine waters were flushed through grain-supported fabrics. Precipitation of syntaxial overgrowth cements reflects the distribution of echinoderm debris and is also most common in the porous grain-supported fabrics. The predominantly non-luminescent CL character of the syntaxial overgrowths is suggestive of marine pore fluids and/or oxidising conditions, although they may also form under shallow burial conditions (Flügel, 2004). The early dissolution of aragonitic bioclasts from shallow photic deposits in: (1) inner-shelf mounds and (2) outer-shelf platforms from the upper terminal buildups and (3) mid to upper part of the lower backstepping to aggradational sequence is most likely linked to subaerial exposure. Support for subaerial exposure-related leaching comes from: (a) dissolution occurring prior to full lithification, (2) partial infill of biomolds by bladed or blocky cements of probably marine or meteoric origin (see below) and (3) leaching only affecting very shallow water deposits. Early leaching is seen in deposits that formed around

the time of eustatic sea level lowstands, although eustasy, tectonic uplift and allogenic buildup of the sediments to sea level may all have been involved in exposure. Mechanical fracturing and grain breakage are interpreted to be due to compaction of the largely unlithified deposits as they underwent progressive burial.

Neomorphism of micrite and aragonitic bioclasts to calcite began under shallow burial conditions since this feature post-dates mechanical compaction. Neomorphism and associated calcitisation into pore spaces is a pervasive feature of inner-shelf carbonates and just those associated with interdigitation and/or admixing of siliciclastics in mid- to outer-shelf settings (Figure 25). Pervasive neomorphism of other shelf carbonates that developed adjacent to humid equatorial landmasses has been linked to terrestrial-derived aquifer flow (Hendry et al., 1999; Wilson, 2012; Madden and Wilson, 2012). Delta^{18}O V-PDB values of –4.5 to –7.9‰ for marine bioclasts, matrix (commonly neomorphosed) and neomorphic granular mosaic to equant cements plot more negatively than many other Miocene marine bioclasts from SE Asia (δ^{18}O V-PDB values of –4.2‰ to –1.5‰; Ali, 1995; Wilson and Evans, 2002). The more negative δ^{18}O values of the inner shelf components than the global norm may be a reflection of lower salinities, or an apparently slightly brackish signature, due to significant terrestrial runoff into the seas around SE Asia (Tomascik et al., 1997; Wilson, 2008; Madden and Wilson, 2012; 2013). The Anderson and Arthur (1983) equation (Equation 1) provides a means to derive Miocene δ^{18}O seawater values for the region, and also the possibility of evaluating the potential origins of fluids involved in cement precipitation:

$$T=16 - 4.14(\delta^{18}O_{CALCITE} - \delta^{18}O_{SEAWATER}) + 0.13(\delta^{18}O_{CALCITE} - \delta^{18}O_{SEAWATER})^2 \quad (1)$$

A Miocene $\delta^{18}O$ seawater value for the region of –2‰ to 0‰ V-SMOW has been derived using this equation and the observed range of calcitic bioclast values ($\delta^{18}O$ values of –4.2‰ to –1.5‰; Ali, 1995; Wilson and Evans, 2002) for SE Asian Oligocene–Miocene seawater and an assumed ocean surface temperature of 25 °C (Neogene of coastal Borneo; Ali, 1995). A $\delta^{18}O$ value of –8‰ to –4‰ V-SMOW is suggested for possible meteoric parent fluids on the basis of $\delta^{18}O$ values of meteoric precipitation in SE Asia of –6‰ to –4‰ at low elevations (Bowen and Wilkinson, 2002) and up to –8‰ for the whole of Borneo (Anderson and Arthur, 1983). Using a temperature gradient of 30 °C/km for one of the wells from this study (Hall, 2002b) together with the onset depth of stylolite and dissolution seam formation of 500–1000 m (Nicolaides and Wallace, 1997) the temperatures of pre-stylolite and stylolite-associated features are inferred to be 25–40°C and >40–55 °C, respectively. The neomorphic granular mosaic cements are shallow-burial features that pre-date stylolite formation (i.e. formed at 25–40°C) and inputting the data outlined directly above into the Arthur and Anderson equation (1983) calculated values of $\delta^{18}O$ V-SMOW are 0 to –4‰. Since neomorphism is an *in situ* replacement of originally marine bioclasts or micrite any additional diagenetic fluid contributing to that of the original rock-derived marine signature is likely to have been of brackish or meteoric origin (Figure 25). The dull- to slightly bright-luminescent CL character of the neomorphosed matrix and cements are consistent with precipitation from reducing fluids and/or those with Fe^{2+} ions. Values of –0.6 to +1.6‰ $\delta^{13}C$ V-PDB are consistent with marine $\delta^{13}C$ values. For the cements these $\delta^{13}C$ values indicate a lack of soil zone processes, and that a seawater or rock-derived source of carbon with marine $\delta^{13}C$ values was inherited by the precipitating fluids (Hendry et al., 1999; Madden and Wilson, 2012; 2013). In comparison, the equant fracture filling cements with values of –9.6 and –10.1‰ $\delta^{18}O$ V-PDB if formed at temperatures of >40–55 °C would have calculated

V-SMOW $\delta^{18}O$ values more negative than –2 to –5, i.e. most consistent with derivation from brackish and/or meteoric waters. The $\delta^{13}C$ V-PDB values of –1.8 and –7.4‰ for these fracture filling cements are suggestive of organically sourced CO_2 mixed at different proportions with host-rock derived carbon with higher $\delta^{13}C$ values (cf. Warrlich et al., 2010). Overall, precipitation from meteoric groundwaters is inferred for the neomorphic cements on the basis of their: (1) $\delta^{18}O$ values, (2) $\delta^{13}C$ values indicating a lack of soil zone processes, and (3) shallow burial origin. Poikilotopic calcite cements were only seen in carbonates from inner-shelf settings and/or outer-shelf ones associated with siliciclastic input, as with the neomorphic cements. Morad *et al.* (2000) note that poikilotopic cements and neomorphic calcite are commonly associated with meteoric to shallow burial diagenesis in humid tropical clastic successions. The occurrence of calcite cements formed during shallow burial diagenesis in Miocene siliciclastics from outcrops onshore, and subsurface deposits offshore, Malaysia gives credence to the inference of terrestrial-derived aquifer flow causing alteration of marine shelf sediments (Almond et al., 1990; Ibrahim and Madon, 1990; Madon and Abolins, 1999; Breitfeld, pers. comm., 2013). However, detailed geochemistry has yet to be undertaken of cements in the siliciclastic formations. Additionally the extensive dissolution of feldspars during early burial diagenesis has also been linked to flushing of meteoric water in subsurface siliciclastics offshore Malaysia (Ibrahim and Madon, 1990).

Delta^{18}O V-PDB values of –2.4 to –5.4‰ for marine bioclasts, matrix and blocky to equant cements from the outer-shelf carbonates plot mostly within the same field as many other Miocene marine bioclasts from SE Asia ($\delta^{18}O$ V-PDB values of –4.2‰ to –1.5‰; Ali, 1995; Wilson and Evans, 2002). In terms of their stable isotopes, and paucity of neomorphic or poikilotopic cements (except in samples with admixed siliciclastics or those interbedded

with siliciclastics during the middle build-out phase) there is little evidence for a brackish or meteoric signature during deposition or calcite cementation (Figure 25). The elements that plot most negatively from the outer-shelf deposits are the blocky to mainly equant cements with $\delta^{18}O$ V-PDB values of –3.6 to –5.4‰. Post-dating mechanical compaction, but pre-dating most stylolite development inferred $\delta^{18}O$ SMOW values for the outer-shelf calcite cements are –3.3 to +1.2‰ using a temperature range on 25–40 °C, i.e. most consistent with precipitation from fluids of marine derivation. Values of –1.1 to +0.6‰ $\delta^{13}C$ V-PDB are also consistent with marine $\delta^{13}C$ values, and for the cements indicate a lack of soil zone processes, and that a seawater or rock-derived source of carbon with marine $\delta^{13}C$ values was inherited from the precipitating fluids. The geometries of these blocky and equant cement are most commonly associated with phreatic and particularly for equant cements burial diagenetic environments (Flügel, 2004).

Development of chemical compaction features post-dating calcite cementation indicates progressive burial of inner- and outer-shelf carbonates to burial depths greater than ~500–1000 m (Nicolaides and Wallace, 1997; Machel, 2004). Samples studied are currently at depths between 620–4570 m, and those from <750 m from the SW Serunai High outer shelf deposits show least chemical compaction. The development of dissolution seams in more siliciclastic-rich samples compared with stylolites in more calcitic, well-cemented samples is a commonly documented trend from other studies (Wanless, 1979; Railsback, 1993). The formation of microdolomite rhombs along dissolution seams indicates their development in a burial setting post-dating the onset of chemical compaction. The ‘dusty’ appearance of many of the microdolomite rhombs indicates they are predominantly replacive, incorporating micritic or calcitic inclusions from the original matrix of samples (cf. Warren, 2000; Gregg and Sibley, 1984; Sibley and Gregg, 1987). The clear dolomite cements

with predominantly planar, but also curved crystal faces are indicative of temperatures less than, and greater than, 50–60 °C, respectively (Warren, 2000). Delta^{18}O values for dolomite (–5.2 to –7.4‰ V-PDB) at 40 to 60 °C convert to formation fluids of –0.3 to –6.3‰ V-SMOW (after Land, 1983). The more negative V-SMOW values calculated for the dolomites are consistent with their precipitation from meteoric fluids, whereas the less negative values may reflect a mixed marine-meteoric signature or silicate alteration reactions between pore fluids and siliciclastics (Morad, 1998). The sequence of dolomite replacement, dissolution of calcite and dolomite 'overgrowth' as occurs in the NW Borneo shelf carbonates is very common in other dolomitised successions (Machel, 2004).

Reservoir quality development

With porosity generally <4% and commonly <1–2%, and limited pore connectivity reservoir quality is low in inner-shelf carbonates and those admixed and/or interdigitating with shelf clastics in mid- to outer-shelf settings. The predominantly low to moderate depositional energies and proximity to siliciclastic influx resulted in carbonates rich in micrite or clays with little interconnected primary porosity (Figures 9, 16 and 25). Diagenesis mainly occurred in meteoric to predominantly burial settings, with compaction, neomorphism and cementation reducing pore space. Although early, probable meteoric leaching affected some inner shelf and/or shallow photic deposits, the secondary pores after leaching of aragonitic bioclasts are mainly filled with blocky, poikilotopic and equant cements and any remaining porosity does not appear well connected. The paucity of early marine cements from the low-energy deposits results in samples with little resistance to compaction-induced porosity reduction. The pervasive neomorphism of aragonite to calcite and association calcitisation into pore spaces that result in low porosity deposits are most

likely linked to alteration from terrestrially-derived meteoric groundwaters in shallow to deep burial environments. Subsurface fluid flow may be enhanced along bed parallel dissolution seams, but retarded perpendicular to them. Major influences on the lack of apparent reservoir quality development are therefore: (1) development in low energy settings on a broad marine shelf, (2) proximity to an adjacent humid landmass with meteoric aquifer circulation into inner shelf carbonates or perhaps channelled through shelf siliciclastics to more outer-shelf settings (Hendry et al., 1999; Wilson, 2012; Madden and Wilson, 2012).

Mid- to outer-shelf carbonates not associated with encroachment of shelf siliciclastics have the best reservoir quality, i.e. those in the core of mid-shelf mounds or from 'build-out' or backstepping to aggradational shelf-margin successions. There is a strong facies control on reservoir quality with the moderate to high energy, coarse grained grain/rudstones retaining best porosity. Porosity in grainstones from the mid-shelf mounds, the West Baram Hinge Zone, and the SW Serunai High shelf margin deposits were noted up to 5–8%, 3–20% and 10–35%, respectively, although not all pores are interlinked. Porosity is mainly intergranular, intragranular, intercrystalline and biomoldic, the later mainly associated with leaching near clear dolomite cements. Precipitation of early marine cements partially infilling pore space was important in preservation of primary porosity through providing resistance to the effects of later compaction. High energy deposits from the SW Serunai High have the highest porosity due to the additional presence of locally developed meniscate cements and a paucity of burial compaction related features (at 620–883 m they are the shallowest deposits studied). Although early dissolution of aragonitic bioclasts affected some samples, such as those from the terminal backstepping to aggradational sequence on the Baram High, much of this secondary porosity was occluded

with drusy to blocky/equant calcite cements. The late phase of dissolution associated with saddle dolomite formation enhanced remaining porosity and occurred during burial. Both clear dolomite cementation and associated leaching is most prevalent in the more porous samples, probably reflecting the presence of pathways for dolomitising and leaching fluids. Factors that resulted in good reservoir potential are: (1) high to moderate energies and the formation of grain-supported textures with good primary porosity, (2) presence of some early intergranular cementation to provide some rigidity and resistance to potential compaction effects, (3) no or limited early neomorphism and association calcitisation and limited later burial cements, and (4) late dissolution associated with dolomitisation.

Comparisons with other attached and isolated systems

The pervasive neomorphism and associated calcitisation that is a major cause of low reservoir quality in the shelf carbonates off NW Borneo has been linked to terrestrial-derived aquifer flow in other shelf carbonates that developed adjacent to humid equatorial landmasses (Hendry et al., 1999; Wilson, 2012; Madden and Wilson, 2012). Additionally the low energies that resulted in little primary porosity within inner shelf deposits are a common feature of broad siliciclastic shelves in the equatorial tropics lying as they do outside the typhoon belt (Tomascik et al., 1997). As a consequence of a vertically contracted biotic depth zonation, many terrestrial-runoff influenced systems develop with low relief (Wilson and Lokier, 2002; Wilson, 2005). Upright or toppled skeletons of reefal organisms are typically surrounded by clastic-matrix and the paucity of reefal frameworks result in gently sloping margins (Wilson and Lokier, 2002). The low relief mounded carbonates from the inner shelf of North Borneo therefore have both limited trap development and reservoir quality as a consequence of their depositional setting adjacent

to a humid equatorial landmass and the associated carbonate-siliciclastic interactions and terrestrially-driven groundwater aquifer flow. The original hypothesis that potential reservoir development in attached carbonate shelf systems will be strongly influenced by local environmental conditions associated with their development in the equatorial tropics adjacent to large landmasses appears to hold for the NW Borneo shelf and has resulted in low reservoir potential.

A growing body of research indicates that continental-derived meteoric groundwater flow from islands is strongly impacting the diagenesis of coastal, shelf and even some isolated carbonate platforms in SE Asia. Coral patch reefs that developed seaward of the Mahakam Delta in Borneo show pervasive early neomorphic replacement of aragonite by calcite and associated calcite cementation (Wilson, 2012; Madden and Wilson, 2012). Patch reefs contain 5–80% admixed siliciclastic component, formed coevally with near-continuous terrestrial influx and show no evidence of subaerial exposure or meteoric leaching (Wilson and Lokier, 2002; Wilson, 2005; Madden and Wilson, 2012). The neomorphism and calcitisation is an early diagenetic alteration formed during shallow burial. Flushing of meteoric groundwater flow (confined aquifer of James and Choquette, 1984), perhaps with an upland source derivation, plus/minus a minor seawater component is the inferred altering fluid (Madden and Wilson, 2012). Evidence for this interpretation is: 1) neomorphism retaining some structure of the original aragonite components that pre-dates most compaction (dissolution seams and stylolites, but not all mechanical compaction), 2) paucity of meteoric soil zone indicators (few negative $\delta^{13}C$ values), 3) $\delta^{18}O$ values consistent with derivation from meteoric waters including an upland source, or partially consistent with SE Asian seawater, 4) temperatures of up to ~55°C consistent with shallow burial depths and the regional geotherm. It is inferred that meteoric groundwater associated with

the ‘evet-wet’ climate of Borneo was focussed via aquifers through the adjacent deltaics causing extensive early alteration and cementation of the patch reefs (Madden and Wilson, 2012). Similar diagenetic features in a range of coastal carbonates indicate that meteoric groundwater flow is likely to have been a more important influence in the equatorial tropics than previously recognised (Netherwood and Wight, 1992; Meyers and Lohmann, 1985; Hendry et al., 1999; Moore, 2001; Wilson and Hall, 2010).

Recent research has shown that isolated carbonate platforms now caught up in fold and thrust belt development in the Luconia Province of North Borneo and Papua New Guinea are also strongly influenced by continental derived groundwaters (Warrlich et al., 2010; Wilson, 2012). Diagenesis relating to continental groundwaters in these isolated systems post-dates early diagenetic features (e.g. subaerial exposure related leaching) and may result in: 1) extensive or partial dolomitisation, and 2) burial leaching (Warrlich et al., 2010; Wilson, 2012). Recent work as shown that there is more interdigitation of siliciclastics with the Luconia carbonates than previously thought and that perhaps these systems should no longer be regarded as truly isolated carbonates (Kosa, 2012). Early calcite cements from the Luconia E11 platform have $\delta^{18}O$ and $\delta^{13}C$ isotopic signatures very similar to the inner-shelf and/or outer-shelf siliciclastic-associated carbonates described here. Warrlich et al. (2010) inferred that the early calcite cements as well as the dolomites in the E11 platform were precipitated from meteoric water, but most likely introduced laterally through permeable deltaic units rather than associated with subaerial exposure, i.e. the meteoric continental aquifer model as inferred herein (cf. Hendry et al., 1999; Taberner et al., 2002). As with this study, Warrlich et al. (2010) inferred that the ‘high rainfall and mountains in nearby Borneo appear to be sufficient to account for the required hydraulic head and water volumes’ to drive both early calcitisation and burial dolomitisation in Luconia. There is some

evidence that the dolomitisation and perhaps the associated late leaching of mid to outer shelf carbonates from the NW Borneo Shelf is also linked to aquifer-driven meteoric flow derived from the Borneo landmass or a mixed marine-meteoric source. It therefore appears that in shelf carbonates proximal to large humid equatorial landmasses and/or those with an early diagenetic connection to terrestrial driven aquifer flow via shelf siliciclastic deposits meteoric aquifer related diagenesis has a detrimental impact on reservoir quality. However, where continental-derived aquifer flow, perhaps with evolved character, affects carbonates distal from large humid landmasses and/or late in their diagenetic history subsurface aquifer-related diagenesis may have a positive impact on reservoir development. Late fracture filling calcite cements in Luconia have negative $\delta^{18}O$ and negative $\delta^{13}C$ values comparable with the fracture filling cements in inner shelf carbonates described here. Significant volumes of organically derived CO_2 are inferred during fracturing perhaps 'sourced by fluids from a deep-seated aquifer with salinities lower than seawater that are mixed in variable proportions with local compaction-derived fluids and a recurrent supply of organogenic CO_2' (Warrlich et al., 2010). Within the Luconia Province, 'fault trends in the older Tertiary section, subsidence profiles, evolution of source-rock kitchen areas, hydrocarbon migration, and overpressures are considered as key elements controlling the distribution of late diagenetic fluids' and some of these may also be applicable for the NW Borneo Shelf.

There is some evidence that carbonate systems from the siliciclastic dominated shelf of East Borneo show similar trends in deposits, sequence development, diagenesis and variations in reservoir quality to those on the NW Borneo Shelf. The sampled inner- and outer-shelf carbonates from East Borneo, however, are not from the same geological Epoch spanning the Miocene to Pleistocene. Inner shelf carbonates from East Borneo are the

Miocene delta-front patch reefs described directly above. These patch reef have a siliciclastic influence throughout their depositional history, developed under low energy conditions, and were significantly affected by diagenesis linked to continental-derived aquifer flow, with all factors having a detrimental impact on reservoir potential (Wilson and Lokier, 2002; Hook and Wilson, 2003; Wilson, 2005; Madden and Wilson, 2012). Miocene patch reefs that formed proximal to the delta front have similar geometries to the NW Borneo examples with low relief, gently sloping margins, but are slightly smaller being on the order of kilometres across and tens of metres thick (Wilson, 2005). Lower to Middle Miocene patch reef deposits in East Borneo are inferred to have developed best during transgressive phases, again similar to inner shelf carbonates in NW Borneo (Wilson, 2005). Latest Miocene to Pleistocene mid- and outer-shelf carbonates on the East Borneo shelf from 3-D seismic and well data consist of localised transgressive carbonate buildups and transgressive to highstand localised or stacked shelf margin sequences, respectively (Roberts and Sydow, 1996; Saller et al., 2010). Individual shelf margin sequences are elongate parallel to the shelf margin and up to kilometres to tens of kilometres long, hundreds of metres thick and up to a few kilometres wide. Coral-rich or bioclastic packstones and grainstones dominate the shelf-margin buildups, though partially dolomitised wackestones and siliciclastic mudstones are associated with maximum flooding surfaces (Saller et al., 2010). Mid-shelf buildups are on the order of magnitude of hundreds of metres to a few kilometres across and tens of metres thick and predominantly grew on faulted highs (Saller et al., 2010). Mid-shelf carbonates studied in cuttings include bioclastic packstones, grainstones and wackestones with some dolomitisation (Saller et al., 2010). Diagenetic features are variably developed in latest Miocene to Pleistocene mid-shelf and shelf margin deposits and include fibrous to prismatic cements (shelf margin), equant calcite

cement, dissolution, calcitisation of aragonite, and partial dolomitisation (Saller et al., 2010). Porosity is reported to be up to 20–35% and highest in the shelf margin deposits with pore types including inter-, and intra-granular (some cement lined) as well as moldic (Saller et al., 2010). The diagenetic features and pore types of mid- and outer-shelf deposits appear comparable to those from NW Borneo. Additional geochemistry is not available on samples from East Borneo and diagenetic feature have been variably and very tentatively linked to marine diagenesis (fibrous cements and questionably the dolomites), perched freshwater lenses above siliciclastics and subaerial exposure (Saller et al., 2010). Saller et al. (2010) noted that the prograding siliciclastics that commonly downlap onto carbonates during highstand, falling-stage, and/or lowstand systems tracts may be problematic for sealing stratigraphic traps in the carbonate buildups. From both the NW and East Borneo shelves the second hypothesis of this manuscript appears to hold: that there are significant (and apparently comparable) variations in carbonate and potential reservoir development across broad land-attached shelves from the equatorial tropics.

Conclusions

Considerable variation in deposition, diagenesis and reservoir potential of carbonate systems from across the siliciclastic-dominated NW Borneo shelf strongly reflect: environmental variability across the shelf, sequence development through time, siliciclastic-carbonate interactions and probable aquifer-driven groundwaters influencing carbonate alteration. Other influences include antecedent topography with deeply underlying tectonic highs, siliciclastic deposit morphologies and location of earlier carbonate buildups all affecting subsequent carbonate development. Tectonics through uplift, differential subsidence and active faulting influenced clastic runoff, aquifer charge, localised

accommodation space for carbonate development on both local-fault-related and regional-shelf scales, positions of the shelf margin and fault related margin collapse. The humid equatorial monsoonal climate resulted in significant surface siliciclastic and nutrient run-off to the shelf as well as groundwater flow affecting equatorial carbonate development and diagenesis together with windward-leeward differentiation in shelf margin areas.

Inner- to mid-shelf carbonates – Inner- to mid-shelf systems consist of laterally persistent layered sheet-like deposits that are probably interbedded carbonate-siliciclastic units and correlative thicker localised mounded carbonates all of Early Miocene age. Samples were only available from the mounded carbonate deposits. Mounded carbonate features had low-relief, gently-sloping margins and are up to 100–200 m thick and 2–10 km across. Molluscs, larger benthic foraminifera and corals are common components from the mounded carbonates indicating shallow photic depths consistent with patch reef development, although reefal frameworks may not have been present. The abundance of micrite and clay to medium-sand-grade siliciclastics within the groundmass of samples resulted in low primary porosity and is due to the predominantly low energy conditions and proximity to siliciclastic input in inner-shelf areas. Although some samples have been affected by early leaching of aragonite most show pervasive neomorphic granular mosaic, poikilotopic, blocky or equant calcite cements. These cements post-date some compaction, replace aragonite and occlude primary and secondary porosity, resulting in final porosity generally <4%, and commonly <2%. In addition to low reservoir potential of inner-shelf carbonates the size and geometry of the mounded features result in limited potential volumes for any hydrocarbon entrapment and the interdigitation and/or overlying shelf siliciclastics may result in poor sealing. The neomorphic and poikilotopic cements are inferred to be related to alteration from meteoric groundwaters derived from the Borneo

landmass. This link to interpreted aquifer flow is on the basis of: (1) cement geometries, (2) their paragenetic timing relative to shallow and deeper burial features, and (3) their geochemistry (values of –4.5 to –7.9‰ δ^{18}O V-PDB equivalent to δ^{18}O V-SMOW values of 0 to –4‰ at 25–40°C and δ^{13}C V-PDB values of –0.6 to +1.6‰). Most deposits from mid-shelf mounds are similar to those from the inner shelf. However, deposits from the cores of mid-shelf mounds include grainstones with porosities of up to 8% linked to retention of some primary porosity, less pervasive cementation than most inner-shelf deposits and some late leaching.

Outer-shelf and shelf-margin carbonates - Outer shelf carbonates form a stacked carbonate succession >1400 m thick on the West Baram High that span much of the Miocene, and a more sheet-like carbonate deposit ~260 m thick of latest Middle Miocene age over the SW part of the Serunai High. On the West Baram High carbonates form: (1) an initial backstepping to aggradational succession that is covered in siliciclastics, (2) followed by a series of 'build-out' to aggradational carbonates that interdigitate with siliciclastics, that are (3) overlain by a terminal backstepping to aggradational carbonate succession. Carbonates in close proximity to, and associated with encroachment of, siliciclastics are similar to those from the inner shelf areas. Grain/rudstones are common in outer shelf deposits particularly from the backstepping to aggradational units indicative of moderate to high energy conditions. Corals are abundant in the grain/rudstones from the West Baram High and are suggestive of reefal to near-reefal conditions, whereas larger benthic foraminifera dominated deposits from the SW Serunai High area. Retention of significant primary porosity (up to 35%) was seen in samples with some early cementation, resulting in resistance to compaction, and/or those from the SW Serunai High margin that are buried to depths of <900 m. Calcite cementation is less pervasive than in inner shelf deposits and

includes isopachous fringing, blocky and equant morphologies, with all cement precipitation linked to marine-derived rather than meteoric fluids. Late dolomite cements, some with saddle geometries, and those replacing matrix may be linked to alteration via meteoric aquifer flow on the basis of their geochemistry. Moderate to excellent reservoir quality with porosities of up to 20–35% is linked to grain/rudstones units that have: (1) retained some primary porosity, (2) less fine grained matrix and less calcite cementation than in inner-shelf deposits, (3) fractures, and (4) some late leaching associated with dolomitisation.

Proximity to the Borneo landmass and the associated terrestrial runoff, meteoric groundwater flow and local environmental conditions on the shelf in general resulted in low reservoir potential in inner-shelf areas and generally enhanced potential in shelf-margin carbonates. Trends in carbonate deposition, diagenesis and reservoir potential from the NW Borneo shelf appear comparable to those from East Borneo and may apply to other carbonate systems developed on predominantly clastic shelves bordering large-scale humid equatorial landmasses.

Acknowledgements

We acknowledge company support and thank Petronas (Carigali) for providing additional funds for diagenetic analyses and allowing publication. Moyra Wilson completed the petrographic work, field study and co-ordinated and/or undertook the additional diagenetic analyses. Steven Dorobek completed the seismic characterisation. Peter Lunt undertook the regional subsurface evaluation, biostratigraphy and fieldwork. Eva Chang completed the SEM and stable isotopic study together with some petrographic analyses as part of her Honours study, whilst supervised by Moyra at Curtin University. The use of equipment,

scientific and technical assistance of the Curtin University Electron Microscope Facility, which is partially funded by the University, State and Commonwealth Governments is acknowledged. Annette George, Zahra Seyedmehdi and Grzegorz Skrzypek all from the University of Western Australia (UWA), Perth, are thanked for their assistance in use of the CL luminoscope and in running the stable isotope analyses, respectively. Toni Simo and Mario Wannier provided constructive manuscript reviews. This is for Megan – who has gazed from the shore and wondered!

References

Adams, C.G., 1970. A reconsideration of the East Indian Letter Classification of the Tertiary. British Museum of (Natural History), Geology 19, 87–137.

Agostinelli, E., Tajuddin, M.R.A., Antollielli, E., and Aris, M.M. 1990. Miocene-Pliocene palaeogeographic evolution of a tract of Sarawak offshore between Bintulu and Miri. Geological Society of Malaysia, Bulletin 27, 117–135.

Ali, M.Y. 1995. Carbonate cement stratigraphy and timing of diagenesis in a Miocene mixed carbonate-clastic sequence, offshore Sabah, Malaysia: constraints from cathodoluminesence, geochemistry, and isotope studies. Sedimentary Geology 99, 191–214.

Almond, J., Vincent, P. and Williams, L.R. 1990. The application of detailed reservoir geological studies in the D18 Field, Balingian Province, offshore Sarawak. Geological Society of Malaysia, Bulletin 27, 137–159.

Anderson, T.F., and Arthur, M.A. 1983, Stable isotopes of oxygen and carbon and their application to sedimentologic and paleoenvironmental problems. *In* Arthur, M.A., Anderson, T.F., Kaplan, I.R., Veizer, J., and Land, L.S., (eds.). Stable Isotopes in Sedimentary Geology. SEPM, Short Course no. 10, 1–1 – 1–151.

Bachtel, S.L., Kissling, R.D., Martono, D., Rahardjanto, S.P., Dunn, P.A., and MacDonald, B.A. 2004, Seismic stratigraphic evolution of the Miocene–Pliocene Segitiga Platform, East Natuna Sea, Indonesia: the origin, growth, and demise of an isolated carbonate platform, in Eberli, G.P., Masafero, J.L., and Sarg, J.F., eds., Seismic Imaging of Carbonate Reservoirs and Systems. American Association of Petroleum Geologists, Memoir 81, p. 291–308.

Barckhausen, U, and Roeser, H.A.. 2004. Seafloor Spreading Anomalies in the South China Sea Revisited. *In* Continent-ocean interactions within East Asian marginal seas. P. Clift, P. Wang, W. Kuhnt, and D. Hayes (eds.) Washington: American Geophysical Union. 121–125.

Bathurst, R.G.C., 1966, Boring algae, micrite envelopes and lithification of molluscan biosparites. Geological Journal 5, 15 – 32.

Blow, W.H., 1969. Late Eocene to Recent planktonic foraminiferal biostratigraphy. Proceedings 1st Plankt. Conf., Geneva 1967, 1, 199–422.

Blow, W.H., 1979. The Cainozoic Globigerinida. Brill, E.J., Leiden, 1412p.

Bowen, G.J. and Wilkinson, B. 2002. Spatial distribution of $\delta^{18}O$ in meteoric precipitation. Geology 30, 315–318.

Briais, A., Patriat, P. and Tapponnier, P. 1993. Updated interpretation of magnetic anomalies and seafloor spreading stages in the South China Sea: Implications for the Tertiary tectonics of Southeast Asia. Journal of Geophysical Research 98, 6299–6328.

Dickson, J.A.D., 1965. A modified staining technique for carbonates in thin section. Nature, 205, 587.

Dunham, R.J., 1962. Classification of carbonate rocks according to depositional texture. *In:* Ham, W.E. (Ed.), Classification of carbonate rocks. American Association of Petroleum Geologists, Memoir, 1, 108–121.

Embry, A.F. and Klovan, J.E. 1971. A late Devonian reef tract on northeastern Banks Island, Northwest Territories. Canadian Petroleum Geologist, Bulletin 19, 730–781.

Erlich, R.N., Barrett, S.F., Bai Ju, G., 1990. Seismic and geologic characteristics of drowning events on carbonate platforms. AAPG Bulletin 74, 1523–1537.

Erlich, R.N., Longo, A.P, Hyare, S., 1993. Response of carbonate platform margins to drowning: Evidence of environmental collapse. In: Loucks R.G., Sarg, J.F. (Eds.). Carbonate sequence stratigraphy. American Association of Petroleum Geologists, Memoir 57, 241–266.

Epting, M. 1980, Sedimentology of Miocene carbonate buildups, Central Luconia, offshore Sarawak. Geological Society of Malaysia, Bulletin 12, 17–30.

Flügel, E., 2004, Microfacies of carbonate rocks. Analysis, interpretation and application; Springer-Verlag, Berlin, 976 p.

Fulthorpe, C.S. and Schlanger, S.O. 1989, Paleo-oceanographic and tectonic settings of early Miocene reefs and associated carbonates of offshore southeast Asia. American Association of Petroleum Geologists, Bulletin 73, 729–756.

Gradstein, F.M., Ogg, J.G. and Smith, A.G., (Eds.), 2004. A Geologic Time Scale 2004, Cambridge University Press, UK. 589 pp.

Gregg, J.M., and Sibley, D.F. 1984, Epigenetic dolomitization and the origin of xenotopic dolomite texture. Journal of Sedimentary Petrology 54, 908–931.

Gunther, A. 1990. Distribution and bathymetric zonation of shell boring endoliths in recent reef and shelf environments: Cozumel, Yucatan (Mexico). Facies 22, 233 – 262.

Hall, R. 1996. Reconstructing Cenozoic SE Asia. *In* Hall, R., and Blundell, D.J. (Eds.). Tectonic Evolution of Southeast Asia. Geological Society of London, Special Publication 106, 153–184.

Hall, R. 2002a. Cenozoic geological and plate tectonic evolution of SE Asia and the SW Pacific: computer-based reconstructions, model and animations. Journal of Asian Earth Sciences 20, 353–431.

Hall, R. 2002b. SE Asian heat flow: Call for new data. Indonesian Petroleum Association Newsletter 4, 20–21.

Hall, R. and Nichols, G. 2002. Cenozoic sedimentation and tectonics in Borneo: climatic influences on orogenesis. In: Sediment Flux to Basins: Causes, Controls and Consequences. Jones, S.J. and Frostick, L.E. (Eds). Geological Society, London, Special Publication 191, 5–22.

Hallock, P., 2005, Global change and modern coral reefs: New opportunities to understand shallow-water carbonate depositional processes: Sedimentary Geology 175, p. 19–33.

Hamilton, W. 1974. Map of sedimentary basins of the Indonesian region. United States Geological Survey Map-I-875-B, U.S. Geological Survey, Reston, VA, USA.

Hamilton, W. 1979. Tectonics of the Indonesian region. United States Geological Survey Professional Paper 1078, 345 p.

Haq, B.U., Hardenbol, J. & Vail, P.R. 1987. Chronology of fluctuating sea levels since the Triassic. Science, 235, 1156–1165.

Hazebroek, H.P., Tan, D.N.K. and P. Swinburn. P. 1994. Tertiary evolution of the offshore Sarawak and Sabah Basins, NW Borneo, American Association of Petroleum Geologists Bulletin 78, 1144–1145.

Hendry, J.P., Taberner, C., Marshall, J.D., Pierre, C., and Carey, P.F. 1999. Coral reef diagenesis records pore-fluid evolution and paleohydrology of a siliciclastic basin margin succession (Eocene South Pyrenean foreland basin, northeastern Spain). Geological Society of America Bulletin 111, 395–411.

Hinz, K. and Schlüter, H.U. 1985. Geology of the Dangerous Grounds, South China Sea and the continental margin of Southwest Palawan: results of SONNE cruises SO-23 and SO-27. Energy, 10, 297–315.

Holloway, N.H., 1982. The stratigraphic and tectonic evolution of Reed Bank, North Palawan and Mindoro to the Asian mainland and its significance in the evolution of the South China Sea. American Association of Petroleum Geologists Bulletin 66, 1357–1383.

Hook, J. and Wilson, M.E.J. 2003. Stratigraphic relationships of a Miocene mixed carbonate-siliciclastic interval in the Badak field, East Kalimantan, Indonesia. Proceedings of the 29th Indonesian Petroleum Association, 398–412.

Hutchison, C.S. 2005. Geology of North-West Borneo: Sarawak, Brunei and Sabah. Elsevier, London, 421 p.

Hutchison, C.S., Bergman, S.C., Swauger, D.A. and Graves, J.E. 2000. A Miocene collisional belt in north Borneo: Uplift mechanism and isostatic adjustment quantified by thermochronology. Journal of the Geological Society of London, 157, 783–793.

Ibrahim, N.A. and Madon, M. 1990. Depositional environments, diagenesis, and porosity of reservoir sandstones in the Malong Field, offshore West Malaysia. Geological Society of Malaysia, Bulletin 27, 27–55.

James, N.P. and Choquette, P.W. 1984. Diagenesis 9 - Limestones – the meteoric diagenetic environment. Geoscience Canada 11, 161–194.

King, R.C., Tingay, M.R.P., Hillis, R.R., Morley, C.K. and Clark, J. 2010. Present-day stress orientations and tectonic provinces of the NW Borneo collisional margin. Journal of Geophysical Research 115, B10415, doi:10.1029/2009JB006997.

Kosa, E. 2012. Wings, Mushrooms and Christmas Trees: Insights from Carbonate Seismic Geomorphology into the Tectono-Stratigraphic Evolution of Central Luconia; Miocene-Present, Offshore Sarawak, NW Borneo, Malaysia. AAPG Search and Discovery Article #90155©2012 AAPG International Conference & Exhibition, Singapore, 16–19 September 2012. http://www.searchanddiscovery.com/abstracts/html/2012/90155ice/abstracts/kos.htm (accessed 25/09/2012).

Lokier, S.W., Wilson, M.E.J. and Burton, L.M. 2009. Marine biota response to clastic sediment influx: a quantitative approach. Palaeogeography, Palaeoclimatology, Palaeoecology 281, 25–42.

Land, L.S., 1983. The applications of stable isotopes to studies of the origin of dolomite and to problems of diagenesis of clastic sediments. *In* Arthur, M.A., Anderson, T.F., Kaplan, I.R., Veizer, J., and Land, L.S., (eds.), Stable Isotopes in Sedimentary Geology. SEPM, Short Course no. 10, 4–1 – 4–22.

Lunt, P. and Allan, T., 2004. A history and application of larger foraminifera in Indonesian biostratigraphy, calibrated to isotopic dating. GRDC Workshop on Micropalaeontology, 109 pp.

Machel, H.G., 2004, Concepts and models of dolomitization: A critical reappraisal. *In* Braithwaite, C.J.R., Rizzi, G., and Darke, G., (eds.), The Geometry and Petrogenesis of Dolomite Hydrocarbon Reservoirs. Geological Society of London, Special Publication 235, 7 – 63.

Madden, R.H.C. and Wilson, M.E.J. 2012. Diagenesis of delta-front patch reefs: a model for alteration of coastal siliciclastic-influenced carbonates from humid equatorial regions. Journal of Sedimentary Research 82, 871-888.

Madden, R.H.C. and Wilson, M.E.J. 2013. Diagenesis of a SE Asian Cenozoic carbonate platform margin and its adjacent basinal deposits. Sedimentary Geology, 286–287, 20–38.

Madon, M.B.H. 1999a. Geological Setting of Sarawak. In: The Petroleum Geology and Resources of Malaysia. PETRONAS, Kuala Lumpur, Malaysia. 273–290.

Madon, M.B.H. 1999b. Basin types, tectono-stratigraphic provinces, structural styles. In: The Petroleum Geology and Resources of Malaysia. PETRONAS, Kuala Lumpur, Malaysia, 77–112.

Madon, M.B.H. and Abolins, P. 1999. Balingian Province. *In* The Petroleum Geology and Resources of Malaysia. PETRONAS, Kuala Lumpur, Malaysia, 343–368.

Martini, E., 1971. Standard Tertiary and Quaternary calcareous nannoplankton zonation. *In*: Farinacci, A. (Ed.), Conference Planktonic Microfossils, Proceedings, Rome, 1970, 2, pp. 739–785.

Mat–Zin, I.C. and Tucker, M.E. 1999. An alternative stratigraphic scheme for the Sarawak Basin. Journal of Asian Earth Science 17, 215–232.

Mazzullo, J. and Graham, A.J., (Eds.), 1988. Handbook for Shipboard Sedimentologists. ODP Technical Notes 8.

McArthur, J.M. and Howarth, R.J., 2004. Strontium isotope stratigraphy. *In*: Gradstein, F.M., Ogg, J.G. and Smith, A.G. (Eds.), A Geologic Time Scale 2004, Cambridge University Press. pp. 96–105.

McArthur, J.M., Howarth, R. and Bailey, T.R., 2001. Strontium Isotope Stratigraphy: LOWESS version 3. Best fit line to the marine Sr-isotope curve for 0 to 509 Ma and accompanying look-up table for deriving numerical age. Journal of Geology 109, 155–169.

Meyers, W.J., and Lohmann, K.C., 1985. Isotope geochemistry of regionally extensive calcite cement zones and marine components in Mississippian limestones, New Mexico. In: Harris, P.M. and Schneidermann, N. (eds.) Carbonate Cements, Tulsa, OK, SEPM Special Publication 36, 223–239.

Mitchum, R.M. Jr, Vail, P.R., Thompson III, S., 1977. Seismic stratigraphy and global changes of sea level, Part 2: The depositional sequence as a basic unit for stratigraphic analysis. *In:* Payton, C.E. (Ed.), Seismic Stratigraphy-Application to Hydrocarbon Exploration, American Association of Petroleum Geologists, Memoir 26, 53–62.

Moore, C.H., 2001. Carbonate Reservoirs, Porosity Evolution and Diagenesis in a Sequence Stratigraphic Framework. Amsterdam, Elsevier, 444 p.

Morad, S., 1998. Carbonate cementation in sandstones: distribution patterns and geochemical evolution. *In* Morad, S, (ed.), Carbonate Cementation in Sandstones. International Association of Sedimentologists Special Publication 26, 1–26.

Morad, S., Ketzer, J.M., and Ros, L.F.D., 2000. Spatial and temporal distribution of diagenetic alterations in siliciclastic rocks: implications for mass transfer in sedimentary basins. Sedimentology 47, 95–120.

Morley, C.K., Back, S., Van Rensbergen, P., Crevello, P. and Lambiase, J.J. 2003. Characteristics of repeated, detached, Miocene-Pliocene tectonic inversion events, in a large delta province on an active margin, Brunei Darussalam, Borneo. Journal of Structural Geology 25, 1147–1169.

Netherwood, R. and Wight, A., 1992. Structurally-controlled, linear reefs in a Pliocene Delta-front setting, Tarakan Basin, Northeast Kalimantan. In: Siemers, C.T., Longman, M.W., Park, R.K.,

Kaldi, J.G. (Eds.). Carbonate rocks and reservoirs of Indonesia. Indonesian Petroleum Association Core Workshop Notes 1, Ch. 3.

Nicolaides, S., and Wallace, M.W. 1997. Pressure dissolution and cementation in an Oligo-Miocene non-tropical limestone (Clifton Formation), Otway Basin, Australia. *In:* James, N.P. and Clarke, J.A.D., (eds.), Cool Water Carbonates. SEPM, Special Publication 56, 249 – 261.

Noad, J., 2001, The Gomantong Limestone of eastern Borneo: a sedimentological comparison with the near-contemporaneous Luconia Province: Palaeogeography, Palaeoclimatology, Palaeoecology 175, p. 273–302.

Perry, C.T., 1999. Biofilm-related calcification, sediment trapping and constructive micrite envelopes: a criterion for the recognition of ancient grass-bed environments? Sedimentology, 46, 33 – 45.

Railsback, L.B., 1993. Lithologic controls on morphology of pressure-dissolution surfaces (stylolites and dissolution seams) in Paleozoic carbonate rocks from the Mideastern United States. Journal of Sedimentary Petrology 63, 513 – 522.

Roberts, H.H. and Sydow, J. 1996. The offshore Mahakam Delta: Stratigraphic response of late Pleistocene to modern sea level cycle. Indonesian Petroleum Association, Proceedings 25th Annual Convention, 147–161.

Saller, A.H., Reksalegora, S., and Bassant, P., 2010, Sequence stratigraphy and growth of shelf margin and middle shelf carbonates, *in* Morgan, W.A., George, A.D., Harris, P.M., Kupecz, J.A. and Sarg, J.F., (eds.), Cenozoic Carbonates of Australasia. SEPM Special Publication 95, p. 147 – 174.

Sanders, D. and Baron–Szabo, R.C. 2005. Scleractinian assemblages under sediment input: their characteristics and relation to the nutrient input concept. Palaeogeography, Palaeoclimatology, Palaeoecology 216, 139–181.

Sibley, D.F., and Gregg, J.M. 1987. Classification of dolomite rock textures. Journal of Sedimentary Petrology 57, 967–975.

Skryzypek G., and Paul, D., 2006. $\delta^{13}C$ analysis of calcium carbonate: comparison between the GasBench and elemental analyzer techniques. Rapid Communications in Mass Spectrometry 20, 2915–2920.

Spalding, M. D., Ravilious, C. & Green, E. P. 2001. World Atlas of Coral Reefs. University of California Press, Hong Kong, 424 p.

Taberner, C., Marshall, J.D., Hendry, J.P., Pierre, C., and Thirlwall, M.F., 2002. Celestite formation, bacterial sulphate reduction and carbonate cementation of Eocene reefs and basinal sediments (Igualada, NE Spain). Sedimentology 49, 171–190.

Taylor, B. and Hayes, D.E. 1983. Origin and history of the South China Sea Basin. In: Hayes, D.E (Ed.). The tectonic and geologic evolution of Southeast Asian Seas and Islands: Part 2. American Geophysical Union, Geophysical Monograph 27, 23–56.

Tomascik, T., Mah, A.J., Nontji, A. and Moosa, M.K. 1997. The Ecology of the Indonesian Seas. Oxford University Press, Singapore, 1388 p.

Vahrenkamp, V.C., David, F., Duijndam, P., Newall, M. and Crevello, P. 2004. Growth architecture, faulting, and karstification of a Middle Miocene carbonate platform, Luconia province, offshore Sarawak, Malaysia. In: Eberli, G.P., Masafero, J.L. and Sarg, J.F. (Eds.) Seismic imaging of carbonate reservoirs and systems. American Association of Petroleum Geologists Memoir 81, 329–350.

van de Vlerk, I.M. and Umbgrove, J.H.F., 1927. Tertiaire gidsforaminifern van Nederlandsch Oost-Indiè. Wetensch. Meded. Dienst Mijnbouw Nederlandsch Oost-Indiè 6, 3–31.

Wang, P. and Li, Q. 2009. Oceanographical and Geological Background. In: Wang, P. and Li., Q. (eds.) The South China Sea – Paleooceanography and Sedimentology. Springer, Developments in Paleoenvironmental Research 13, 25–73.

Wanless, H.R., 1979. Limestone response to stress: pressure solution and dolomitization. Journal of Sedimentary Petrology 49, 437 – 462.

Wannier, M. 2009. Carbonate platforms in wedge-top basins: An example from the Gunung Mulu National Park, Northern Sarawak (Malaysia). Marine and Petroleum Geology 26, 177–207.

Warren, J., 2000. Dolomite: Occurrence, evolution and economically important associations. Earth-Science Reviews 52, 1 – 81.

Warrlich, G., Taberner, C., Asyee, W., Stephenson, B., Esteban, M., Boya-Ferrero, M., Dombrowski, A. and Van Konijnenburg, J.–H. 2010. The impact of postdepositional processes on reservoir properties: two case studies of Tertiary carbonate buildup gas fields in Southeast Asia (Malampaya and E11). In: Morgan, W.A., George, A.D, Harris, P.M., Kupecz, J.A. and Sarg, J.F. (Eds.). Cenozoic Carbonate Systems of Australasia. SEPM Special Publication 95, 99–127.

Wilson M.E.J. 2002. Cenozoic carbonates in Southeast Asia: implications for equatorial carbonate development. Sedimentary Geology 147, 295–328.

Wilson, M.E.J. 2005. Equatorial delta-front patch reef development during the Neogene, Borneo. Journal of Sedimentary Research 75, 116–134.

Wilson, M.E.J. 2008, Global and regional influences on equatorial shallow marine carbonates during the Cenozoic. Palaeogeography, Palaeoclimatology, Palaeoecology 265, 262–274.

Wilson, M.E.J. 2011. SE Asian carbonates: tools for evaluating environmental and climatic change in the equatorial tropics over the last 50 million years. In: Hall, R., Cottam., M.A., and Wilson, M.E.J. (Eds.). The SE Asian gateway: history and tectonics of Australia-Asia collision. Geological Society of London Special Publication 355, 347–369.

Wilson, M.E.J., 2012. Equatorial carbonates: an earth systems approach. Sedimentology 59, 1–31.

Wilson, M.E.J. & Evans, M.J. 2002. Sedimentology and diagenesis of Tertiary carbonates on the Mangkalihat Peninsula, Borneo: implications for subsurface reservoir quality. Marine and Petroleum Geology, 19, 873–900.

Wilson, M.E.J. and Hall, R. 2010. Tectonic influence on SE Asian carbonate systems and their reservoir quality. In: Morgan, W.A., George, A.D, Harris, P.M., Kupecz, J.A. and Sarg, J.F.

(Eds.). Cenozoic Carbonate Systems of Australasia. SEPM Special Publication 95, 13–40.

Wilson, M.E.J. and Lokier, S.J. 2002. Siliciclastic and volcaniclastic influences on equatorial carbonates; insights from the Neogene of Indonesia. Sedimentology 49, 583–601.

Wilson, M.E.J., Chambers, J.L.C, Evans, M.J., Moss, S.J. and Satria Nas, D. 1999. Cenozoic carbonates in Borneo: Case studies from Northeast Kalimantan. Journal of Asian Earth Science 17, 183–201.

Witkowski, F.W., Blundell, D.J., Gutteridge, P., Horbury, A.D., Oxtoby, N.H., and Qing, H. 2000. Video cathodoluminescence microscopy of diagenetic cements and its applications. Marine and Petroleum Geology 17, 1085–1093.

Zachos, J., Pagani, M., Sloan, L., Thomas, E., and Billups, K., 2001. Trends, rhythms, and aberrations in global climate 65 Ma to present. Science 292, 686–693.

Figures and Tables

Figure 1) Simplified geological map of north Borneo showing the location of the research area. Major outcropping and subsurface Cenozoic and modern carbonates are illustrated, as are areas of Cenozoic delta progradation (modified from Wilson et al. 1999; Spalding et al., 2001; Wilson 2002; Madden and Wilson, 2012).

Figure 2A) Schematic cross sections across the NW Borneo collisional margin during the Late Cretaceous and Oligocene to Miocene, illustrating subduction of the proto-South China Sea plate beneath the Crocker-Rajang Accretionary Complex. **(B)** A schematic map illustrating the plate configuration at the NW Borneo collisional margin during the Eocene to Miocene with the study area highlighted (modified from King et al., 2010; after Madon, 1999a).

Figure 3A) Simplified map of the Balingian Province, showing the sub-provinces, depocentres, and structural features (after Madon, 1999b). Well locations are those featured on Figure 4. **(B)** Basement TWT (two way time) map of the East Balingian Sub-Province.

Figure 4) Simplified, approximate west to east transect through Tertiary strata from the Sarawak shelf highlighting carbonate deposits. Inset map shows line of section through subsurface wells (identified by letters) and onshore outcrops. The approximate position of the Neogene shelf margin is shown on the inset map and wells within 5–10 km of the margin are considered to be in outer shelf or shelf margin locations. The position of the

shelf margin may have varied during the Cenozoic (Agostinelli et al., 1990, Madon, 1999a), and the shelf-margin location illustrated best reflects that for Miocene deposits. Distribution of well and outcrop samples are plotted against the timescale of Gradstein et al. (2004) with biostratigraphic zones shown (following van der Vlerk and Umbgrove, 1927; Blow, 1969; 1979; Martini; 1971; Adams, 1970; Lunt and Allan, 2004). The definition of the Batu Gading and Melinau outcrops as platforms that formed in 'wedge top basin' settings follows Wannier (2009). The Subis Limestone although shown under the 'inner shelf' heading may have characteristics most comparable with an isolated buildup (Wannier, pers. comm. 2013), and at 500 m, is thicker than inner shelf deposits described from the subsurface in the text. New strontium isotope ages follow the 'look-up' tables of McArthur and Howarth (2004).

Figure 5) Regional SW-NE seismic line across mid to outer shelf settings with carbonate development highlighted. Sequences are after Mat–Zin and Tucker (1999), following the definition of Mitchum et al. (1977), with boundaries of sequences shown in green and the ages of the base of the sequences given as: T2 S – 23–22.5 Ma, T3 S – 18.0–18.5 Ma, T4 S – 11–13 Ma, T5 S – 5.2–5.3 Ma. Notes on wells: (1) Top NN5 (highest *Sphenolithus heteromorphus*). Event marked correlates to slight folding in well Y and the end of the broad outer shelf carbonate platform. (2) Top limestone is well-dated as mid NN2 (nannofossils in mudstone SWC immediately above limestone), lowest Tf on larger benthic foraminifera from Side Wall Cores (SWCs) in the limestone, supported by Sr dating at 20.0 Ma. The base limestone is still within the Miocene as *Miogypsina* is found in mudstones at TD. (3) Shift from shallow shelf mudstones and silts to very shallow and sand-rich sediments above. The more marine mudstones below are dated as close to the

NN10-NN11 boundary (c. 8–8.5 Ma). (4) At this point is the disappearance of *Fohsella peripheroronda* and that of *Sphenolithus hetermorphus* both within a section of consistently good fauna, i.e. 13.5–14 Ma. Above is an abrupt shallowing from middle neritic, open marine to shallow, inner neritic, up hole that is probably a sequence boundary (marked). (5) Well Y projected onto line evolution datum of *Neogloboquadrina humersosa*. This point is also a significant, long lasting shift from shallow marine to probably littoral and more sand-rich environments up-hole. (6) A limestone bed in the well (faulted up on this line) contains both *Nephrolepidina* and *Miogypsina* indicating an age older than c. 12.7 to 13 Ma (within Lower Tf) and thereby older than the top of T3S (Cycle III/IV). (7) Overpressure in deep marine mudstones above the carbonates. No age index markers in the mudstone, but environment in top limestone interpreted as outer neritic to bathyal. (8) In the limestone there is *Flosculinella* aff. *fennemai* but no record of *Alveolinella. Borelis melo* occurs indicating an age no older than late Miocene. The whole fauna is Upper Tf, post c. 12.7 Ma. This is distinctly younger than the thin limestones near TD in well Y. Sr dating suggests an age ranging from 7 to 8 Ma near the top of the limestone and 10.5–11 Ma near TD.

Figure 6) Regional, generalized stratigraphic framework for the Miocene carbonate sequences identified in this study from the West Baram Line fault zone region. Regionally, the Aquitanian carbonate sequences extend farther to the west and southwest, which is not shown in this schematic diagram. Also shown are generalized platform morphologies, long-term behavior of platform margins (i.e., progradation, aggradation, dowstepping, backstepping, or drowning), and integration with other

selected siliciclastic seismic horizons (siliciclastics are shown stippled). Well penetrations are illustrated schematically.

Figure 7) Typical chaotic to subparallel seismic reflector geometries from Aquitanian inner shelf mounded and sheet-like inner-shelf carbonate deposits. Chaotic reflector character likely reflects karstification and potential secondary porosity development within these carbonate intervals. Lowstand deltaics that downlap onto the carbonates are also apparent. Toplap truncation surface (highlighted) at the top of the lowstand delta indicates the former position of sea level when the delta formed.

Figure 8) Seismic image showing possible evidence for karstification in the Aquitanian carbonate strata. Potential karst-related features include sinkhole features, inclined or rotated blocks, collapse features, and overall chaotic character of reflectors. Possible incised valley features and channels associated with the overlying siliciclastics that cut down into the upper surface of the carbonates can be mapped over several tens of kilometres.

Figure 9) Plane-polarised light thin-section photomicrographs from Aquitanian inner-, and inner- to mid-shelf mounded carbonates (Wells D and W: see Figure 4). (A) Coral (lower part of image) showing micritisation, replacement and infill of chambers by granular mosaic to equant or poikilotopic calcite. Concavo-convex point contact, enhanced by dissolution seam development, between larger benthic foraminifera and coral. Groundmass includes siliciclastics and microdolomite rhombs and these are concentrated along dissolution seam. (B) Bioclastic packstone including coral fragment encrusted in

laminar coralline algae (left), fragmented branching coralline algae, echinoderm material and imperforate foraminifera, including *Austrotrillina.* (C) Partial neomorphism of fine matrix (which includes quartz grains) and replacement of molluscs by granular mosaic calcite. Coralline algae and agglutinated foraminifera present. (D) Bioclastic packstone with mollusc dissolved out and infilled by blocky non-ferroan calcite, minor moldic, intercrystalline porosity remains. Other bioclasts include echinoderm material, larger benthic foraminifera and miliolids. (E) Bioclastic packstone with some siliciclastics in matrix. Biomolds after molluscs and probably corals are infilled with bladed and blocky, then coarse poikilotopic cements. (F) Neomorphosed bioclastic packstone with matrix and some aragonitic bioclasts such as *Halimeda* neomorphically replaced to granular mosaic calcite. Coral fragment (on left) with 'ghost' trace of septa now includes poikilotopic calcite cement. Compaction-related dissolution seams present in matrix. (G) Coral (left) showing replacement and infill of chambers by granular mosaic to equant or poikilotopic calcite. Groundmass includes siliciclastics and microdolomite rhombs. (H) Recrystallised larger benthic foraminifera and coralline algae pack/grainstone showing dolomitisation and some insoluble siliciclastic content along irregular dissolution seam that cross-cuts area with granular cements. Dissolution and/or intercrystalline porosity present adjacent to seam. (I) Recrystallised coralline algae grainstone showing granular/blocky cement around grains, some preservation of primary intergranular porosity and secondary biomoldic porosity. Pores are partially filled by non-staining saddle dolomite (with curved crystal faces) and there is some leaching of nearby bioclasts, including coralline algae.

Figure 10) Plane-polar (PL) and cathodoluminescent (CL) thin-section photomicrograph pairs from Aquitanian inner-, and inner- to mid-shelf mounded carbonates (Wells D and W: see Figure 4). (A/A') Upper part of image shows bright to dull luminescent recrystallised coral (C) now composed of granular mosaic calcite with dull-luminescent micritic infill of boring. Other bioclasts including coralline algae (CA) and larger benthic foraminifera (LBF) show dull luminescence. Admixed siliciclastic-micritic matrix (SM) with some microdolomite rhombs and fragmented bioclasts is mainly non-luminescent with bright 'flecks'. (B/B') Different field of view from same sample as A/A' showing similar features with the addition of brightly luminescent equant calcite cements infilling fractures (F) and shelter porosity (S). Dolomite cements (D) and the microdolomites are both non-luminescent. (C/C') Brightly-luminescent, laminar coralline algae (CA) and imperforate foraminifera (I) in more dull-luminescent micritic matrix (M). Coral (C) and *Halimeda* (H) replaced by granular mosaic calcite show dull-luminescence. Fracture (F) filling equant cements are more brightly luminescent, whereas microdolomite (D) is non-luminescent.

Figure 11) Paragenetic sequence of diagenetic events affecting inner-, and inner- to mid-shelf low- and moderate-energy deposits, respectively, from Aquitanian mounded carbonates. Relative timing of events is on the basis of petrographic observations.

Figure 12) Cross-plot of $\delta^{18}O‰$ V-PDB versus $\delta^{13}C‰$ V-PDB for calcite and dolomite components and cements from inner- to outer-shelf carbonates. Samples from outer shelf settings affected by siliciclastic influx are also included in the inner to mid-shelf components. The $\delta^{18}O$ values of typical SE Asian marine elements are after Ali (1995) and

Wilson and Evans (2002) with those for Borneo groundwaters after Anderson and Arthur (1983) and Bowen and Wilkinson (2002; see text for details).

Figure 13) Seismic image showing extensive Aquitanian carbonates overlain by more localised Burdigalian and younger platforms. The Burdigalian platforms directly above the dark blue horizon are steep-sided and have high relief (~300 ms). The Burdigalian systems initiated during a regional rise in relative sea-level, which forced carbonate deposition to backstep toward regional highs. The steep, apparently aggradational SW sides of a number of the post-Aquitanian platforms likely reflect windward margins and more the inclined, progradational NE sides of the platform are likely to be leeward margins. Internal seismic facies are not obvious within any carbonate sequence.

Figure 14) Seismic image across the West Baram Hinge Line area showing Miocene carbonate platform development, sequence geometries and the interaction between carbonates, siliciclastics and structures. Aquitanian and possibly older carbonate development (below the dark blue seismic pick) was extensive across the shelf. However, an apparent break in carbonate development 25–40 km back from the hinge zone may reflect a region of structural 'sag' linked to inferred uplift and incipient fault break through in the hinge zone region. During the Burdigalian siliciclastics prograde out across the shelf and carbonates backstep towards the bathymetric high of the hinge zone area (pink seismic pick). This is followed by relatively flat-topped carbonate platforms intermittently building out over (towards the SW on this image, e.g. orange horizons), and interdigitating with the shelf siliciclastics. The interdigitating shelf

siliciclastics intermittently prograde out across the shelf (towards the NE on this image), and locally over the shelf margin. During the Tortonian, carbonates backstepped to the shelf margin area and were restricted to a series of localised carbonate buildups that experienced diachronous downlapping and covering by siliciclastics. The location of carbonate platform and buildup development in the hinge line area appears to be strongly linked to structural highs associated with inferred strike-slip faulting and probable flower structure development. Thickness changes in carbonate strata as well as growth strata are associated with many of the faults (e.g. light green and dark green seismic picks).

Figure 15) Seismic image showing extensive Aquitanian (and possibly older) carbonates (pale blue to dark blue seismic 'picks') overlain by downlapping Burdigalian siliciclastics. During the Burdigalian, carbonates backstep towards the shelf margin (NE on this image) followed by relatively flat-topped carbonate platforms intermittently building out over (towards the SW on this image), and interdigitating with the shelf siliciclastics. In the upper part of the image, carbonate platforms that interdigitate with the siliciclastics show stacked development (e.g. orange, red and green seismic picks). Many of the flat-topped carbonate platforms developed along individual horizons aggraded to a common 'base level' (e.g. orange and red seismic picks; although strata has been tilted northeastward by later deformation). There is slight asymmetry to many platform profiles, with steeper SW, probably windward margins and more gently inclined NE leeward margins.

Figure 16) Plane-polarised light thin-section photomicrographs from Burdigalian outer-shelf and shelf-margin carbonate deposits from the West Baram Hinge Zone area from between 4570 and 4414 m that date to around 19.0–18.7 Ma (Well G: see Figure 4). Samples are from the backstepping sequence immediately post-dating widespread Aquitanian shelf-wide carbonate deposition and pre-dating siliciclastic progradation over the shelf margin and are shown in order of deepest (A) to shallowest (I) within this interval. (A) Larger benthic foraminifera bioclastic packstone showing sutured contacts between grains and dissolution seams with fracture filled by equant calcite cement. (B) Bioclastic grainstone with foraminifera, coralline algae and replaced aragonitic components including shells (original shape highlighted by micrite envelopes). Dolomite cements partially infill pores usually after leaching of aragonitic bioclasts and equant to poikilotopic calcite cements are common. (C) Equant to granular mosaic calcite cement replacing coral and infilling chambers. Some chambers are filled or partially filled with micrite. Micritisation highlights original walls of the coral, and in places the calcite cements cross-cut the micritic rims (i.e. neomorphism and associated calcitisation into pore space). (D) Silty bioclastic pack/wackestone with larger foraminifera, miliolids, coralline algal and echinoderm debris. (E) Bioclastic pack/grainstone with coralline algae, small and larger benthic foraminifera. Dolomite and equant to poikilotopic calcite cements infill pores, some after leaching of aragonitic bioclasts. (F) Larger benthic foraminifera and coralline algal bioclastic grainstone. Fractures through coralline algae and other pore spaces are filled with equant calcite cement. (G) Bioclastic pack/wackestone including miliolids and coralline algae. Fractures and pores after leached out aragonitic bioclasts are filled with granular mosaic to equant calcite cements. (H) Siliciclastic bioclastic packstone with microdolomite rhombs in matrix.

Minor porosity along dissolution seam. (I) Gastropod, echinoderm plate, coralline algae, imperforate, perforate and planktonic foraminifera in bioclastic packstone.

Figure 17) Plane-polarised light thin-section photomicrographs from outer-shelf and shelf-margin carbonate deposits from the West Baram Hinge Zone area. Samples are from the first 'build-out' carbonate sequence directly proceeding the phase of siliciclastic progradation over the shelf margin from 3837–3847 m that date to between 15.7–15.3 Ma (A–D: Well G, Burdigalian to Langhian: see Figure 4) and those from the aggradational terminal carbonate deposits between 3400–3440 m that date to around 11.4–7.0 Ma (E–I: Well Z, Tortonian: see Figure 4). Samples are shown in order of deepest (A) to shallowest (I) within these intervals. (A) Larger benthic foraminifera bioclastic packstone with dolomite partially infilling/replacing matrix and concentrated along a dissolution seam below the larger foraminifera. Minor intergranular, matrix and fracture porosity. (B) Larger benthic foraminifera and echinoderm-rich bioclastic grainstone with syntaxial overgrowths on echinoderm material. Dolomite partially infills intergranular porosity and there was late leaching of bioclasts (top left). (C) Larger benthic foraminifera and echinoderm-rich bioclastic grainstone with abundant syntaxial overgrowths on echinoderm material. Dolomite partially infills intergranular porosity and there is minor late leaching of bioclasts (particularly coralline algae). (D) Larger benthic foraminifera bioclastic grainstone with dolomite partially infilling intergranular porosity. (E) Coral bioclastic grainstone with drusy to blocky non-ferroan calcite cement replacing aragonitic components and infilling intergranular pore spaces. Minor moldic/intergranular porosity remains, and is partially filled by dolomite. (F) Coral

bioclastic float/packstone with drusy to blocky non-ferroan calcite cement replacing aragonitic components and infilling intergranular pore spaces. Minor moldic porosity remains. (G) Coral and coralline algal-rich bioclastic grainstone with blocky non-ferroan calcite cement replacing aragonitic components and infilling intergranular pore spaces and fractures. Minor intergranular/fracture porosity partially filled by minor dolomite. (H) Coral and coralline algal-rich bioclastic grain/packstone with blocky non-ferroan calcite cement infilling after dissolved out aragonitic components. Late dissolution and minor dolomitisation are apparent. (I) Coral-rich bioclastic grainstone with drusy to blocky non-ferroan calcite cement infilling pores after dissolved out aragonitic components and partially cementing along fractures.

Figure 18) Plane-polarised light thin-section photomicrographs from Serravallian outer-shelf carbonate deposits overlying the SW Serunai High (Well A: see Figure 4). (A) Dolomitised bioclastic wackestone showing intragranular porosity in chambers of foraminifera and some intercrystalline porosity in dolomitised fine-grained matrix. Dolomite rhombs also seen in chambers of foraminifera. (B) Larger benthic foraminifera bioclastic grainstone showing excellent porosity, with pore spaces 'supported' by slightly meniscate, blocky cement (with cement partially dolomitised (see Figure 16e)). (C) Dolomitised silty bioclastic pack/wackestone with fine, subangular quartz grains showing dolomitization of fine matrix and dissolution of bioclasts. (D) Dolomitised silty bioclastic grain/pack/wackestone (from coarser grain/packstone area) showing isopachous fringing cement partially occluding primary intergranular porosity. (E) Foraminifera bioclastic grainstone showing excellent porosity, with pore spaces 'supported' by slightly

meniscate, blocky cement (now partially replaced by dolomite). (F) Dolomitised bioclastic wackestone showing intragranular porosity in chambers of foraminifera and some intercrystalline porosity in dolomitised fine-grained matrix (including some leaching of bioclastic material).

Figure 19) Scanning electron microsope images from Burdigalian to Langhian outer-shelf and shelf-margin carbonate deposits from the West Baram Hinge Zone area from the first 'build-out' carbonate sequences directly proceeding the phase of siliciclastic progradation over the shelf margin from 3837–3847 m that date to between 15.7–15.3 Ma (Well G: see Figure 4). Instrument operating conditions and scales are shown at the base of each plate. (A) Partially recrystallised micritic matrix in chambers of coralline algae. Original bioclast walls have been leached with some remaining calcite microspar and microdolomite rhombs precipitated. Rhombs of dolomite partially replacing matrix (E) and infilling pore spaces (B and C) or fractures (D). (F) Blocky to equant calcite cement partially infilling pore. (G–I) Rhomb shaped dolomite crystals partially infilling pores and affected by leaching.

Figure 20) Scanning electron microsope images from outer-shelf and shelf-margin carbonate deposits from the West Baram Hinge Zone area from the Tortonian aggradational terminal carbonate deposits between 3400 and 3440 m that date to around 11.4–7.0 Ma (Well Z: see Figure 4). Instrument operating conditions and scales are shown at the base of each plate. (A) Pore space partially infilled by blocky calcite cement. (B and C) Large

calcite crystal formed as a syntaxial overgrowth on echinoderm material in region of intergrown blocky to equant calcite crystals. Minor kaolinite-like clay beneath syntaxial overgrowth. (D–E) Kaolinite or similar related clay mineral infilling pores. (F) Kaolinite or similar related clay mineral concentrated in region of dissolution seam in which rhomb-shaped dolomite crystals have been precipitated. (G–I) Leaching of bioclasts, including chamber walls of coralline algae (H and I). In 'G' a fracture cutting the bioclast was filled by calcite prior to leaching. In 'I' there is also an echinoderm plate with overgrowth cement (centre) and (right) regions of micritic matrix with microporosity as well as intergrown blocky to equant calcite crystals.

Figure 21) Plane-polar (PL) and cathodoluminescent (CL) thin-section photomicrograph pairs from outer-shelf and shelf-margin carbonates. (A/A' and B/B') Burdigalian to Langhian samples from the first of the 'build-out' carbonate sequences directly proceeding the phase of siliciclastic progradation over the shelf margin in the Baram Hinge Zone area (i.e. from depths of 3837–3847 m and dated between 15.7 and 15.3 Ma). (C/C' and D/D') Tortonian samples from the youngest aggradational to backstepping terminal shelf margin carbonate sequences in the Baram Hinge Zone (i.e. from depths of 3400–3440 m and dated between 7.0 and 11.4 Ma). For all samples bioclasts including (larger) benthic foraminifera ((L)BF) coralline algae (CA), echinoderm debris (E) and micritic matrix (M) show dull- to bright-luminescence with these components having brighter more orange luminescence from 3837 to 3847 m whereas those from 3400 to 3440 m show more magenta tones. Dissolution seams and/or stylolites (S) have bright- (B/B') or non-luminescence (A/A' and C/C'). Microdolomites developed along seams or stylolites may

show zoned bright- and non-luminescence (A/A'). Blocky cements around bioclasts (A/A') and equant calcite cements infilling pore space, replacing corals (C) and infilling fractures (F) are non-luminescent.

Figure 22) Paragenetic sequence of diagenetic events affecting outer-shelf low-, to high-energy carbonates on the West Baram High of late Early and Middle Miocene ages (15–19 Ma – Burdigalian to Langhian, Well G). Plot on the right applies to the backstepping sequence immediately post-dating widespread Lower Miocene shelf-wide carbonate deposition from between 4570 and 4414 m and dating to around 19.0–18.7 Ma. Plots on the left and the middle apply to the first 'build-out' carbonate sequences directly proceeding the phase of siliciclastic progradation over the shelf margin from 3837 to 3847 m that date to between 15.7 and 15.3 Ma. Relative timing of events is on the basis of petrographic observations.

Figure 23) Paragenetic sequence of diagenetic events affecting outer-shelf moderate-, to high-energy deposits from the terminal backstepping to aggradational carbonate sequences on the West Baram High of Tortonian age (7.0–11.4 Ma, Well Z). Relative timing of events is on the basis of petrographic observations.

Figure 24) Paragenetic sequence of diagenetic events affecting outer-shelf low- to high-energy deposits from the Serravallian carbonates (12–14 Ma) overlying the SW Serunai High (Well A). Relative timing of events is on the basis of petrographic observations.

Figure 25) Schematic illustrating and describing trends in deposition, diagenesis and reservoir quality of carbonate systems from inner-, middle- and outer-shelf settings on the NW Borneo Shelf together with major controlling influences. Simplified version of Figure 4 is the background to the central panel.

Figure 1

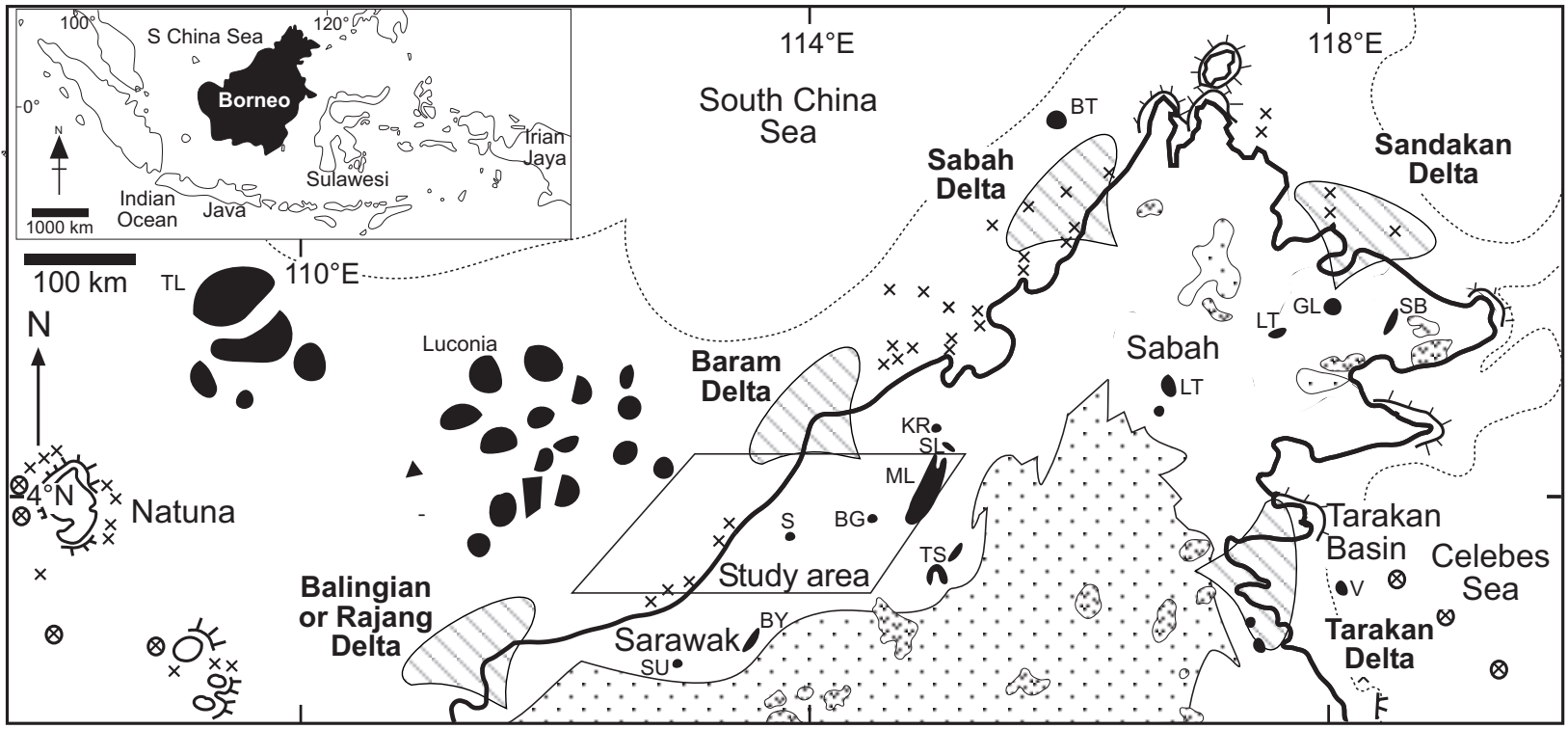

Cenozoic carbonates (outcrop and subsurface) - unit names below

BG - Batu Gading	KR - Keramit Limestone	SL - Selidong Limestone
BT - Balambang Limestone	LT - Limestone in Labang/Tanjong Fms.	SU - Subis Limestone
BY - Bekuyat Limestone	ML - Melinau Limestone	TL - Terumbu Limestone
GL - Gomantong Limestone	S - Bukit Sarang Limestone	TS - Tujoh-Siman Limestone
	SB - Limestone in Sebahat Fm.	V - Vanda Limestone

× Modern patch reefs
⊗ Modern atolls
Modern barrier or fringing reefs
} Mostly after Spalding et al. 2001
Modern shelf margin - 200 m water depth

Location of Neogene to modern deltas (shown schematically)

Cenozoic Volcanics

Areas of Cenozoic clastic sedimentation

Pre-Cenozoic sedimentary, igneous and metamorphic lithologies

Figure 2

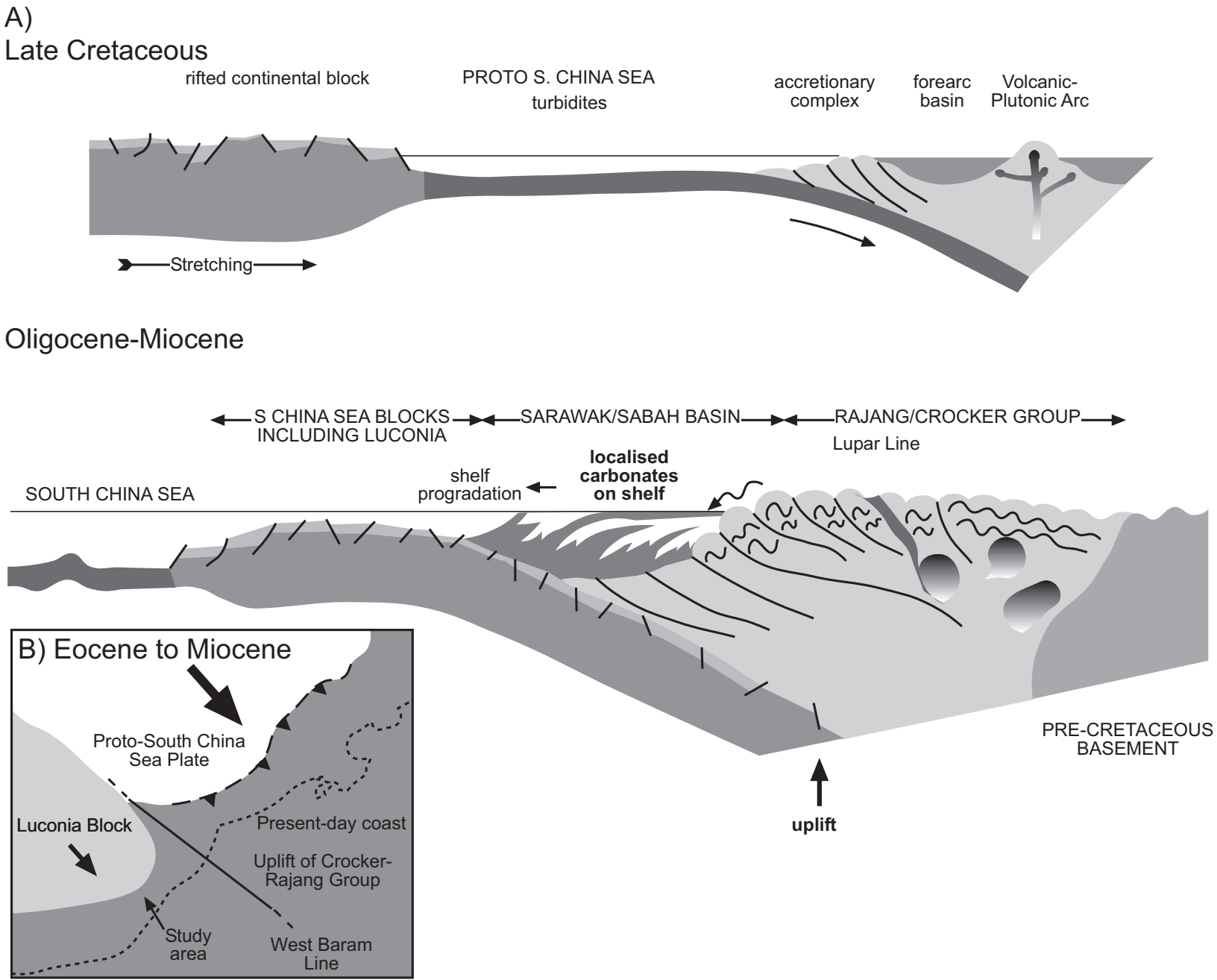
A)
Late Cretaceous
rifted continental block
PROTO S. CHINA SEA
turbidites
accretionary complex
forearc basin
Volcanic-Plutonic Arc
Stretching
Oligocene-Miocene
S CHINA SEA BLOCKS INCLUDING LUCONIA
SARAWAK/SABAH BASIN
RAJANG/CROCKER GROUP
Lupar Line
SOUTH CHINA SEA
shelf progradation
localised carbonates on shelf
PRE-CRETACEOUS BASEMENT
uplift
B) Eocene to Miocene
Proto-South China Sea Plate
Luconia Block
Present-day coast
Uplift of Crocker-Rajang Group
Study area
West Baram Line

Figure 3

Click here to download high resolution image

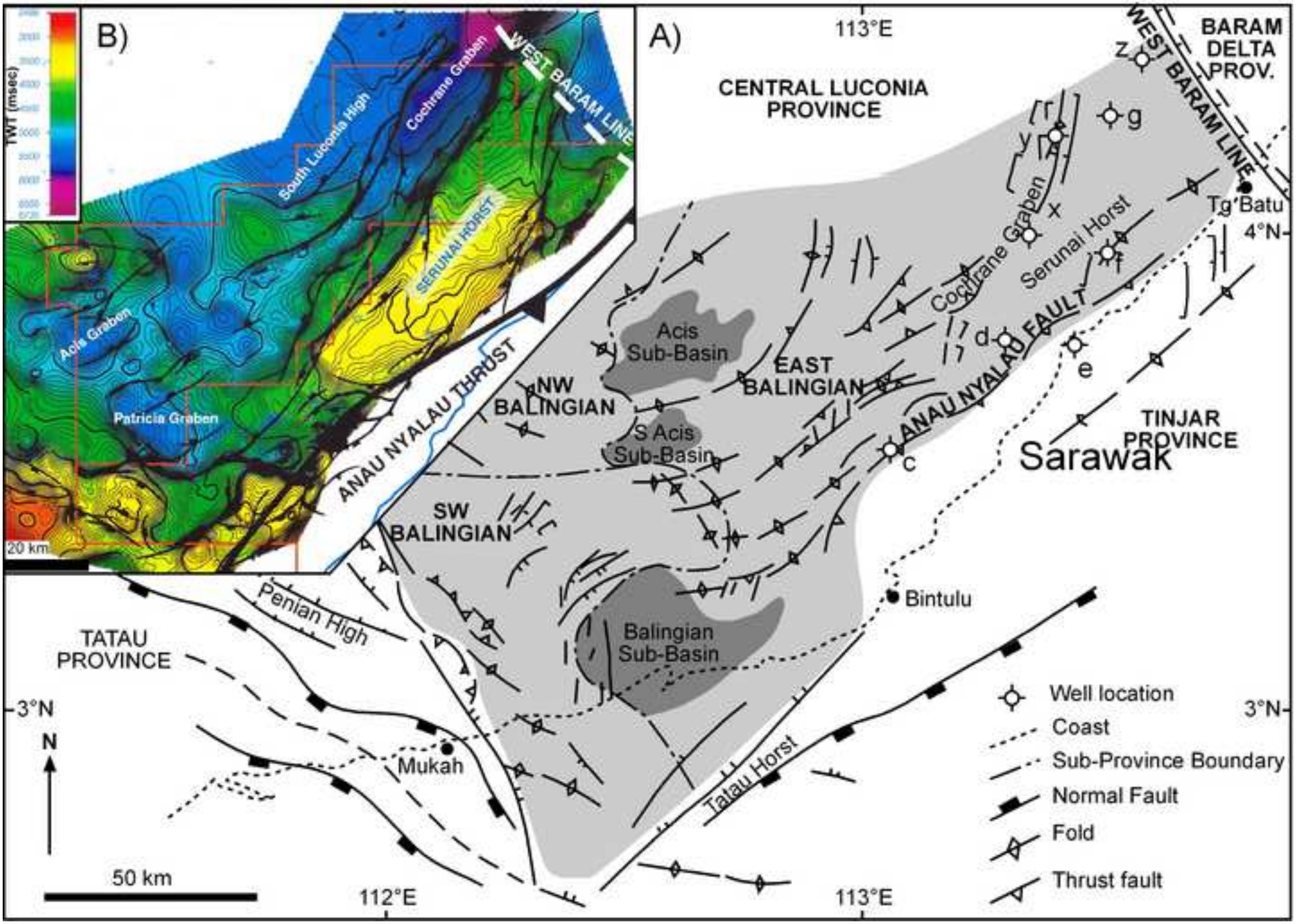

Figure 4

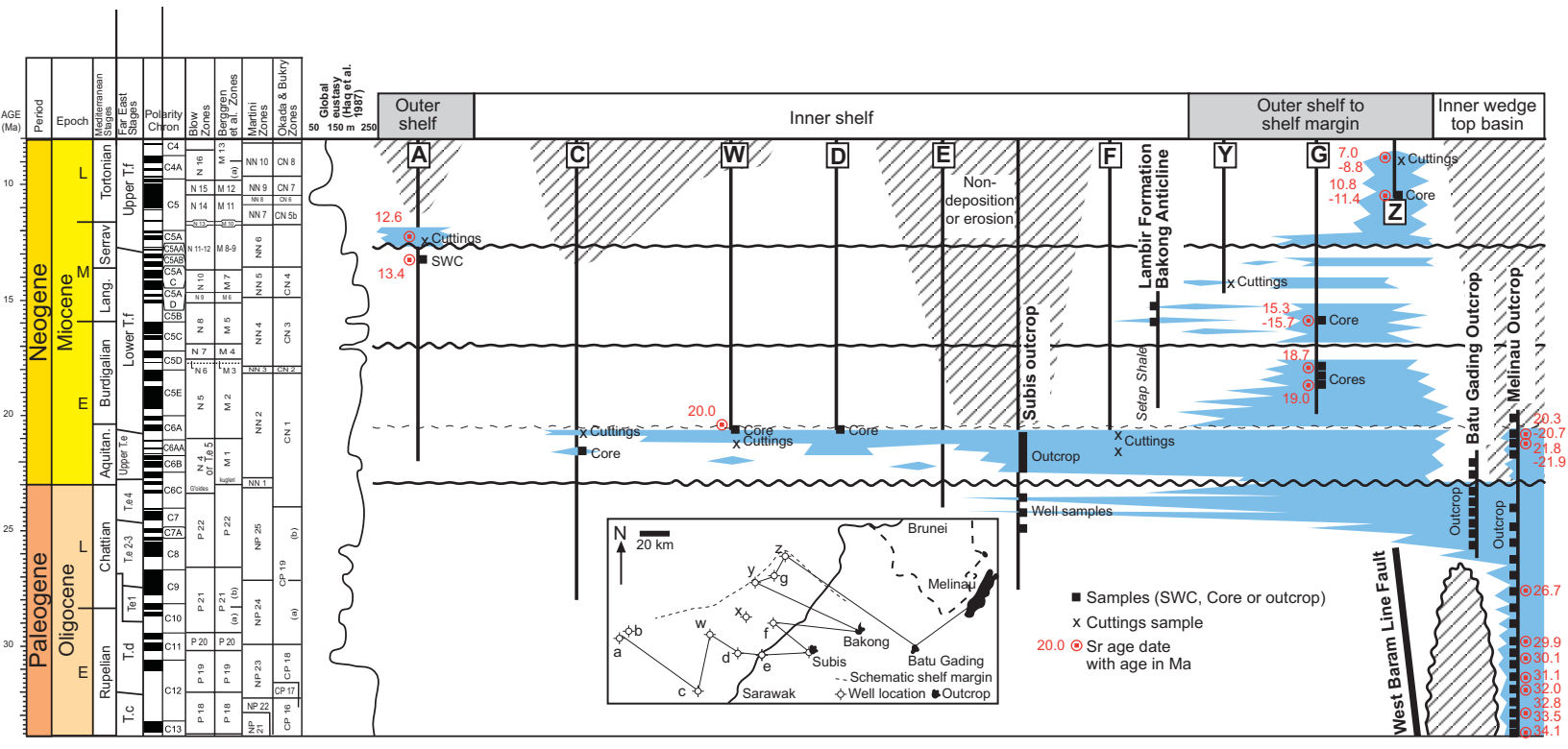
AGE (Ma)
Period
Epoch
Mediterranean Stages
Far East Stages
Polarity Chron
Blow Zones
Berggren et al. Zones
Martini Zones
Okada & Bukry Zones
Global sea-level (Haq et al. 1987)
50 150 m 250
Neogene
Miocene
Paleogene
Oligocene
Tortonian
Serrav.
Lang.
Burdigalian
Aquitan.
Chattian
Rupelian
Upper T.f
Lower T.f
T.e
T.d
T.c
Outer shelf
Inner shelf
Outer shelf to shelf margin
Inner wedge top basin
A
C
W
D
E
F
Y
G
Z
Non-deposition or erosion
Subis outcrop
Lambir Formation
Bakong Anticline
Setap Shale
Batu Gading Outcrop
Melinau Outcrop
West Baram Line Fault
12.6
13.4
Cuttings
SWC
Core
20.0
7.0
-8.8
10.8
-11.4
15.3
-15.7
18.7
19.0
Cores
Outcrop
Well samples
N
20 km
Brunei
Melinau
Bakong
Subis
Batu Gading
Sarawak
Schematic shelf margin
Well location
Outcrop
Samples (SWC, Core or outcrop)
Cuttings sample
Sr age date with age in Ma
20.3
20.7
21.8
21.9
26.7
29.9
30.1
31.1
32.0
32.8
33.5
34.1

Figure 5

Click here to download high resolution image

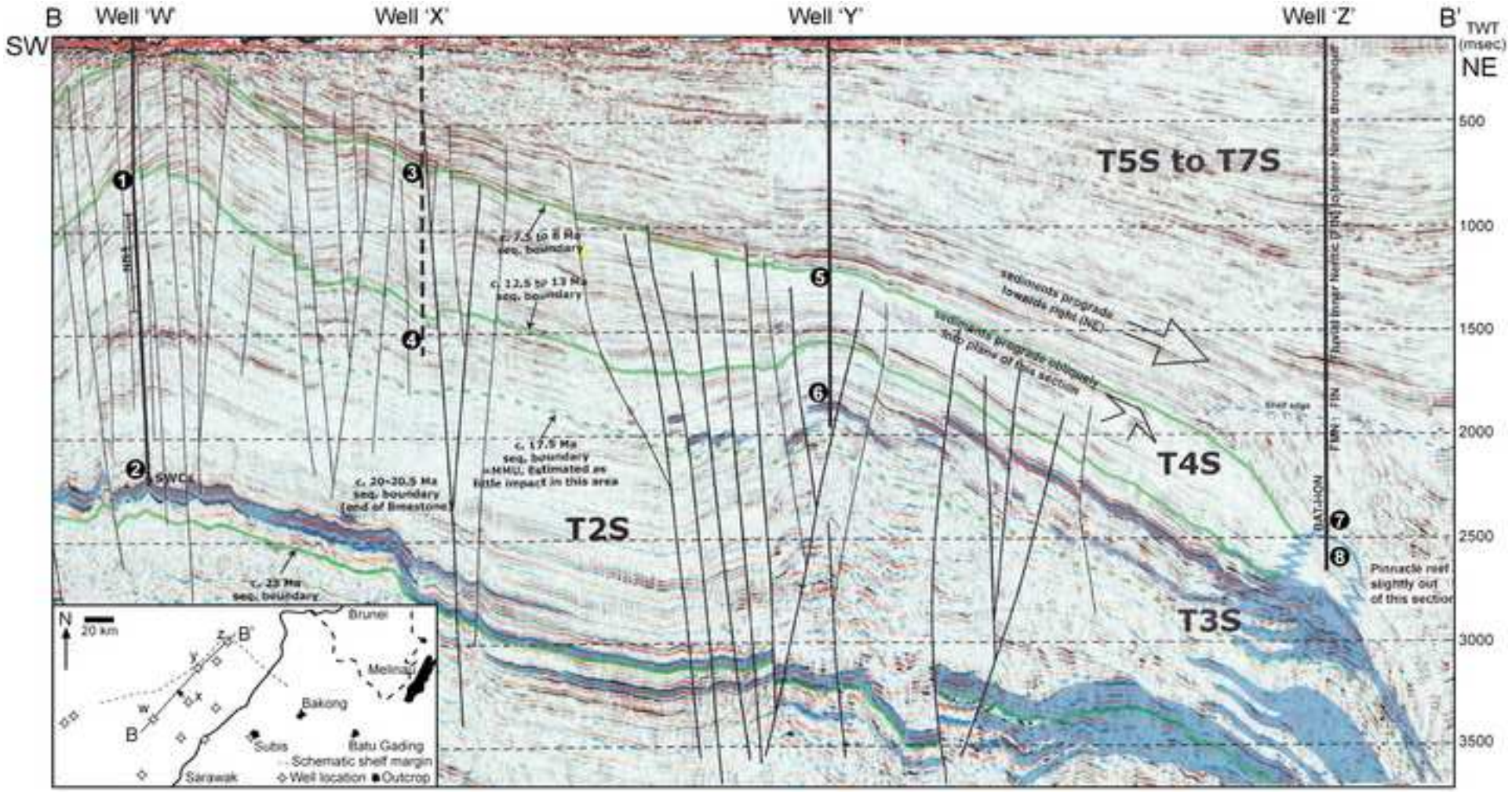

Figure 6

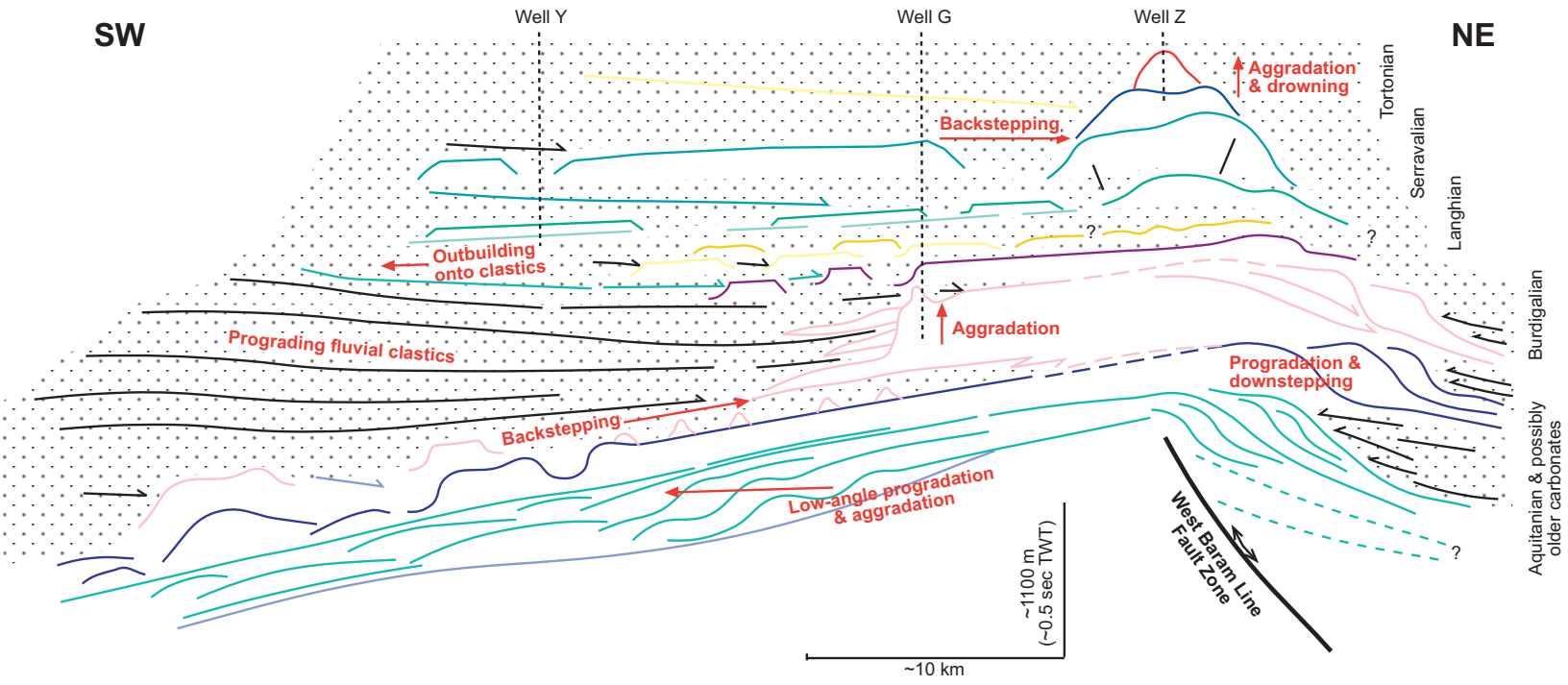
SW
NE
Well Y
Well G
Well Z
Aggradation & drowning
Backstepping
Tortonian
Serravalian
Langhian
Burdigalian
Aquitanian & possibly older carbonates
Outbuilding onto clastics
Prograding fluvial clastics
Aggradation
Progradation & downstepping
Backstepping
Low-angle progradation & aggradation
West Baram Line Fault Zone
~1100 m (~0.5 sec TWT)
~10 km
?

Figure 7

Click here to download high resolution image

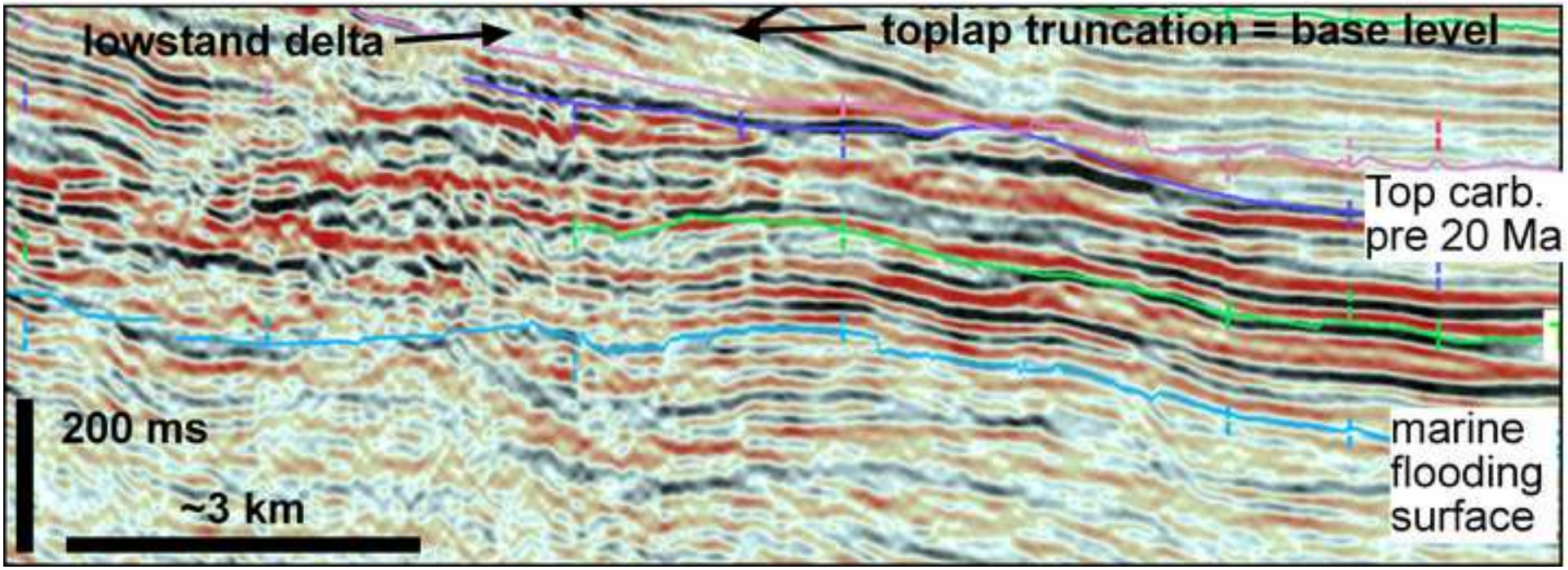

Figure 8

Click here to download high resolution image

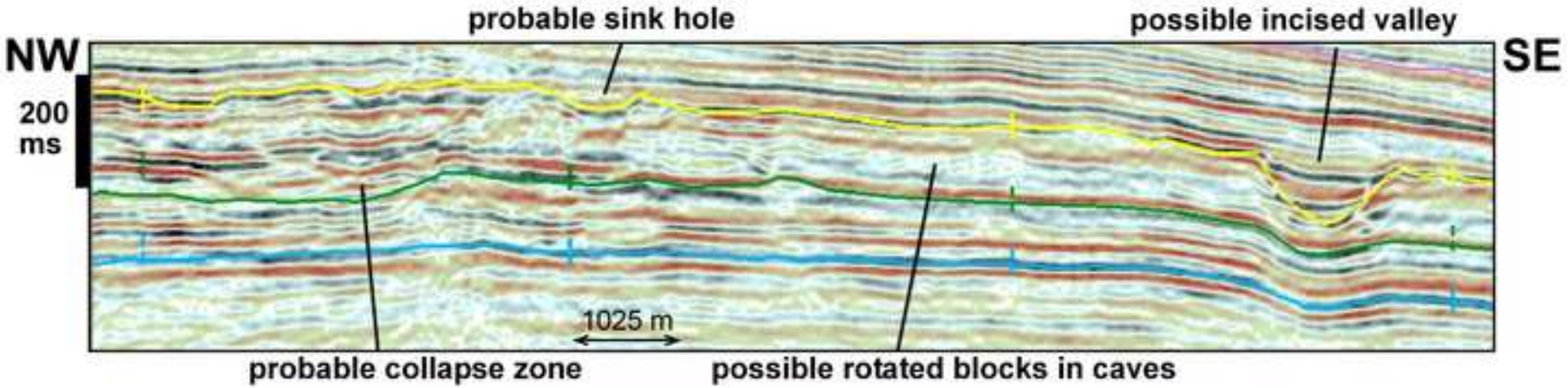

Figure 9

Click here to download high resolution image

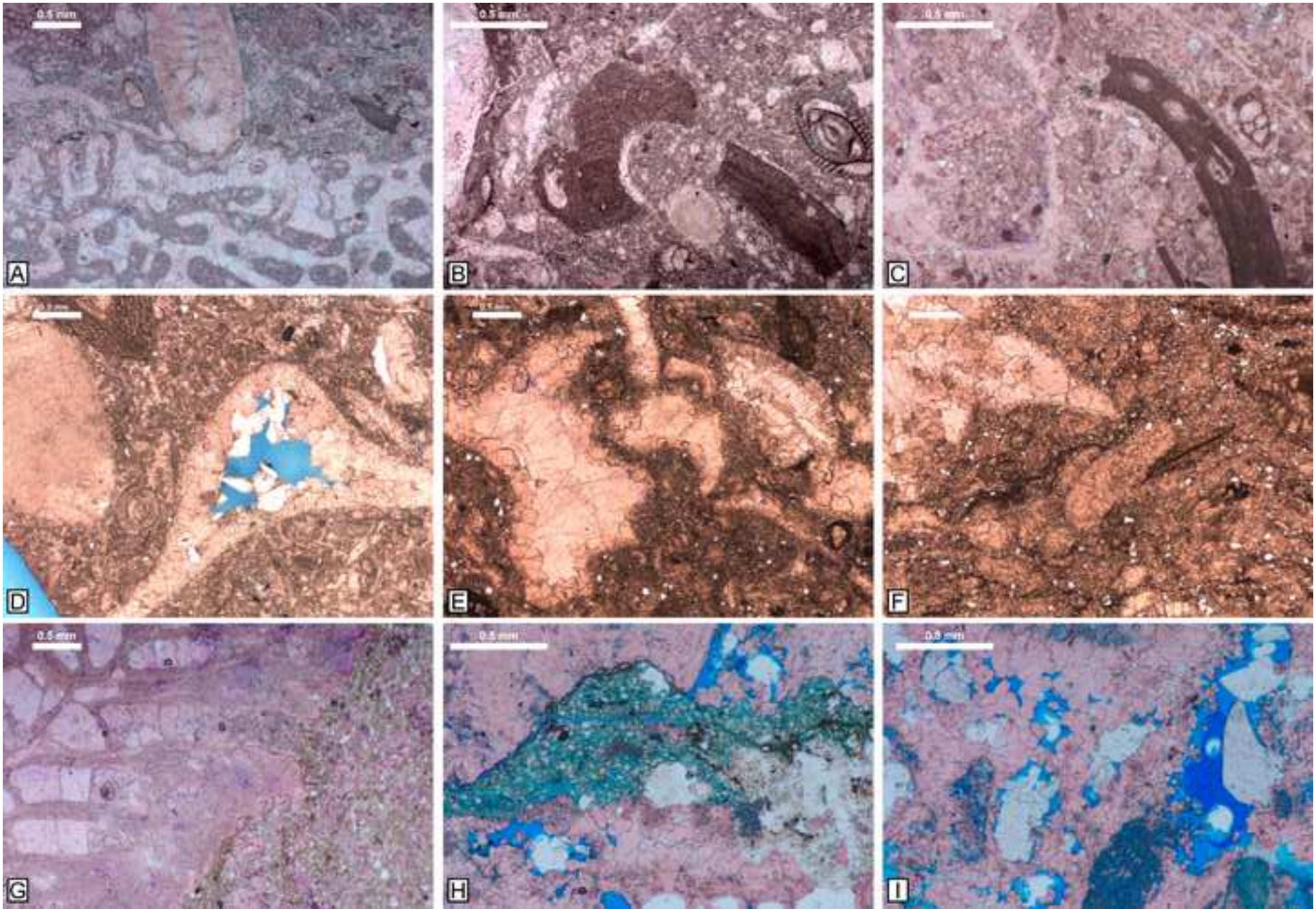

Figure 10

Click here to download high resolution image

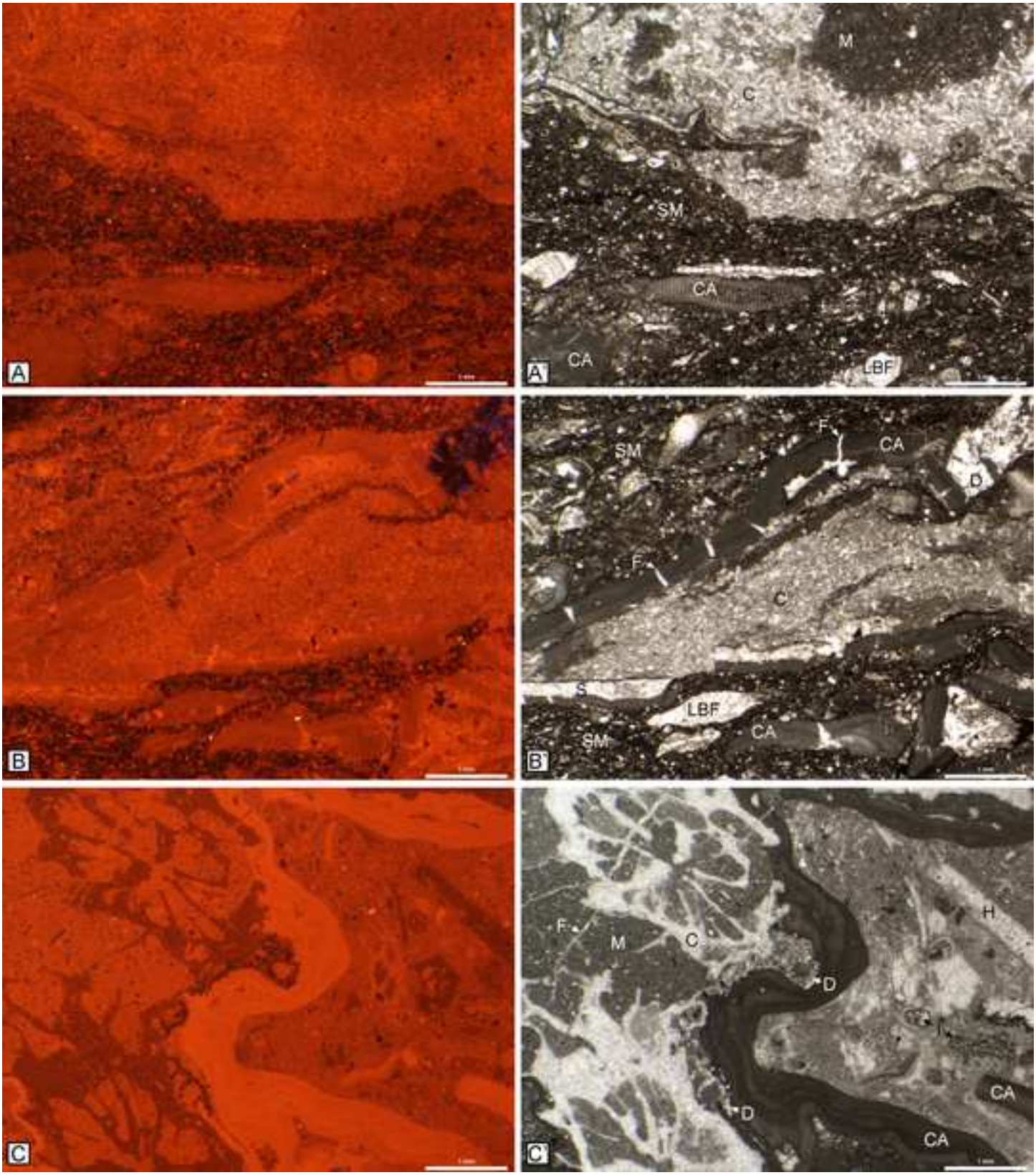

Figure 11

Click here to download high resolution image

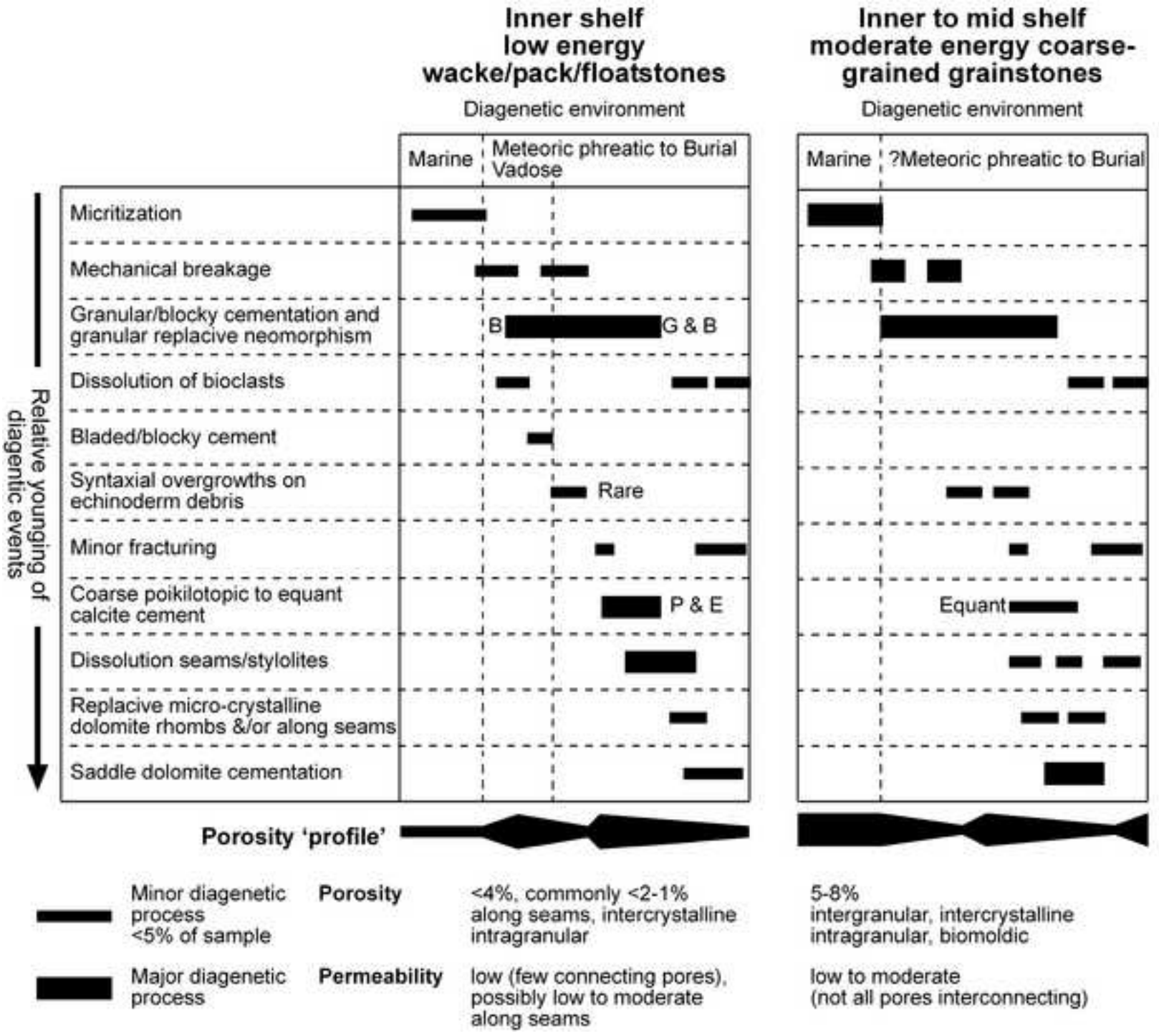

Figure 12

Click here to download high resolution image

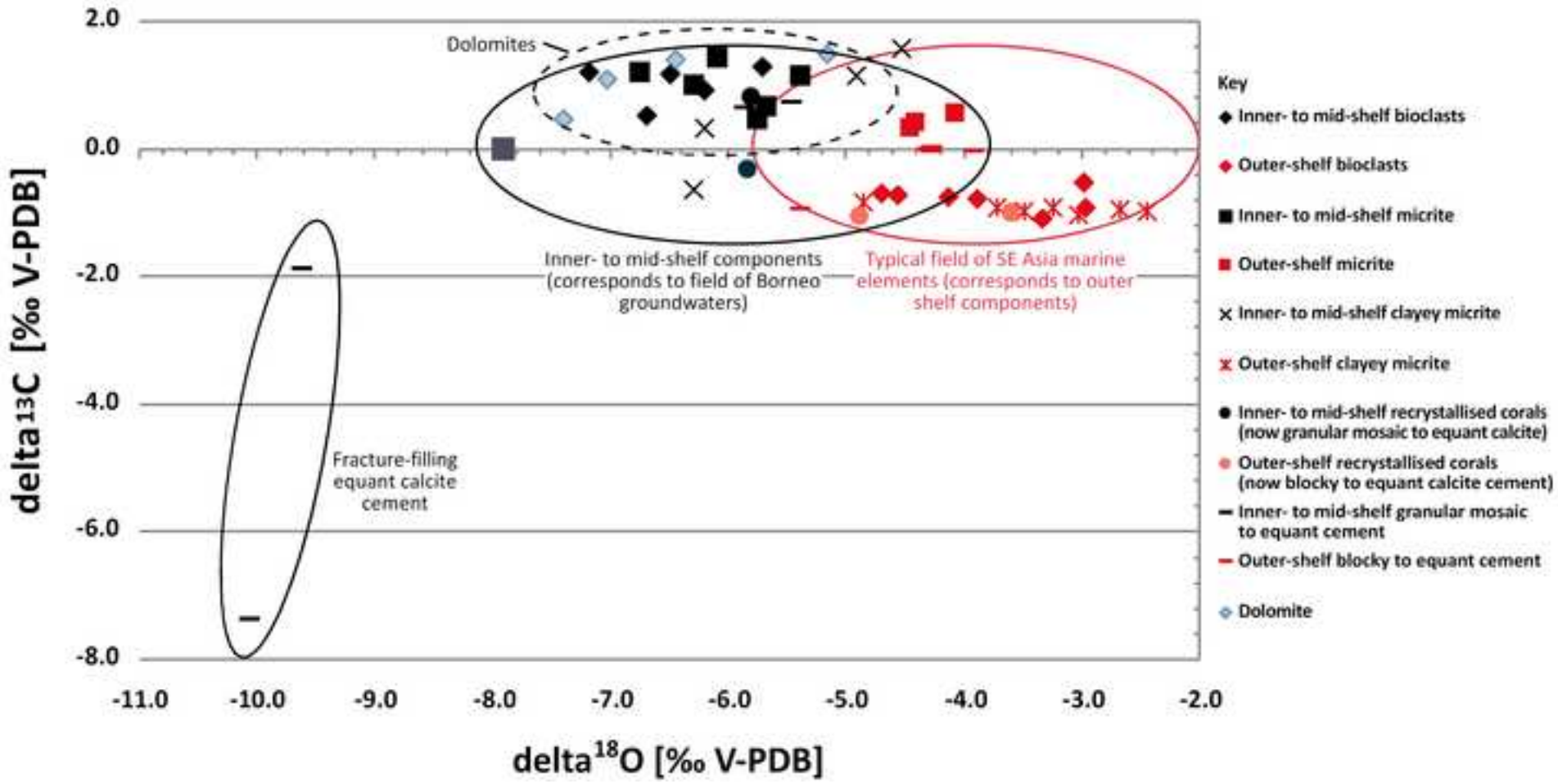

Figure 13

Click here to download high resolution image

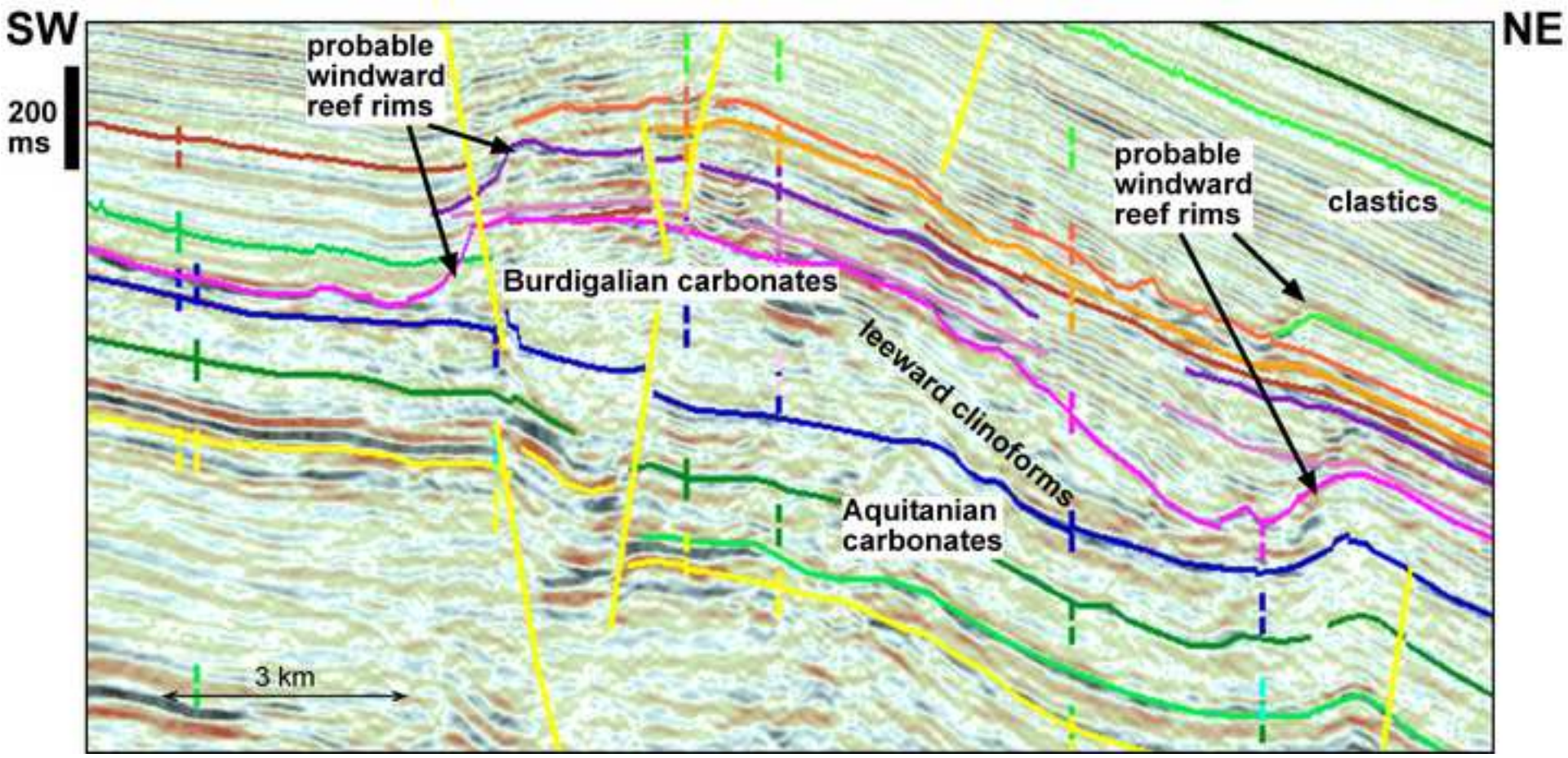

Figure 14

Click here to download high resolution image

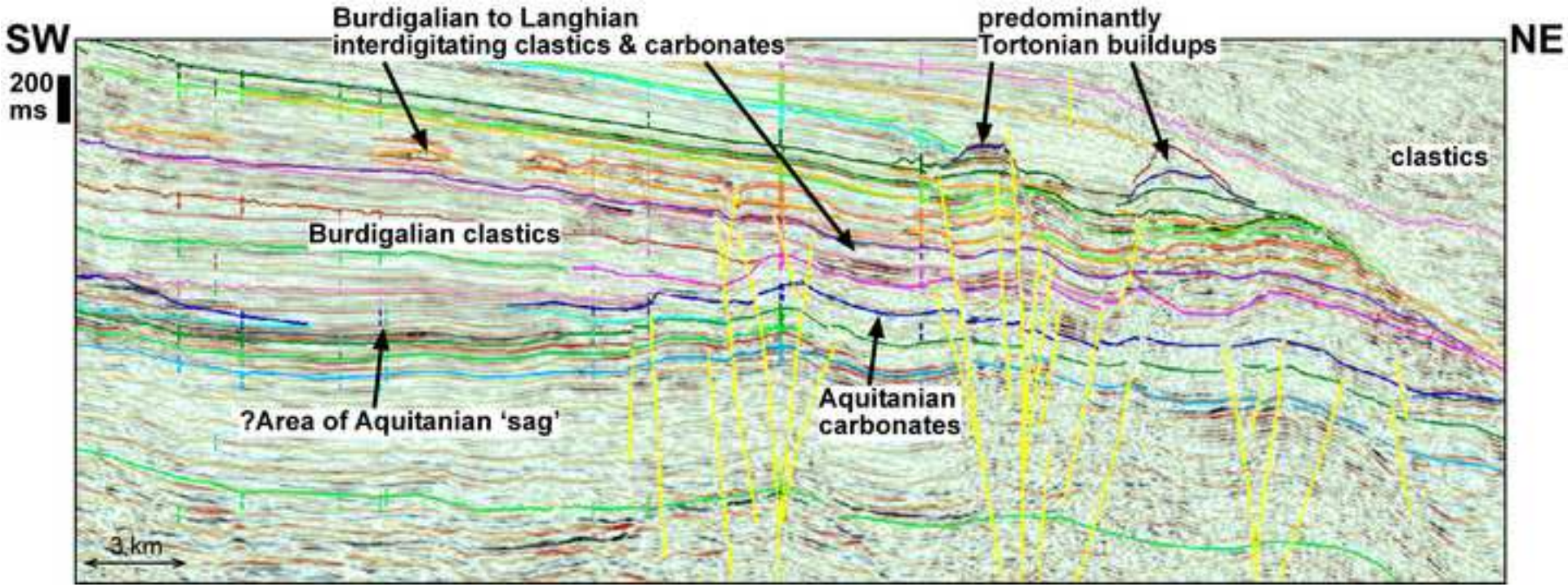

Figure 15

Click here to download high resolution image

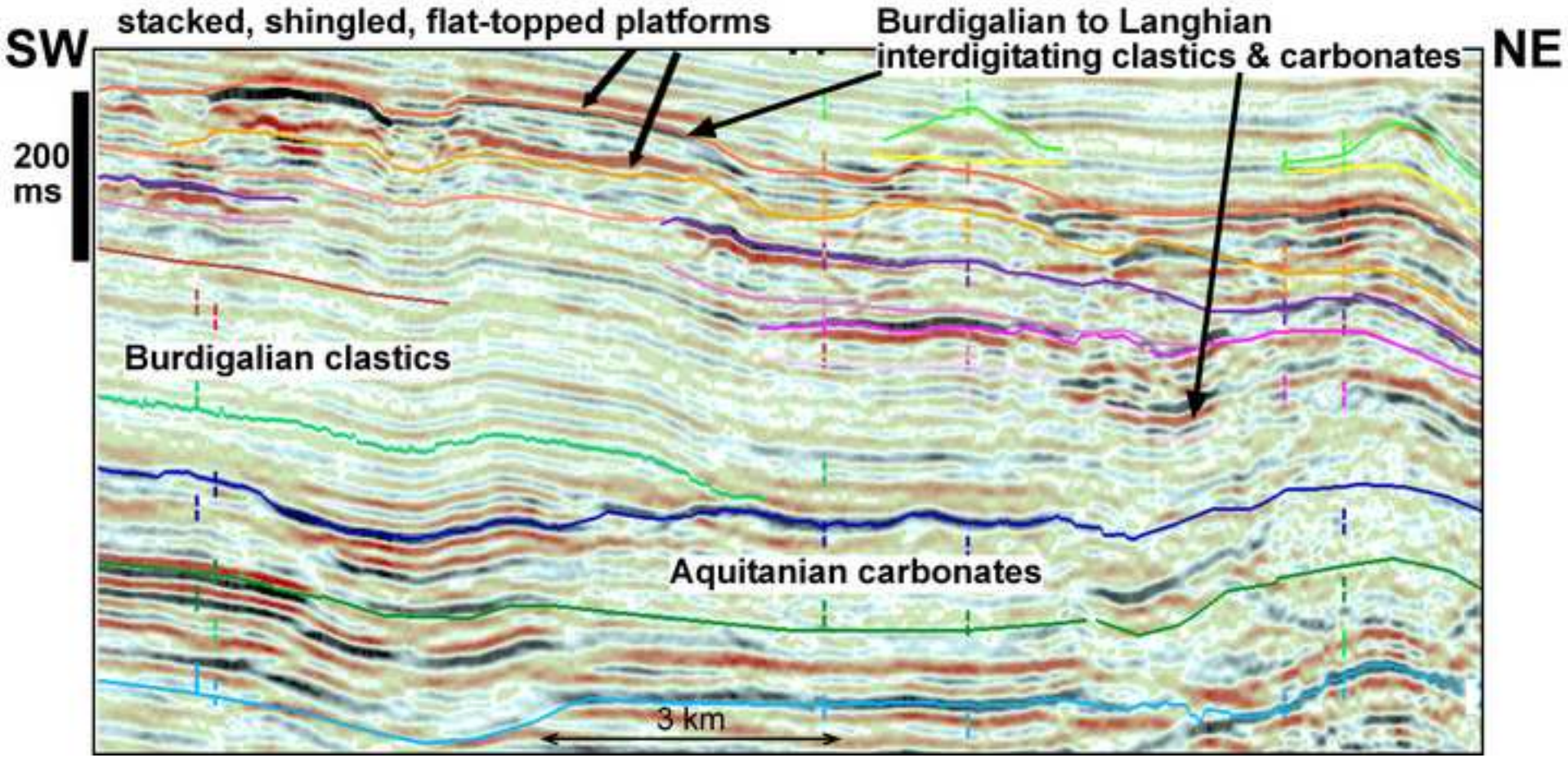

Figure 16

Click here to download high resolution image

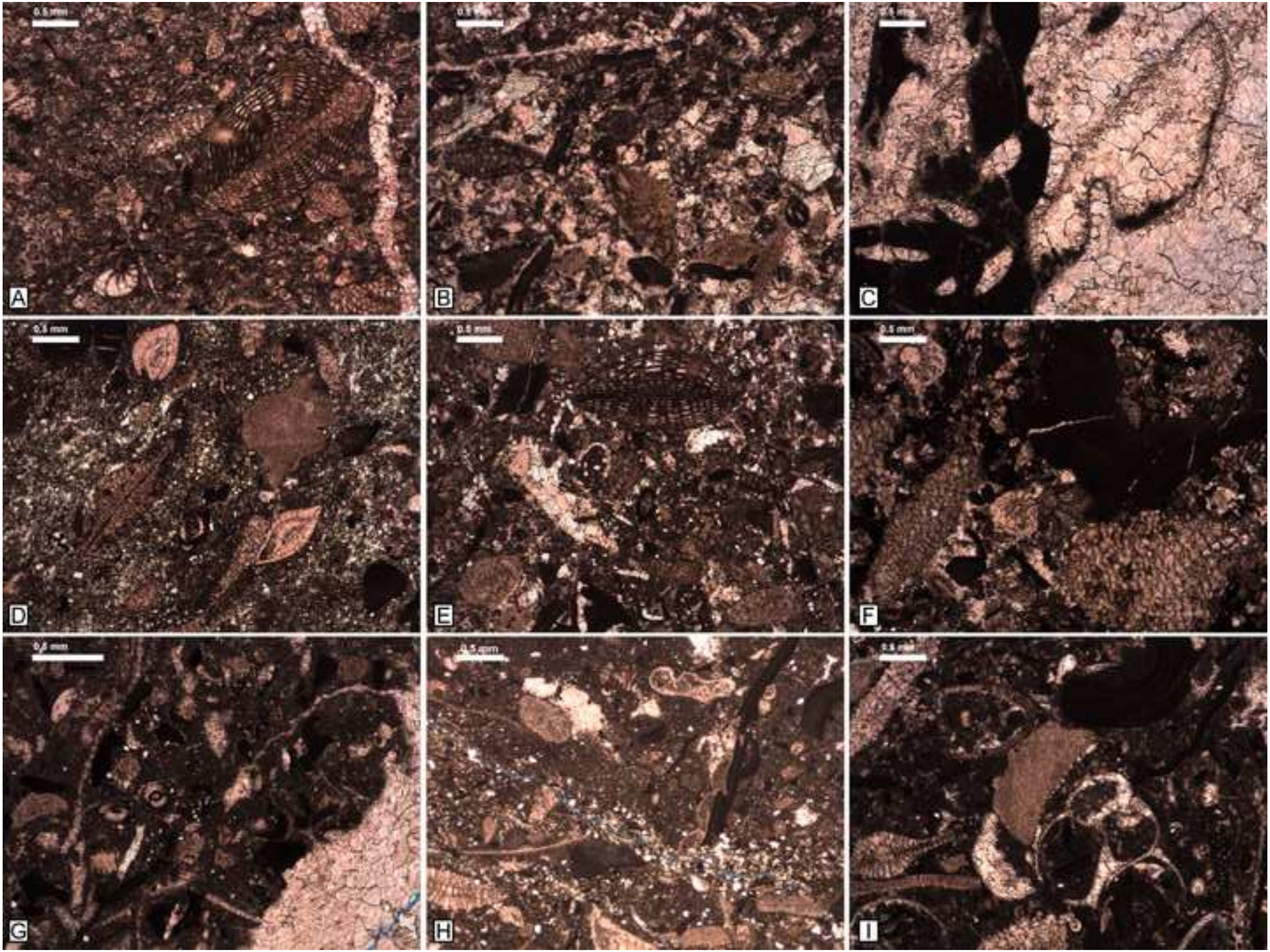

Figure 17

Click here to download high resolution image

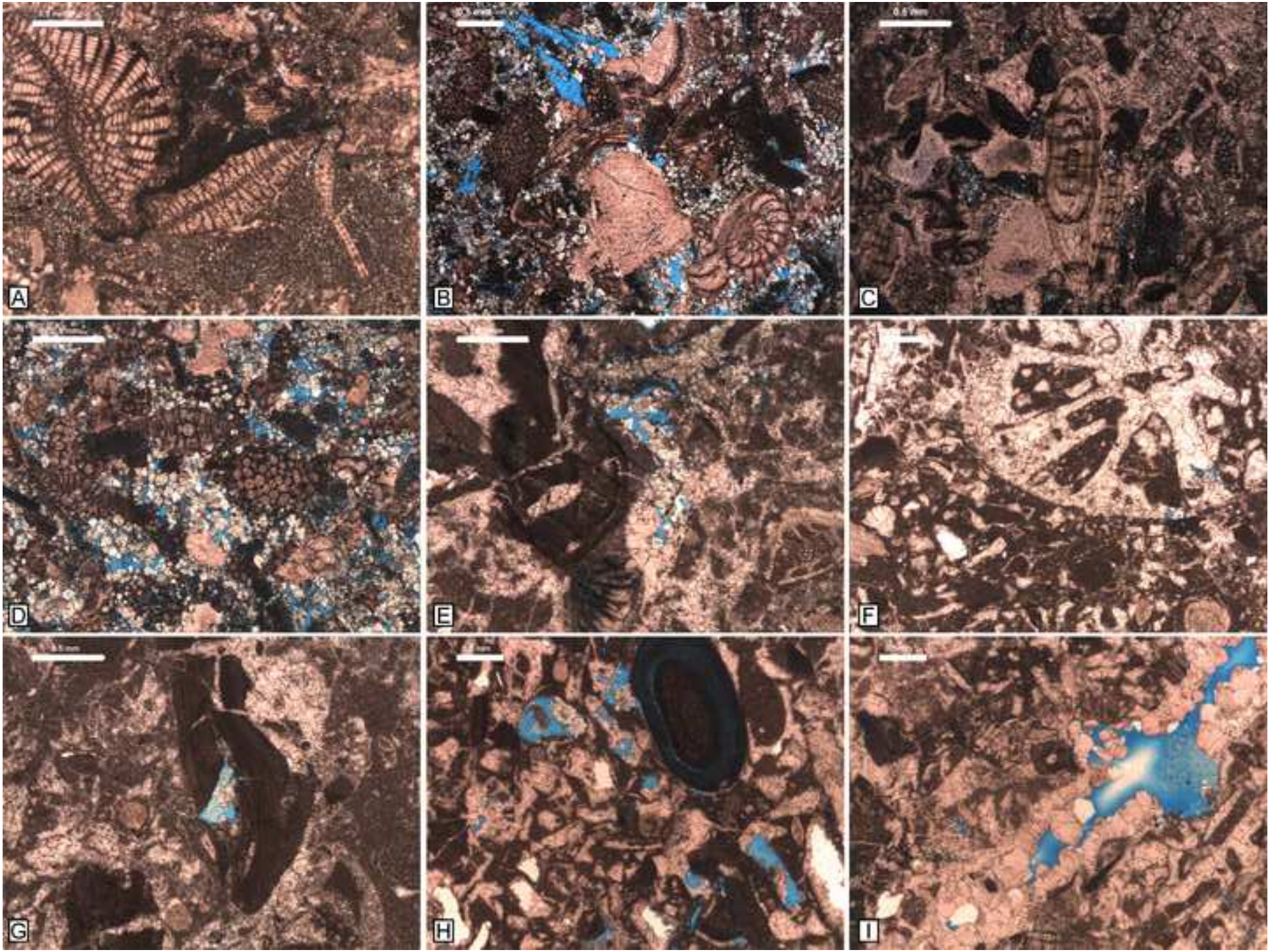

Figure 18

Click here to download high resolution image

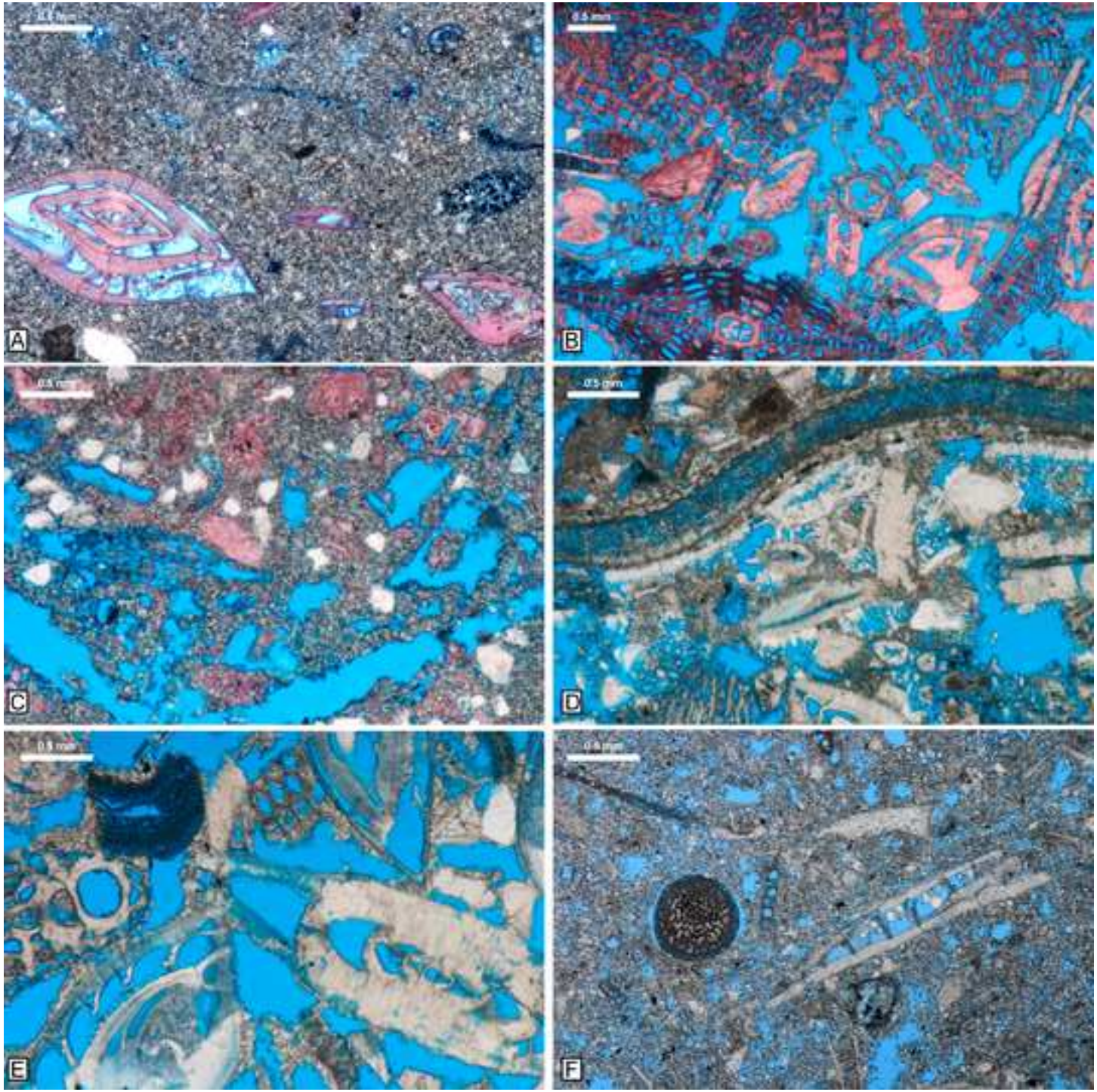

Figure 19

Click here to download high resolution image

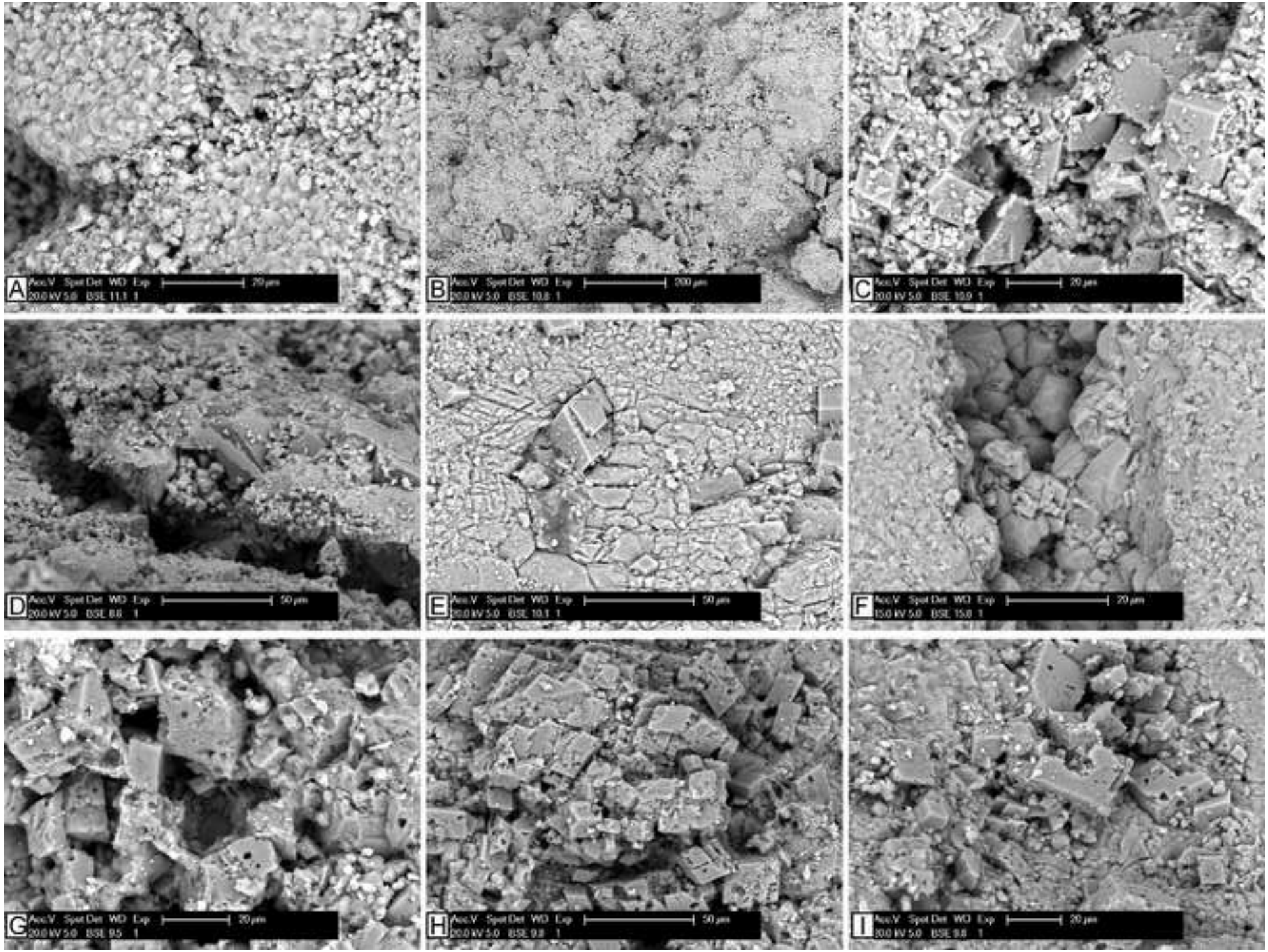

Figure 20

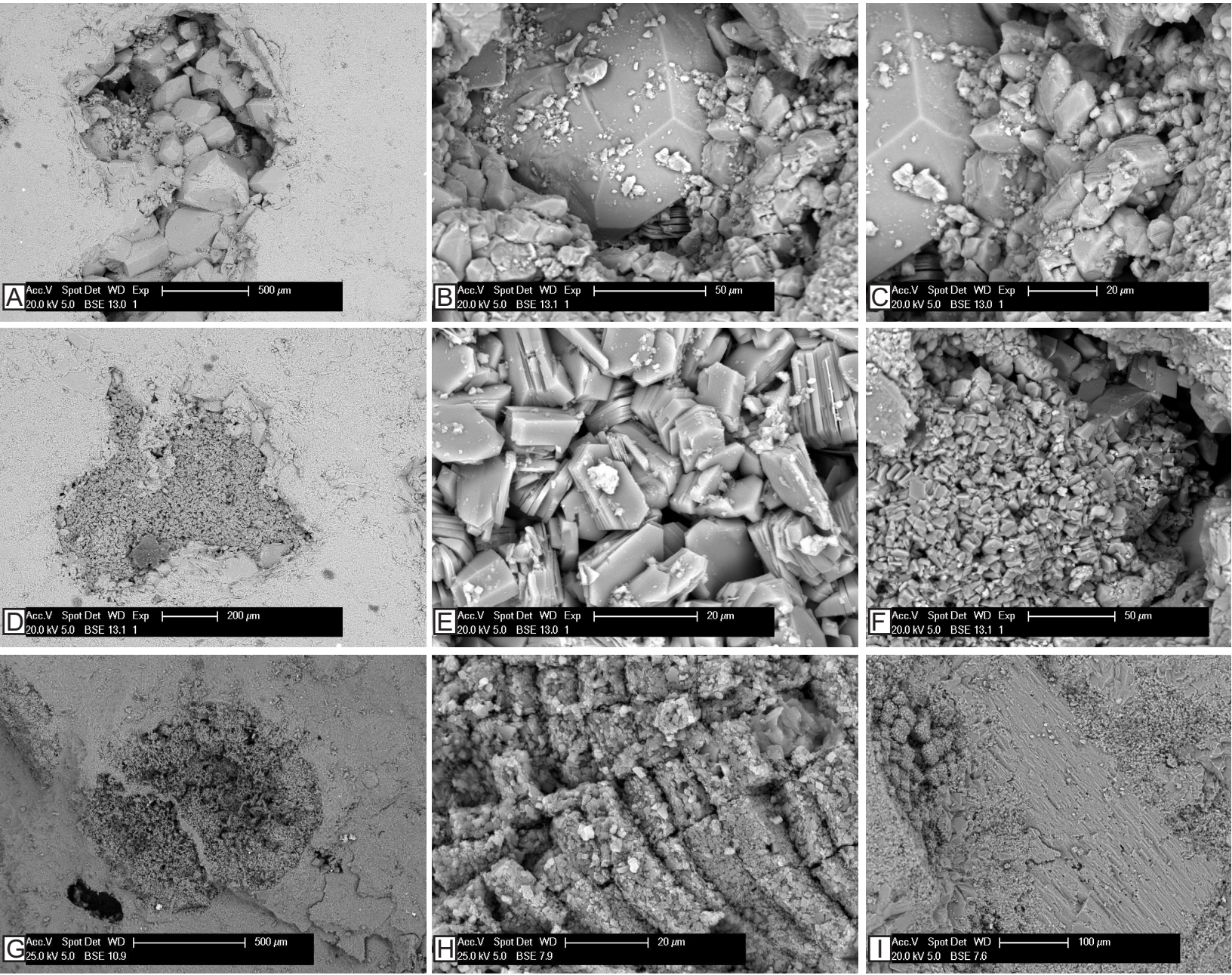
A
Acc.V Spot Det WD Exp 500 µm
20.0 kV 5.0 BSE 13.0 1
B
Acc.V Spot Det WD Exp 50 µm
20.0 kV 5.0 BSE 13.1 1
C
Acc.V Spot Det WD Exp 20 µm
20.0 kV 5.0 BSE 13.0 1
D
Acc.V Spot Det WD Exp 200 µm
20.0 kV 5.0 BSE 13.1 1
E
Acc.V Spot Det WD Exp 20 µm
20.0 kV 5.0 BSE 13.0 1
F
Acc.V Spot Det WD Exp 50 µm
20.0 kV 5.0 BSE 13.1 1
G
Acc.V Spot Det WD 500 µm
25.0 kV 5.0 BSE 10.9
H
Acc.V Spot Det WD 20 µm
25.0 kV 5.0 BSE 7.9
I
Acc.V Spot Det WD 100 µm
20.0 kV 5.0 BSE 7.6

Figure 21

Click here to download high resolution image

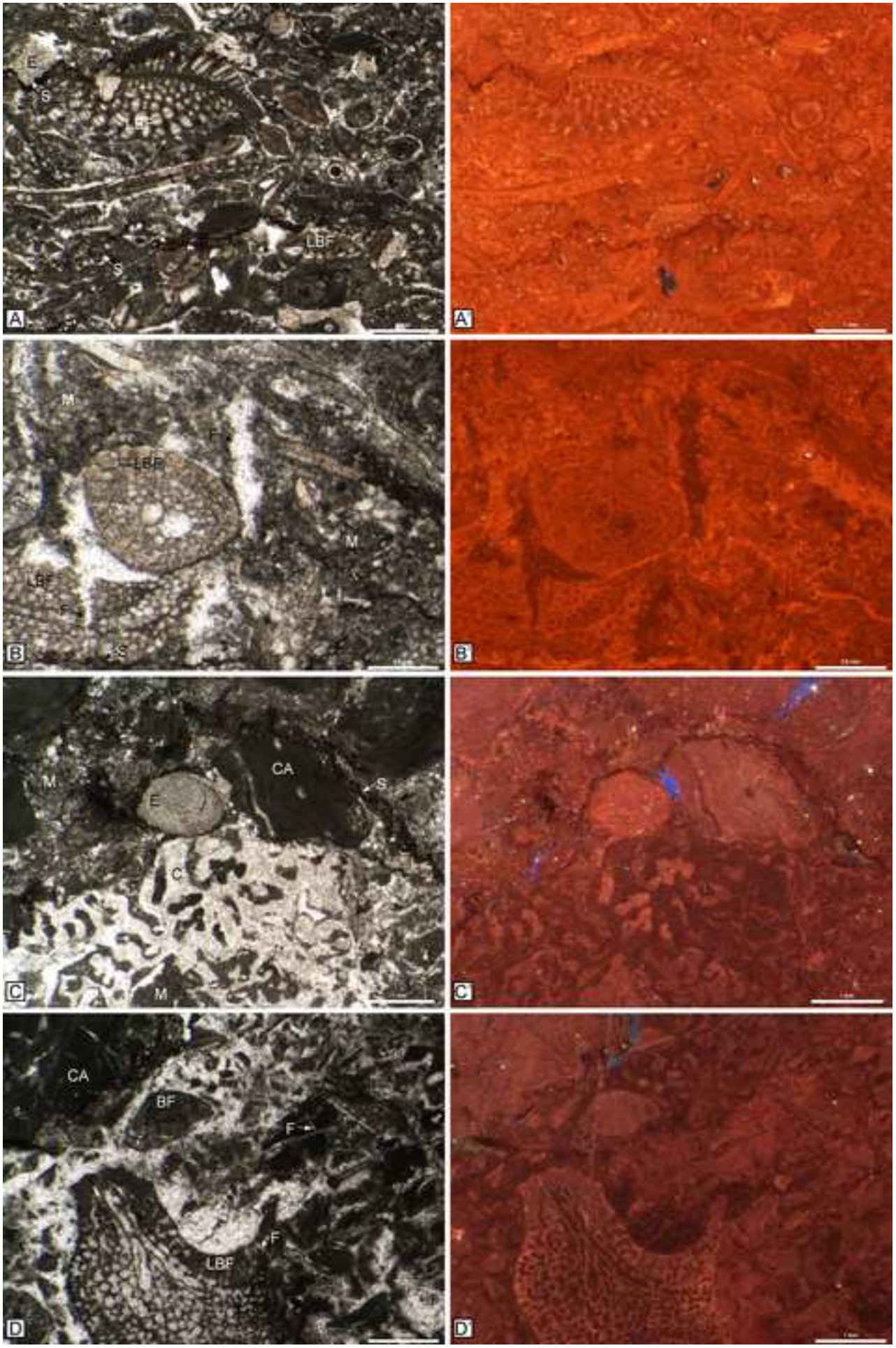

Figure 22

Click here to download high resolution image

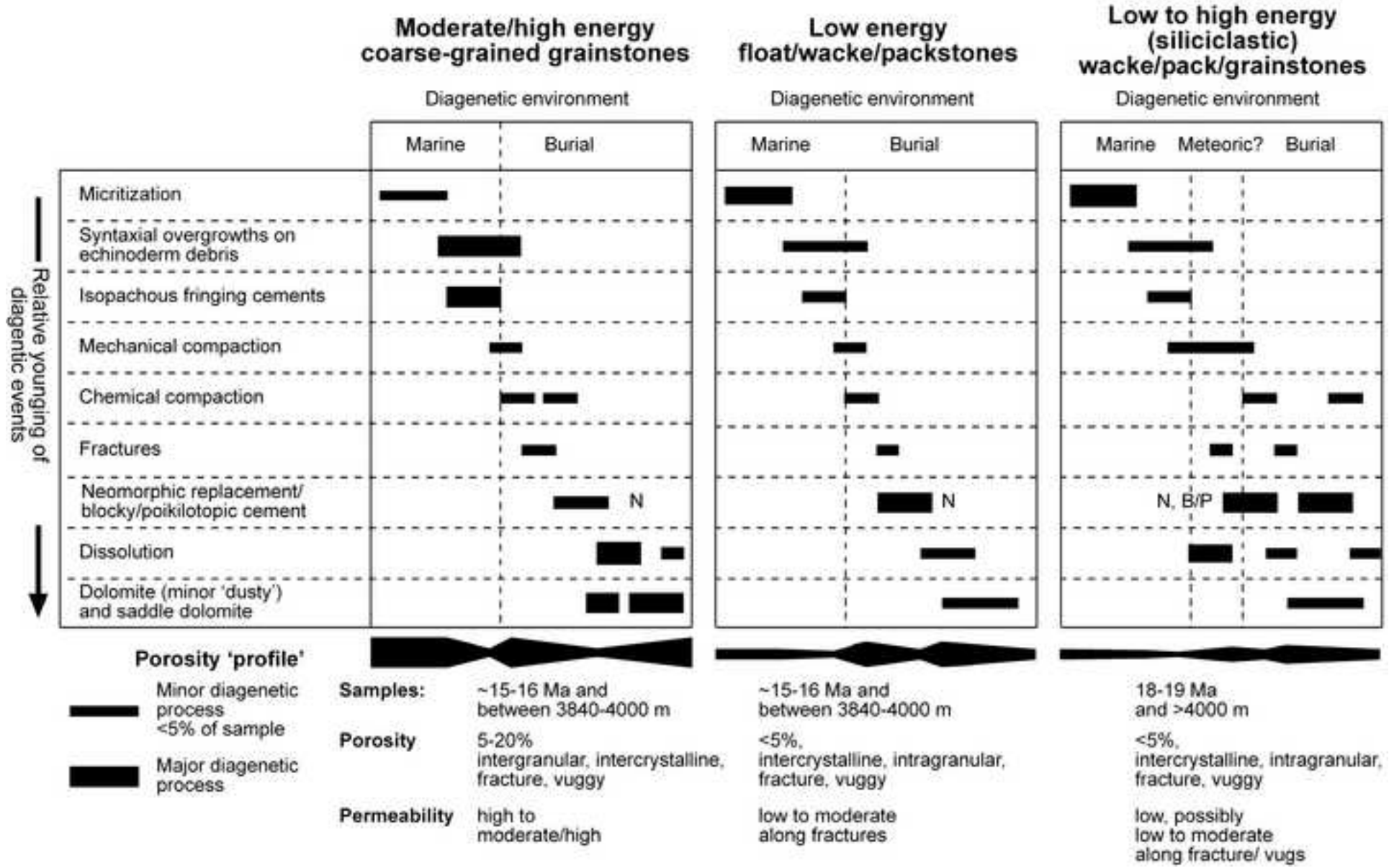

Figure 23
Click here to download high resolution image

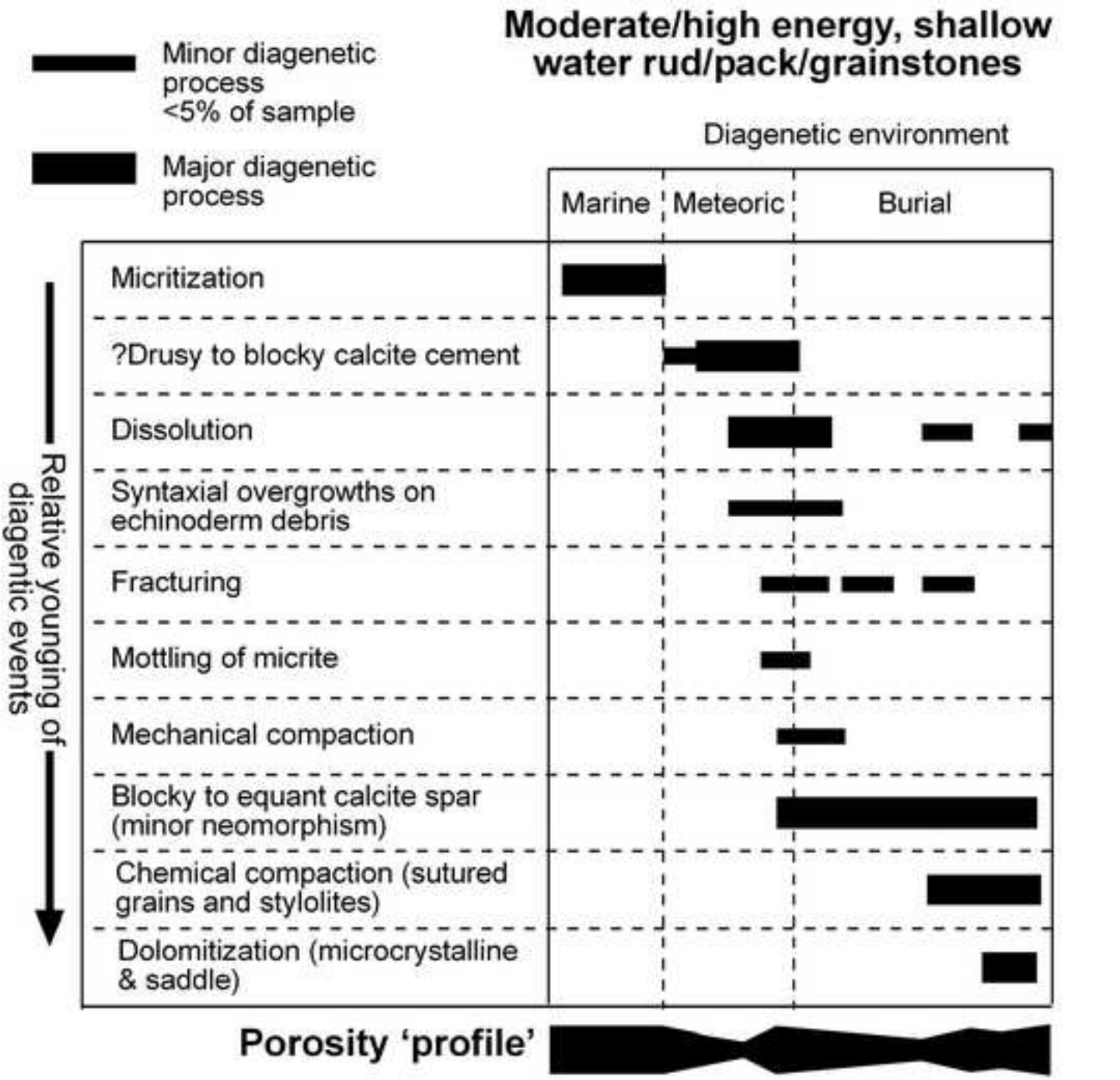

	High energy, shallow water rud/grainstones	Moderate/high energy, shallow water rud/grain/packstones
Porosity	5-15% intercrystalline, intragranular fractures/stylolites, vuggy biomoldic	<6% intercrystalline, intragranular fractures/stylolites, vuggy biomoldic
Permeability	low to moderate - moderate to good (not all inter-connecting pores)	low to moderate (not all inter-connecting pores)

Figure 24

Click here to download high resolution image

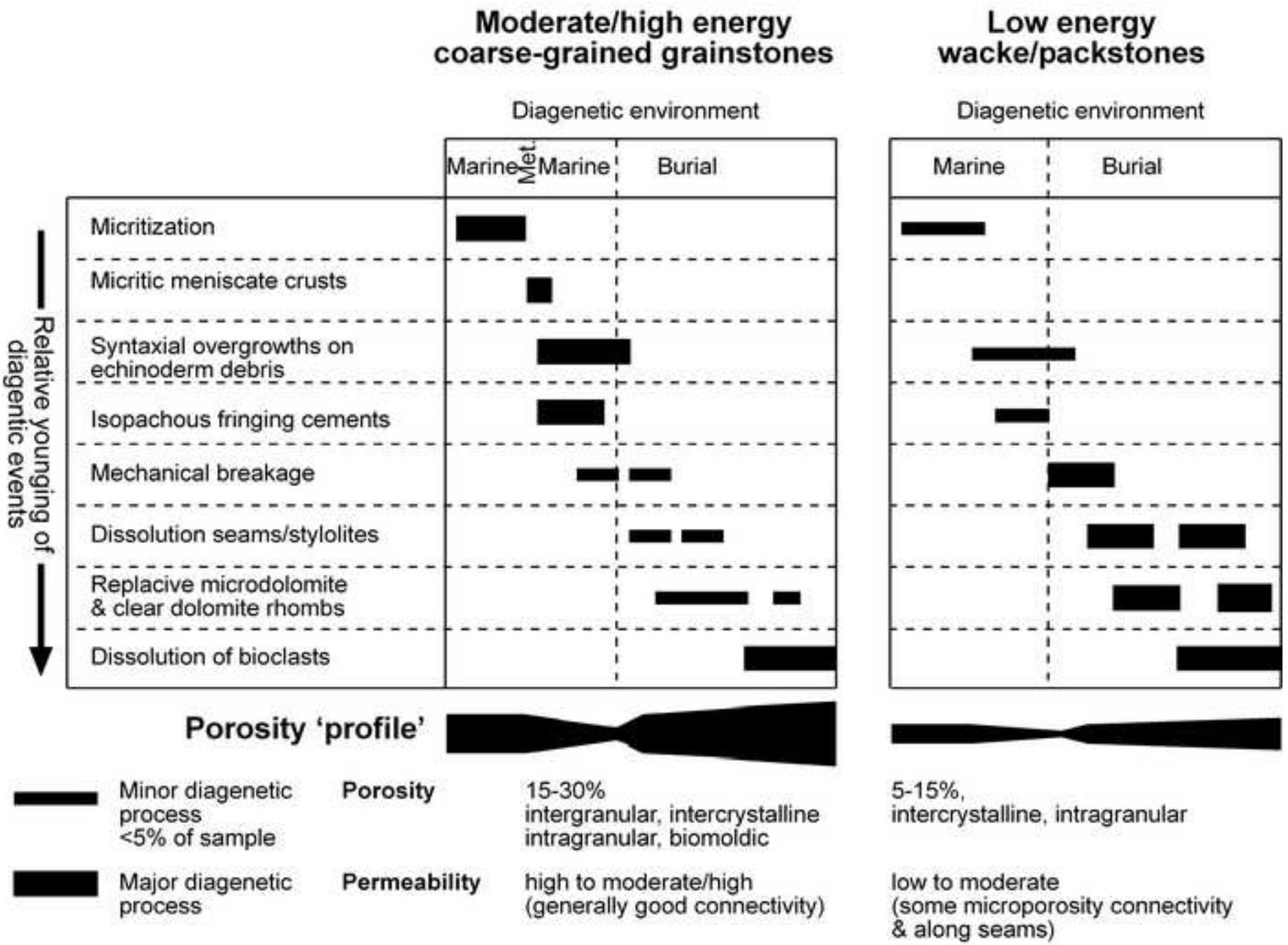

Figure 25

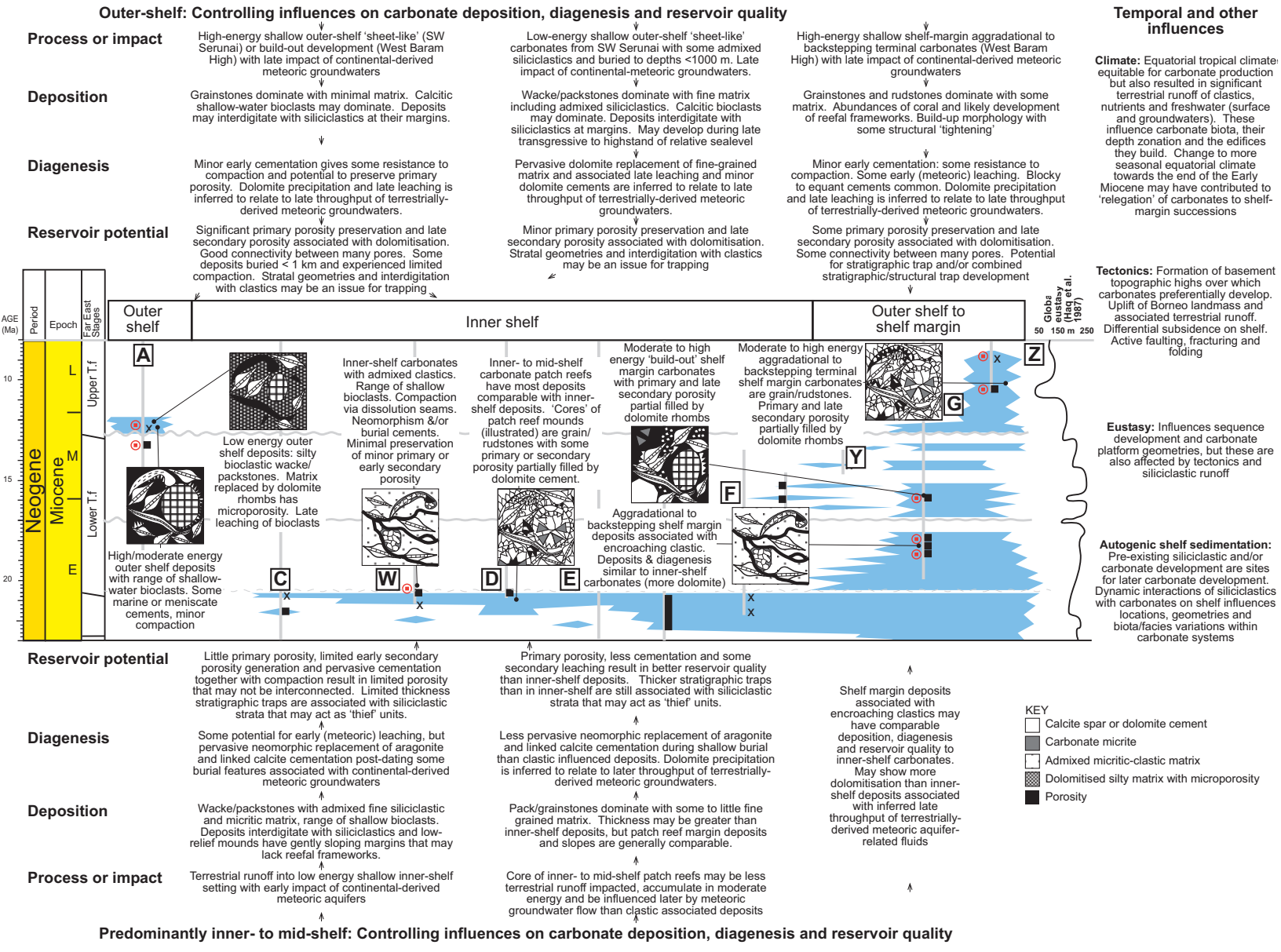
Outer-shelf: Controlling influences on carbonate deposition, diagenesis and reservoir quality
Process or impact
High-energy shallow outer-shelf 'sheet-like' (SW Serunai) or build-out development (West Baram High) with late impact of continental-derived meteoric groundwaters
Low-energy shallow outer-shelf 'sheet-like' carbonates from SW Serunai with some admixed siliciclastics and buried to depths <1000 m. Late impact of continental-meteoric groundwaters.
High-energy shallow shelf-margin aggradational to backstepping terminal carbonates (West Baram High) with late impact of continental-derived meteoric groundwaters
Deposition
Grainstones dominate with minimal matrix. Calcitic shallow-water bioclasts may dominate. Deposits may interdigitate with siliciclastics at their margins.
Wacke/packstones dominate with fine matrix including admixed siliciclastics. Calcitic bioclasts may dominate. Deposits interdigitate with siliciclastics at margins. May develop during late transgressive to highstand of relative sealevel
Grainstones and rudstones dominate with some matrix. Abundances of coral and likely development of reefal frameworks. Build-up morphology with some structural 'tightening'
Diagenesis
Minor early cementation gives some resistance to compaction and potential to preserve primary porosity. Dolomite precipitation and late leaching is inferred to relate to late throughput of terrestrially-derived meteoric groundwaters.
Pervasive dolomite replacement of fine-grained matrix and associated late leaching and minor dolomite cements are inferred to relate to late throughput of terrestrially-derived meteoric groundwaters.
Minor early cementation: some resistance to compaction. Some early (meteoric) leaching. Blocky to equant cements common. Dolomite precipitation and late leaching is inferred to relate to late throughput of terrestrially-derived meteoric groundwaters.
Reservoir potential
Significant primary porosity preservation and late secondary porosity associated with dolomitisation. Good connectivity between many pores. Some deposits buried < 1 km and experienced limited compaction. Stratal geometries and interdigitation with clastics may be an issue for trapping
Minor primary porosity preservation and late secondary porosity associated with dolomitisation. Stratal geometries and interdigitation with clastics may be an issue for trapping
Some primary porosity preservation and late secondary porosity associated with dolomitisation. Some connectivity between many pores. Potential for stratigraphic trap and/or combined stratigraphic/structural trap development
Temporal and other influences
Climate: Equatorial tropical climate equitable for carbonate production but also resulted in significant terrestrial runoff of clastics, nutrients and freshwater (surface and groundwaters). These influence carbonate biota, their depth zonation and the edifices they build. Change to more seasonal equatorial climate towards the end of the Early Miocene may have contributed to 'relegation' of carbonates to shelf-margin successions
Tectonics: Formation of basement topographic highs over which carbonates preferentially develop. Uplift of Borneo landmass and associated terrestrial runoff. Differential subsidence on shelf. Active faulting, fracturing and folding
Eustasy: Influences sequence development and carbonate platform geometries, but these are also affected by tectonics and siliciclastic runoff
Autogenic shelf sedimentation: Pre-existing siliciclastic and/or carbonate development are sites for later carbonate development. Dynamic interactions of siliciclastics with carbonates on shelf influences locations, geometries and biota/facies variations within carbonate systems
AGE (Ma)
Period
Epoch
Far East Stages
Neogene
Miocene
L
M
E
Upper T.f
Lower T.f
10
15
20
Outer shelf
Inner shelf
Outer shelf to shelf margin
Global eustasy (Haq et al. 1987)
50 150 m 250
A
Low energy outer shelf deposits: silty bioclastic wacke/ packstones. Matrix replaced by dolomite rhombs has microporosity. Late leaching of bioclasts
High/moderate energy outer shelf deposits with range of shallow-water bioclasts. Some marine or meniscate cements, minor compaction
C
Inner-shelf carbonates with admixed clastics. Range of shallow bioclasts. Compaction via dissolution seams. Neomorphism &/or burial cements. Minimal preservation of minor primary or early secondary porosity
W
Inner- to mid-shelf carbonate patch reefs have most deposits comparable with inner-shelf deposits. 'Cores' of patch reef mounds (illustrated) are grain/ rudstones with some primary or secondary porosity partially filled by dolomite cement.
D
E
Moderate to high energy 'build-out' shelf margin carbonates with primary and late secondary porosity partial filled by dolomite rhombs
Aggradational to backstepping shelf margin deposits associated with encroaching clastic. Deposits & diagenesis similar to inner-shelf carbonates (more dolomite)
F
Moderate to high energy aggradational to backstepping terminal shelf margin carbonates are grain/rudstones. Primary and late secondary porosity partially filled by dolomite rhombs
G
Y
Z
Reservoir potential
Little primary porosity, limited early secondary porosity generation and pervasive cementation together with compaction result in limited porosity that may not be interconnected. Limited thickness stratigraphic traps are associated with siliciclastic strata that may act as 'thief' units.
Primary porosity, less cementation and some secondary leaching result in better reservoir quality than inner-shelf deposits. Thicker stratigraphic traps than in inner-shelf are still associated with siliciclastic strata that may act as 'thief' units.
Shelf margin deposits associated with encroaching clastics may have comparable deposition, diagenesis and reservoir quality to inner-shelf carbonates. May show more dolomitisation than inner-shelf deposits associated with inferred late throughput of terrestrially-derived meteoric aquifer-related fluids
Diagenesis
Some potential for early (meteoric) leaching, but pervasive neomorphic replacement of aragonite and linked calcite cementation post-dating some burial features associated with continental-derived meteoric groundwaters
Less pervasive neomorphic replacement of aragonite and linked calcite cementation during shallow burial than clastic influenced deposits. Dolomite precipitation is inferred to relate to later throughput of terrestrially-derived meteoric groundwaters.
Deposition
Wacke/packstones with admixed fine siliciclastic and micritic matrix, range of shallow bioclasts. Deposits interdigitate with siliciclastics and low-relief mounds have gently sloping margins that may lack reefal frameworks.
Pack/grainstones dominate with some to little fine grained matrix. Thickness may be greater than inner-shelf deposits, but patch reef margin deposits and slopes are generally comparable.
Process or impact
Terrestrial runoff into low energy shallow inner-shelf setting with early impact of continental-derived meteoric aquifers
Core of inner- to mid-shelf patch reefs may be less terrestrial runoff impacted, accumulate in moderate energy and be influenced later by meteoric groundwater flow than clastic associated deposits
KEY
Calcite spar or dolomite cement
Carbonate micrite
Admixed micritic-clastic matrix
Dolomitised silty matrix with microporosity
Porosity
Predominantly inner- to mid-shelf: Controlling influences on carbonate deposition, diagenesis and reservoir quality